



SOLID STATE ABSTRACTS

*an abstract journal devoted to the
theory, production and use of solid state materials and devices*

VOLUME 1

NUMBER 7

PHYSICS
METALLURGY
ELECTRONICS

SEMICONDUCATORS
PHOSPHORS
MAGNETICS
DIELECTRICS
SUPERCONDUCTORS
METALS

SOLID STATE ABSTRACTS

VOLUME 1, NUMBER 7

April 1961

Abstracts 7846-8154

TABLE OF CONTENTS

Abstracts of the Solid State Literature

Metallurgy and Chemistry of Solids

Thermodynamic Properties of Elements and Alloys	323
Crystal Structure	323
Crystal Imperfections	324
Crystal Impurities (Introduction and Removal)	324
Crystal Surface Structure	326
Structure of Specific Crystals	327
Crystal Growth	327
Crystal Surfaces and Processing	331
Environmental Effects (Including Heat Treatment, Stress, and Radiation Effects)	331

Solid State Physics

General	331
Crystal Physics	332
Electrical Properties	334
Conductivity	336
Other Electrical Properties	338
Magnetic Properties	339
Optical Properties	343
Thermal Properties	345
Mechanical Properties	346

Solid State Devices

Diodes	347
Transistors	348
Magnetoelectric Devices	350

Photodevices	350
Thermal Devices	350
Ferrite Devices	350
Masers	351
Other Solid State Devices	352

Basic Solid State Device Circuits

General	352
Amplifiers	353
Oscillators	356
Switching Circuits	357
Signal Converters	358
Wave Generators	359

Applications of Solid State Devices

Medical and Military	359
Television	360
Telephony and Telemetry	360
Radar and Microwaves	360
Tape Recorders	361
Computers	361
Power	364
Instrumentation	365

Subject Index

Author Index	372
------------------------	-----

Editor: GEOFFREY KNIGHT, JR., Ph.D.

Assistant Editor: JOHN A. MURPHY

PUBLISHED MONTHLY BY

Cambridge Communications Corporation, 238 Main Street, Cambridge 42, Massachusetts, Tel. 491-0710

Subscription Rate: \$25.00 per year. Single Copies and Back Issues: \$2.50. Advertising Rates on Request.

Cambridge Communications Corp. is not prepared to furnish copies of the articles abstracted. However, there are many libraries throughout the country which maintain photocopying services.

SYMBOLS USED IN THE ABSTRACTS

L: Letter to the Editor. A: Only an abstract is given in the reference. R: Only a review is given in the reference. E: Erratum.

The reference numbers in the indices are the abstract numbers, not the page numbers.

Copyright 1961 by Cambridge Communications Corp. Printed in the U.S.A. by the University Press, Inc.

ABSTRACTS OF THE SOLID STATE LITERATURE

METALLURGY AND CHEMISTRY OF SOLIDS

THERMODYNAMIC PROPERTIES OF ELEMENTS AND ALLOYS

Phase Diagram Determination in Alkali Alloy Systems - See 772

846 ALLOYING PROCESSES IN SILICON TECHNOLOGY [In French] by J. J. Brissot (Labs. d'Elect. et de Phys. Appl., Paris); *Acta Electronica*, Vol. 4, No. 4, pp. 493-507, 1960

Theoretical considerations of the composition of metal alloys and of the reading of fusibility diagrams are discussed. These theoretical considerations provide a means of avoiding certain practical difficulties inherent in semiconductor alloying requirements.

847 ORIENTATION-DEPENDENT DISTRIBUTION COEFFICIENTS IN MELT-GROWN InSb CRYSTALS by J. B. Mullin and K. F. Hulme (Roy. Radar Estab.); *J. Phys. Chem. Solids*, Vol. 17, pp. 1-6, Dec. 1960

The anisotropy of the distribution coefficient of Te in melt-grown InSb crystals is discussed. During crystal growth, planar crystallographic facets can develop on the solid-liquid interface. For growth rates of 2 cm/hr, the distribution coefficient for Te on {111} facets of the crystals is shown to be about six times larger than the value recorded off {111} facets. A similar effect has been found for a residual donor impurity. The "acet effect" is not due to a solute-enriched boundary layer. The theoretical significance of the results is discussed.

Distribution of Impurities During Zone Equalization - See 7866

848 DETECTION OF THE α - γ IRON PHASE TRANSFORMATION BY DIFFERENTIAL THERMAL CONDUCTIVITY ANALYSIS by W. F. Claussen (GE Res. Lab.); *Rev. Sci. Instr.*, Vol. 39, pp. 878-881, Aug. 1960

A method of phase change detection in solids involving differential thermal conductivity analysis is described. This method applied to the α - γ transformation of iron at various pressures up to 100,000 atm. This transformation temperature is found to drop continuously with increasing pressure down to 605°C at 100,000 atm.

849 COMPOSITION LIMITS OF STABILITY OF PbTe by R. F. Ebrick and R. S. Allgaier (U.S. Naval Ord. Labs.); *J. Chem.*

Phys., Vol. 32, pp. 1826-1831, June 1960

The heat-treatment of single crystals of PbTe in evacuated silica tubes in the presence of Pb- or Te-rich ingots is described. At the heat-treatment temperatures, which range between 404° and 885°C, the ingot compositions are such that solid, liquid, and vapor phases of PbTe coexist. At a given temperature, the PbTe crystals are therefore as rich in Pb or Te as possible at equilibrium. After quenching the crystals, the resistivity and Hall constant are measured at room temperature and 77°K. Below about 860°C, crystals heated with Pb-rich ingots are n-type. Those heated with Te-rich ingots are p-type at all heat-treatment temperatures. The difference in the concentrations of electrons and holes at room temperature is taken as equal to the difference in concentration of lead and tellurium atoms at the heat-treatment temperature and is used to construct the PbTe solidus lines. The range of stability of PbTe is a maximum near 775°C and is between 49.994 and 50.013 atomic per cent Te, corresponding to carrier concentrations of 3.3×10^{18} electron/cm³ and 7.6×10^{18} holes/cm³, respectively.

CRYSTAL STRUCTURE

X-Ray Diffraction Studies of Pyrographite - See 7851

Morphology of Spiral Growth Layers on BaTiO₃ Crystals - See 7876

Polymorphism in Alkali Halide Phosphors - See 7989

7850 LATTICE SPACINGS AND COLOUR IN THE SYSTEM ALUMINA-CHROMIC OXIDE by J. Graham (Chem. Res. Labs., Melbourne); *J. Phys. Chem. Solids*, Vol. 17, pp. 18-25, Dec. 1960

Precision lattice spacing determinations are developed on well crystallized specimens throughout the system and the measurement of diffuse reflectivity of the samples is presented. There is no anomaly at 8 mol per cent Cr₂O₃ as found by earlier workers; the change in both the colour and the crystal field surrounding the chromium ions is continuous and smooth, although changes in the crystallographic environment of these ions cannot be followed in detail. Atomic parameters have been obtained for pure chromic oxide, revealing that the structure is less distorted than the similar structures of α -alumina and α -Fe₂O₃.

Lattice Constant of Cellulose - See 7936

7851 X-RAY STUDY OF PYROGRAPHITE by O. J. Guentert and C. T. Prewitt (Raytheon); *Bull. Am. Phys. Soc.*, Ser. II,

CRYSTAL STRUCTURE (Cont'd)

Vol. 5, p. 187(A), Mar. 21, 1960

A study of pyrographite samples deposited at different temperatures ranging from 1700° to 2500°C was reported. The basically polycrystalline material was found to consist of groups of parallel and approximately equidistant graphite layers with random layer orientation at the lower deposition temperatures and partial layer order at higher temperatures. The average layer group dimension is of the order of 50 Å at 1700°C and increases to about 500 Å at 2500°C. The increase in the size and layer order with increasing temperature was accompanied by a reduction of the layer spacing from 3.43 Å at 1700°C to 3.35 Å at 2500°C. All samples exhibited preferred orientation in which the layers of the individual layer groups tended to align themselves parallel to the face of deposition. This preferred orientation of the bulk samples increased strongly with increasing deposition temperature.

CRYSTAL IMPERFECTIONS

7852 THE THEORY OF DEFECT STRUCTURE AND SOLID STATE DIFFUSION by E. Brown (Rensselaer Polytech. Inst.); NASA Symp. on the Theory and Mechanism of Diffusion in Solids (A), Oct. 1960

Determination of the atomic configurations around defects in fcc metals, and the corresponding energies from a simple model was reported. Equilibrium configurations of different symmetries were investigated to distinguish the stable complex from the activated one. From the results of these calculations one obtains an activation energy for jumping as well as an activation volume.

7853 DEFECTS IN NATURAL AND SYNTHETIC QUARTZ by G. W. Arnold, Jr. (U.S. Naval Res. Labs.); J. Phys. Chem. Solids, Vol. 13, pp. 306-320, June 1960

Thermoluminescence measurements of quartz (both irradiated and naturally colored) from room temperature to 375°C are discussed. Various peaks of the light intensity vs temperature curves have been identified with absorption maxima in the 190-1000 μμ spectral region. The method is extremely sensitive to radiation dose, well-defined peaks being observed for very short x-irradiation times (~1 sec). Data on x-irradiated natural quartz, smoky quartz and on x-irradiated synthetic quartz with various additives are presented.

Neutron Irradiation Defects in Ge - See 7929

7854 EFFECT OF PRESSURE ON COLOR CENTERS IN Ag⁺-DOPED ALKALI HALIDES by R. A. Eppler and H. G. Drickamer (U. Illinois); J. Chem. Phys., Vol. 32, pp. 1734-1738, June 1960

The effect of pressure on various color centers in silver-doped alkali halides is studied. The crystals include NaCl (two concentrations), KCl, and KBr. The resulting shifts are used to confirm the assignments of some peaks and, in certain cases, to decide among conflicting interpretations.

Solubility of Interstitial Impurities in Ge and Si - See 7869

7855 ETCH PITS AND DISLOCATIONS IN CADMIUM SULPHIDE CRYSTALS by J. Woods (GE, Ltd.); Brit. J. Appl. Phys.,

Vol. 11, pp. 296-302, July 1960

A technique for producing dislocation etch pits on (0001), (0001̄) and {1010} growth faces of CdS crystals is described. Methods are also described whereby the dislocations are decorated by precipitation of either Ga or Cu. The strongest proof that the etch pits are formed where dislocation lines cut the free surfaces is provided by the characteristic etch pattern formed after indentation, the densities of etch pits in intersecting low-angle grain boundaries, and the coincidence of etch pits and decorated lines. Various other observations support the main evidence. It is also shown that the dislocation content can play an important part in determining some of the electrical properties of the crystals. In particular, Cu is rendered ineffective as an acceptor by precipitation; dislocations introduced in cadmium sulphide/chlorine crystals by plastic bending lead to the formation of acceptors.

7856 DISLOCATION MULTIPLICATION IN LITHIUM FLUORIDE CRYSTALS by W. G. Johnston and J. J. Gilman (GE); J. Appl. Phys., Vol. 31, pp. 632-643, Apr. 1960

Experimental observations of dislocation multiplication, of the defect structure left behind by a moving dislocation, and of cross-glide of individual dislocations in LiF crystals are presented. New dislocation loops form at many different sites in the wake of a moving dislocation. These loops have the same Burgers vector as the parent dislocation but do not, in general, lie on the same atomic plane. The rate of formation of new loops depends upon the magnitude of the applied stress. Such creation of new loops leads eventually to the formation of a wide glide band. A moving screw dislocation trails many line defects behind it that lie parallel to its direction of motion. The existence and nature of these trails and the observed dislocation multiplication can be explained in terms of a mechanism which involves the formation, by cross-glide, of jogs on a screw dislocation. This cross-glide multiplication mechanism was originally proposed by Orowan and by Koehler. It is demonstrated that cross-glide occurs easily in LiF, so that this mechanism is plausible. Some interesting complications arise when jogs that are longer than several atomic spacings but less than several hundred are formed. The defect trails exert a dragging of the screw dislocations that is not negligible compared to the yield stress of a crystal.

Dislocations in Ge Dendrites - See 7893

Spin Degeneracy Dependent Statistics of the Occupation of Dislocations - See 7914

Dislocations in LiF Single Crystals - See 7872

Distortion in Alumina-Chromic Oxide Systems - See 7850

CRYSTAL IMPURITIES (Introduction and Removal)

Analysis of Trapping Kinetics of Additively Colored KBr - See 7993

Donor Impurities in InAs - See 7878

7857 CONTINUOUS ZONE REFINING USING CROSS-FLOW by W. G. Pfann (Bell Labs.); U.S. Pat. 2,926,075, Issued Feb. 23, 1960

A continuous zone refining technique utilizing a chamber with multiple parallel compartments connected at their ends by small

CRYSTAL IMPURITIES (Cont'd)

oles is described. Both ends of the first and last compartments are fitted with product tubes, of which two are feeds and two are outlets. A single zone is passed down the length of each compartment simultaneously. When the zone reaches either end of a compartment, the cross-flow holes are all adjacent to liquid zones and liquid feed, forced into the first compartment, will force the contents of the first zone into the second compartment etc., forcing purified product from the last compartment.

One Refined n-Type InAs - See 7878

Solid State Diffusion Model - See 7852

858 DIFFUSION AS A TECHNIQUE FOR THE DOPING OF SILICON [in French] by C. Beauzee (Labs. d'Elect. et de Phys. Appl., Paris); Acta Electronica, Vol. 4, No. 4, pp. 509-532, 1960

The diffusion of impurities and the formation of p- and n-type layers in a Si monocrystal are discussed. Methods for the experimental determination of parameters such as the diffusion constant, surface concentration of impurities, etc., are given. Various diffusion techniques are described, and their application to the construction of solar batteries and power transistors are mentioned.

859 STRAIN ENHANCED DIFFUSION by L. A. Girifalco (NASA); NASA Symp. on the Theory and Mechanism of Diffusion in Solids (A), Oct. 1960

Measurements during plastic deformation of the self-diffusion coefficient of iron during compression, the self-diffusion coefficient of silver during compression and torsion, the diffusion rate of hydrogen through nickel during tension, and the diffusion coefficient of zinc in Al-Zn alloys were reported.

860 THE EFFECT OF PRESSURE ON DIFFUSION by N. Nachtrieb (U. Chicago); NASA Symp. on the Theory and Mechanism of Diffusion in Solids (A), Oct. 1960

The effect of hydrostatic pressure on diffusion was discussed. Pressure, like temperature, permits the characterization of the diffusion process. Dependence of diffusion upon temperature leads to the energy of the process; dependence upon pressure leads to the volume requirement of the elementary step. An activation volume, ΔV_{act} , was defined and provides information on the nature of lattice imperfections by magnitude and sign relationships.

861 RADIATION ENHANCED DIFFUSION by G. J. Dienes (Brookhaven Natl. Lab.); NASA Symp. on the Theory and Mechanism of Diffusion in Solids (A), Oct. 1960

Enhanced diffusion by the introduction of excess vacancies through radiation was discussed. The flux and temperature behavior of diffusion enhancement was shown to be strongly dependent on whether the excess vacancies are removed by migration to fixed sinks, recombination with interstitials, or both. Experiments with α -brass and other metals and alloys were cited.

862 EFFECT OF OXIDE LAYERS ON THE DIFFUSION OF PHOSPHORUS INTO SILICON by R. B. Allen, H. Bernstein, and A. D. Kurtz (Minn. - Honeywell); J. Appl. Phys., Vol. 31, p. 334-337, Feb. 1960

The diffusion of phosphorus from the vapor phase into single crystal Si is described. The experimental data are analyzed in terms of a two-layer diffusion model, leading to the determination of a diffusion constant for phosphorus in the oxide. The resulting diffusion constant at 1150°C is found to be $2.1 \times 10^{-15} \text{ cm/sec}^2$ with an activation energy of 1.4 ev.

7863 ANISOTROPIC DIFFUSION OF COPPER INTO BISMUTH TELLURIDE by R. O. Carlson (GE Res. Labs.); J. Phys. Chem. Solids, Vol. 13, pp. 65-70, May 1960

A marked difference between the penetration of radioactive Cu, parallel to and perpendicular to the cleavage planes in Bi_2Te_3 is reported. The compound readily cleaves perpendicular to the c-axis of the rhombohedral crystal. Room temperature measurements indicate that $D_{||} \sim 10^{-6} \text{ cm}^2/\text{sec}$, while extrapolated $D_{\perp} \sim 3 \times 10^{-15} \text{ cm}^2/\text{sec}$. Minute cracks, except perhaps on an atomic scale, are not believed responsible for the fast parallel diffusion. The fast parallel diffusion can be rationalized on the basis that in this direction, between adjacent tellurium layers, the copper moves through a region of relatively weak electrostatic bonding forces and large layer spacing. In any other direction, covalent and ionic bonding between tellurium and bismuth atoms would make penetration more difficult. Zener's theory is shown to give a reasonable fit to the D_0 values, requiring a negligible entropy term for parallel diffusion and a small entropy term, approximately the Boltzmann factor k, for perpendicular diffusion.

Effect of Dislocation on Diffusion - See 8017

7864 KIRKENDALL EFFECT IN THE Au-Ni SYSTEM by C. J. Meechan (Atomics Int'l.); Bull. Am. Phys. Soc., Ser. II, Vol. 5, pp. 277-278 (A), Apr. 25, 1960

Isothermal diffusion studies on Au-Ni couples at 915°C were discussed. Relative position changes of tungsten wire markers were measured before and after diffusion. Concentration vs penetration curves have been determined as a function of diffusing time from microhardness measurements, following calibration of microhardness as a function of composition on a series of standard alloys. From these measurements, it is found that the width of the interdiffusion zone on the Au-rich side of the original interface is several times greater than the width of the zone on the Ni-rich side. The marker shift is small but measurable and is in the direction of the Au-rich end of the couple. These studies also seem to indicate that the direction of net vacancy flow may be a function of composition in this system.

7865 DIFFUSION OF SULFUR AND SELENIUM IN GALLIUM ARSENIDE by B. Goldstein (RCA Labs.); Bull. Am. Phys. Soc., Ser. II, Vol. 5, p. 374 (A), June 15, 1960

Investigation into the diffusion of S and Se into GaAs from a dilute vapor was reported. The study covered the temperature range from 1000° to 1200°C, and employed radioactive isotopes of these elements and precision sectioning techniques. Penetration profiles were obtained which could be analyzed in terms of the complementary error function. The diffusion coefficients of both S and Se are given by the customary equation $D = D_0 \exp(-E/kT)$, where E, the activation energy, is 4.0 ev for both, and D_0 is $3 \times 10^7 \text{ cm}^2/\text{sec}$ and $1 \times 10^7 \text{ cm}^2/\text{sec}$ for S and Se, respectively. The fact that this activation energy differs from that found for the diffusion of Cd and Zn in GaAs (2.40 ev) suggests that substitutional acceptor and donor impurities diffuse through their respective sublattices in the III-V compound semiconductors. When dense vapors are used, the formation of secondary

CRYSTAL IMPURITIES (Cont'd)

compounds or phases was observed between the vapor and the GaAs. GaS was readily observable by electron diffraction methods for the case of S, and an amorphous phase was clearly visible, but not identifiable, for the case of Se.

Diffusion of Li^+ and B^- in Si - See 7867

Diffusion of Pb and Ga into Ge - See 8029

7866 CONCENTRATION DISTRIBUTION IN A BILLET DURING ZONE EQUALIZATION by V. N. Romanenko (Acad. of Sci.); Soviet Phys. -Solid State, Vol. 1, pp. 1535-1543, May 1960

The impurity concentration distribution in a specimen after successive travel of the liquid zone along the solid billet in two opposite directions is discussed. The problem is treated by means of a Pfann approximation. The two cases most frequently encountered in practice, namely, uniform initial distribution of the impurity, and introduction of the impurity in an initial region of the specimen, are investigated in detail. The calculated and experimental results are compared for the case of a ternary system. The reasons for the deviations resulting from the use of the Pfann approximation are analyzed. The possibilities of employing the method of zone equalization to determine the segregation coefficients and analysis of the phase diagrams are discussed.

7867 RELAXATION PROCESS FOR Li^+ - B^- ION PAIRING by E. M. Pell (GE Res. Labs.); Bull. Am. Phys. Soc., Ser. II, Vol. 5, p. 376 (A), June 15, 1960

The pairing of Li^+ and B^- in Si following their dissociation at high temperature was discussed. The recombination kinetics were determined by measuring resistivity vs time in the temperature range between 2 and 35°C. As pairing proceeds, the resistivity decreases because of the disappearance of the charged impurity scattering associated with unpaired ions. The present results indicate that the pairing of Li^+ and B^- is largely a random process, though there is evidence for a slight correlation between particular Li^+ and B^- ions. The kinetics are characteristic of diffusion limited precipitation to a Coulomb bomb. Diffusion constants of Li^+ calculated from the kinetics are in accord with previous ion drift results.

7868 ASSOCIATION OF VACANCIES WITH CALCIUM IMPURITIES IN POTASSIUM CHLORIDE CRYSTALS by T. Nino-miya (U. Tokyo); J. Phys. Soc. Japan, Vol. 15, pp. 1601-1606, Sept. 1960

Measurements of dc conductivity and dielectric loss in quenched KCl crystals doped with small amounts of CaCl_2 are presented. Evidence for the formation of higher complexes is obtained from decay of conductivity during annealing after quenching. It is also found that the relation between the number of free vacancies, n_v , and that of impurity-vacancy associated pairs, n_p , during decay at a fixed temperature K' is $n_p = K' n_v^{1.91}$. The number of free vacancies is found to decay exponentially with time. The activation energy for decay is estimated to be 0.63 ± 0.1 ev.

7869 THEORY OF SOLUBILITY OF INTERSTITIAL IMPURITIES IN GERMANIUM AND SILICON by K. Weiser (IBM); J. Phys. Chem. Solids, Vol. 17, pp. 149-161, Dec. 1960

A theory of solubility based on estimating the change in energy and in entropy when an impurity is placed in an interstitial site

in the lattice is developed. Two distinct cases are considered, namely, the case of the impurity remaining electrically neutral and the case of the impurity becoming an ionized donor. The species which results in the greater gain in free energy will be predominant in the lattice.

CRYSTAL SURFACE STRUCTURE

7870 ELECTRON DIFFRACTION AND SECONDARY ELECTRON EMISSION STUDIES OF A (100) SEMICONDUCTING DIAMOND SURFACE by H. E. Farnsworth and J. Marsh (Brown U.); Bull. Am. Phys. Soc., Ser. II, Vol. 5, p. 349 (A), June 15, 1960

The effect of surface discontinuity on the position of surface atoms was discussed. When normal incidence on the (100) face was used, the low-energy (below 350 ev) electron-diffraction pattern, after out-gassing of the crystal below 1000°C, contained no half-integral order surface grating beams in either the (100) or (110) azimuths, thus indicating that the positions of the atoms in the surface monolayer are not altered by the surface discontinuity as was found previously for Ge and Si. This result is consistent with the microcleavage experiments of Wolff and Broder. The secondary electron emission coefficient increased from 0.3 at 5 ev to a maximum of 1.45 at 300 to 400 ev for the diamond surface. Heating of the crystal support for 2 days at 1050°C caused a decrease in the intensity of the diffraction pattern. Argon-ion bombardment caused the diffraction pattern to disappear completely. Subsequent heating of the crystal support at 1100°C did not reproduce the diffraction pattern. As a result of this treatment, the maximum secondary emission coefficient decreased to 0.9 at 250 ev. The diamond surface may be regenerated by exposure to aqua regia and subsequent heating in vacuum.

7871 X-RAY REFLECTION STUDIES OF THE ANNEAL AND OXIDATION OF SOME THIN SOLID FILMS by N. Wainfan and L. G. Parratt (Cornell U.); J. Appl. Phys., Vol. 31, pp. 1331-1337, Aug. 1960

The technique of total reflection of x-rays applied to the study of thin films of Cu, Ni, Ge, and Se vacuum-deposited onto polished glass substrates is described. Starting with fresh films smooth enough to exhibit pronounced x-ray interference fringes in the region just beyond the critical angle, the effects of vacuum anneal and oxidation are studied. Changes in the reflection curves are interpreted in terms of possible structural changes in the films. Reflection from layers of particles of carbon or polystyrene latex deposited onto smooth substrates are also studied for comparison.

7872 X-RAY OBSERVATIONS ON CLEAVAGE FACES OF LiF SINGLE CRYSTALS by M. Yoshimatsu (Ragaku Denki, Ltd.) and K. Kohra (U. Tokyo); J. Phys. Soc. Japan, Vol. 15, pp. 1760-1770, Oct. 1960

A study of cleavage faces of LiF single crystals by means of the Berg-Barrett method of x-rays is discussed. Boundary lines of subgrains with small tilt angle show the intensity enhancement as do boundaries lying close to the surface. As to deformation produced by cleaving, more information such as slip directions is obtained than from etch-pit photographs. Furthermore, outcrops of individual dislocations arrayed in a boundary line or scattered in the interior of a grain are resolved. Dislocation half-loops lying close to the surface in a slip line are also ob-

CRYSTAL SURFACE STRUCTURE (Cont'd)

erved. In each type of defect mentioned above the direction of the Burgers vector is determined.

STRUCTURE OF SPECIFIC CRYSTALS

873 OBSERVATIONS ON MnBi FILMS DURING HEAT TREATMENT by L. Mayer (Genl. Mills); J. Appl. Phys., Vol. 31, pp. 346-351, Feb. 1960

Observations of magnetic surface phenomena made during the vacuum heat treatment necessary to develop ferromagnetic MnBi films from their nonmagnetic constituents are described. A vacuum hot stage for a metallurgical microscope was constructed in order to accomplish by means of the Kerr magneto-optic effect this visual observation of incipient ferromagnetism. MnBi films with some areas already magnetic were first observed. The phenomena occurring during evolution of the magnetic state in the areas adjacent to the already magnetic areas could be observed readily and the experiments could be reproduced consistently. Attempts to nucleate this transformation in the vacuum hot stage were only partly successful because reproducibility could not be achieved. Growth of a new magnetic area on MnBi film manifests itself first as an essentially structureless area. This structureless area then becomes an area of antiparallel domains. The size of the domains depends mainly on the duration of the existence of the structureless state. Large domains tend to develop if the structureless state is kept in existence for a short time and vice versa. In addition to the immediate practical goal of improving reproducibility in the preparation of MnBi films, such visual observation of the nascent state of ferromagnetism may also be of general interest to the physics of magnetism.

-Ray Diffraction Studies of Pyrographite - See 7851

874 SYNTHESIS AND CRYSTALLOGRAPHY OF STRUCTURALLY PURE CUBIC AND HEXAGONAL SINGLE CRYSTALS OF ZnS by H. Samelson and V. A. Brophy (Sylvania); 1960 Spring Mtg. Electrochem. Soc. (A)

The synthesis and identification of ZnS single crystals of structurally pure zincblende and wurtzite type were discussed. The structure identifications have been made by means of x-ray single-crystal photographs and by optical microscopy using polarized light. The concept of faults in a close-packed diatomic system was discussed, and the effect of faulting on the single-crystal x-ray diffraction patterns was illustrated.

CRYSTAL GROWTH

875 THEORY OF CRYSTAL GROWTH AND INTERFACE MOTION IN CRYSTALLINE MATERIALS by J. W. Cahn (GE Res. Lab.); Acta Metal., Vol. 8, pp. 554-561, Aug. 1960

The theory of crystal growth for diffuse and for non-singular surfaces is re-examined. It is found that if a critical driving force is exceeded, the surface will be able to advance normal to itself without needing steps; if this driving force is not exceeded lateral step motion is necessary. For extremely diffuse interfaces this critical driving force will be so small that any

measurable driving force will exceed it. For sharp interfaces the critical driving force will be very large, and most growth will occur by lateral step motion. For most systems, however, the critical driving force should be accessible experimentally. The nature of a step in a diffuse interface is discussed and its energy calculated. The conditions for interface motion by classical nucleation or screw dislocation mechanisms are derived.

7876 SPIRAL GROWTH LAYERS ON BARIUM TITANATE CRYSTALS. Part II. by N. V. Glik and V. A. Timofeeva (Inst. Cryst., USSR); Soviet Phys. -Cryst., Vol. 4, pp. 861-866, June 1960

The morphological characteristics of spiral growth layers forming depressions on the faces of barium titanate crystals are examined. The features of the internal morphology of these crystals are indicated. The conditions for the formation of transverse steps intersecting the spiral layers are discussed.

Melt Grown InSb Crystals - See 7847

7877 GROWTH OF LEAD TELLURIDE CRYSTALS BY THE CZOCHRALSKI METHOD by B. B. Houston (U.S. Naval Ord. Labs.); Bull. Am. Phys. Soc., Ser. II, Vol. 5, p. 166 (A), Mar. 21, 1960

The growth of PbTe crystals by a modification of the Czochralski method was discussed. An argon atmosphere was introduced to inhibit evaporation of molten PbTe. Crystals grown by this technique have dislocation densities from 5 to $10 \times 10^4/\text{cm}^2$ and, in some cases, no small-angle boundaries. They show considerable improvement over crystals grown by other methods. Crystals grown by the Bridgman method had $\sim 3 \times 10^5/\text{cm}^2$ dislocations randomly distributed, plus small-angle boundaries separated on the average by 0.3 mm. Crystals grown from the vapor phase had similar densities of randomly distributed dislocations with small-angle boundary separations of 1.0 mm. Crystals were grown from melts containing donor impurities, and from melts with various Pb to Te ratios. Of the latter runs, those which produced single crystals all resulted in p-type material with carrier concentrations of about $3 \times 10^{18}/\text{cm}^3$.

7878 PREPARATION AND PROPERTIES OF INDIUM ARSENIDE by R. H. Harada and A. J. Strauss (Chicago U.); U.S. Gov. Res. Rep., Vol. 33, p. 562 (A), May 13, 1960 PB 137 689

The preparation of zone-refined n-type InAs was discussed. In the preparation, As obtained by reduction of arsenic trichloride and purified by a thermal gradient sublimation technique was utilized. Properties of InAs large single crystals grown by a horizontal modification of the Bridgman technique are described. Electrical measurements on the n-type material are in good agreement with those obtained elsewhere. These results support the view that free carriers in InAs are produced by ionization of donor impurities (principally sulfur) which originate in the arsenic used for synthesis. Compensated samples of InAs have been prepared by doping with cadmium. One such sample exhibits anomalous electrical properties similar to those reported in the literature for samples doped with zinc. Another cadmium-doped sample has a resistivity of 80 ohm-cm at 77°K.

7879 HIGH PURITY SILICON PRODUCTION [in French] by P. Marcel (Cie. Péchiney, St.-Michel-de-Maurienne); Acta Electronica, Vol. 4, No. 4, pp. 465-478, 1960

The main processes for the production of electronic grade Si,

CRYSTAL GROWTH (Cont'd)

the reduction of SiCl_4 by Zn or H and the thermal decomposition of SiI_4 , SiCl_4 , and SiH_4 are discussed. The relative efficiency and future possibilities of these processes are mentioned.

Formation of Ge Films by Thermal Decomposition of GeI_2 - See 7885 and 7887

Pyrolytic Deposition of SiC, Ferrites, and Dielectrics - See 7886

7880 GROWTH OF CRYSTALS by D. C. Reynolds and S. J. Czyzak (USAF); U.S. Pat. 2,947,613, Issued Aug. 2, 1960

A device for growing single crystals from the vapor phase is described. It is applied to the synthesis of sulfides such as cadmium sulfide (CdS), which sublime from the solid phase. In operation, a controlled temperature sublimes a charge of solid material within the crystal-growing furnace retort, and the vapors pass through an orifice into an annular chamber containing a hydrogen sulfide (H_2S) atmosphere. Temperature control permits condensation and crystallization upon the chamber surface, the distance between the orifice and the surface being variable to allow physical growth of the crystal. Crystals have been grown in from 24 to 168 hours.

7881 METHOD FOR GROWING HEXAGONAL HgS SINGLE CRYSTALS by D. L. Kingston and D. C. Reynolds (Aero Res. Labs.); Bull. Am. Phys. Soc., Ser. II, Vol. 5, p. 372 (A), June 15, 1960

The growth of hexagonal HgS crystals from the vapor phase was described. A technique similar to that used for growing cadmium sulfide crystals was used. A charge of mercury sulfide powder is placed in a Vycor tube which is closed at one end with a flat plate to serve as a substrate. This tube is sealed in a larger tube with an atmosphere of H_2S or an inert gas. The whole system is heated so that the charge is at a temperature of approximately 725°C and the substrate at approximately 650°C . A pressure of approximately four atm is used during growth. The growth process involves vaporization of the material from the powder charge and recrystallization on the substrate. The hexagonal structure of the crystals have been verified by x-ray measurements. The crystals possess the characteristic red color of natural cinnabar.

Growth of PbTe Crystals from Vapor Phase - See 7877

7882 PREPARATION OF InAs, InP, GaAs, AND GaP BY CHEMICAL METHODS by D. Effer and G. R. Antell (Metropolitan Vickers); J. Electrochem. Soc., Vol. 107, pp. 252-253, Mar. 1960

A variety of III-V compound synthesis techniques based on the reaction of the lower valency metal halides with As or P are reported. The divalent metal halide and the V-element are run into a reaction tube from individually heated containers, in the proper proportions with a nitrogen carrier gas. Alternatively the liquid halide is reacted with the V-element under nitrogen or the V-element hydride is bubbled through the liquid halide and the complex heated under vacuum. The preferred technique consists of heating the V-element trichloride with excess metal in a sealed tube. Yields of the techniques vary from 65 - 95 per cent.

7883 PREPARATION OF LARGE AREA SINGLE-CRYSTAL CUPROUS OXIDE by R. S. Toth, R. Kilkson, and D. Trivich (Wayne State U.); J. Appl. Phys., Vol. 31, pp. 1117-1121, June 1960

The growth of large area single crystals of Cu_2O by the process of high temperature annealing is described. Initially, Cu_2O was prepared in finely polycrystalline form by the complete oxidation of Cu plate in air at temperatures of 1020°C to 1050°C . Subsequent annealing of the polycrystalline plates at higher temperatures allowed secondary recrystallization to occur. Single crystal grains having surface areas larger than 1 in^2 were grown consistently on Cu_2O plates having thicknesses of 0.010 in. to 0.060 in. In some cases, entire polycrystalline plates were transformed into single crystals, and as a result, individual single crystals having surface areas of 3 in^2 and larger were obtained. The annealing temperature and the annealing time were found to depend markedly on the plate thickness. Thick plates required lower temperatures and longer annealing times than the thinner plates. X-ray analysis of the large grains verified that they were single crystals without excess strain, and indicated preferred orientation, with the (211) and (311) planes predominating. Resistance profile measurements at room temperature on quenched samples showed that a variation in resistance exists through the thickness of the plate.

7884 THE EFFECT OF IMPURITIES ON THE GROWTH OF SYNTHETIC QUARTZ by C. S. Brown and L. A. Thomas (GE Ltd.); J. Phys. Chem. Solids, Vol. 13, pp. 337-343, June 1960

The effect of impurities on the habit and quality of large crystals of synthetic quartz is discussed. The role of Al as a key impurity is evaluated. The manner in which Al, possibly associated with another element, is incorporated into the quartz structure is indicated. The distribution of other impurities is studied by examining the darkening produced by x-irradiation. The over-all investigation seeks to develop a process for the growth of large crystals of synthetic quartz, using silica-rich rocks native to the United Kingdom as the raw material.

Growth of Ni, Fe, Ni-Fe, and Ni-Co Films by Vacuum Deposition - See 7956

7885 SOME ASPECTS OF Ge CRYSTAL GROWTH BY DISPROPORTIONATION OF GeI_2 by R. P. Ruth and S. B. Catalano (Bendix Aviation); Bull. Am. Phys. Soc., Ser. II, Vol. 5, p. 166 (A), Mar. 21, 1960

The preparation of crystalline Ge layers by epitaxy on single-crystal Ge substrate wafers, utilizing the disproportionation of GeI_2 , was discussed. Layers up to 150μ thick have been grown on p-type substrates having (111), (211), (311), (100), and (110) surfaces at average growth rates up to $15 \mu/\text{hr}$. The dependence of the growth rate upon temperature and other experimental conditions has been studied; the effects of these parameters and the crystalline orientation of the interface upon growth rate, degree of monocrystallinity, and conductivity type of the deposited layer have been evaluated with respect to the results of Newman and Wakefield. X-ray diffraction examination, etching studies, and electrical measurements indicate that n-type single-crystal layers are usually formed on (211), (311), and (110) substrate planes, and n- or p-type single-crystal layers on (111) substrate planes. The structure and type of the deposit on (100) planes depends upon the growth rate and temperature involved. The results of some electrical measurements and impurity doping experiments were described.

CRYSTAL GROWTH (Cont'd)

886 RESEARCH ON THE PYROLYTIC DEPOSITION OF THIN FILMS by F. V. Schossberger and S. Spriggs (Armour Res. Found.); U.S. Gov. Res. Rep., Vol. 33, p. 495 (A), May 13, 1960 PB 161 417

The preparation of thin films, particularly the pyrolytic deposition of thin films with high temperature stability, is discussed. Compact polycrystalline films of translucent, yellow β -SiC have been reproducibly prepared on tungsten substrates by the pyrolysis of trimethylchlorosilane vapor at 1 to 2 mm pressure and 1700°C. Unsupported films of β -SiC have been made by dissolving away the tungsten in melted sodium nitrite. Spectrochemical analyses and spectral transmission measurements verify that these films are of high purity. Nonporous films of silica on molybdenum have also been made by the low pressure pyrolysis of tetraethylsilicate; and films of nickel metal mixed with NiO have been prepared with high temperature coefficients of electrical resistance. These films, and films of a number of ferrites such as $(\text{Ni}, \text{Zn})\text{Fe}_2\text{O}_4$, have been made by spraying ethanol-ethyl acetate solutions of metal acetylacetones on alumina substrates heated to 600° to 950°C. Dielectric films adherent to copper have been prepared by the vacuum allying of a titanium-copper-nickel bonding layer, followed by the pyrolytic decomposition of triethanolamine titanate to titanium dioxide. The limits of composition, the conditions of firing, and the optimum thickness required for a flexible alloy layer were determined. Finally, beta-ray back-scattering has been shown to be a useful method for the measurement of film thickness.

887 VAPOR-DEPOSITED SINGLE-CRYSTAL GERMANIUM by R. P. Ruth, J. C. Marinace, and W. C. Dunlap, Jr. (GE); *J. Appl. Phys.*, Vol. 31, pp. 995-1006, June 1960

Formation of germanium layers on single-crystal Ge substrates by the thermal decomposition of GeI_2 is reported. The single-crystal nature of the layers has been established by x-ray and electron diffraction examination and by electrical measurements. The deposition process is described briefly. The crystal growth rate varies with crystal direction, and under certain conditions Ge whiskers appear. The layers as deposited are generally n-type; p ranges from 1 to 5 ohm-cm and μ_H from 200 to 2700 $\text{cm}^2/\text{v-sec}$ at room temperature. A donor level is found approximately 0.2 ev below the conduction band, with a concentration of active centers of about $10^{16}/\text{cm}^3$. Heat treatment at 550°C gradually converts the layers to p-type, for which p is 10 to 40 ohm-cm and μ_H 1500 to 2400 $\text{cm}^2/\text{v-sec}$ at room temperature; an acceptor level is found at about 0.05 ev above the valence band, with a density of active centers of 10^{14} to $10^{15}/\text{cm}^3$. The layers can be doped intentionally to produce either conductivity type, permitting fabrication of junction devices. Although iodine and other impurity atoms are considered, it is concluded that interstitial Ge atoms and lattice vacancies, occurring in unequal numbers at the time of deposition, are the most likely source of the donor and acceptor levels, respectively, and of the observed heat treatment properties.

888 ROLE OF THE TWIN PLANE IN THE DENDRITIC PROPAGATION OF GERMANIUM CRYSTALS by D. R. Hamilton, R. G. Seidensticker, J. W. Faust, Jr., and H. F. John (Westinghouse Res. Labs.); *Bull. Am. Phys. Soc.*, Ser. II, Vol. 5, p. 165 (A), Mar. 21, 1960

The relationship between the preference of Ge dendrites for <211> directional growth and their lamellar twin structure was

presented. A model in which nucleation and growth occur in the 141° re-entrant corners formed by the operation of a twin plane on the {111} growth habit of Ge was proposed. If only one twin plane is present, the crystal is not capable of indefinite <211> extension by nucleation and growth from re-entrant corners, since the corners grow out leaving a 219° ridge structure across which nucleation is difficult. If two twin planes are present, growth from one re-entrant corner serves to create a re-entrance at the second twin plane at a location previously occupied by a ridge structure. The difficulty of nucleation across a ridge is thus circumvented in the two twinned crystal, which can never be entirely bounded by ridges. The doubly twinned crystal was shown to possess easy growth in the six co-planer <211> directions as a consequence of its structure.

7889 LATERAL GROWTH PROCESSES IN DENDRITES OF DIAMOND-LATTICE MATERIALS by H. F. John and J. W. Faust, Jr. (Westinghouse Res. Labs.); *Bull. Am. Phys. Soc.*, Ser. II, Vol. 5, p. 165 (A), Mar. 21, 1960

The complexity of lateral growth processes in dendrites of diamond-lattice materials was discussed. It was observed that lateral growth processes are generally independent of the central twin structure. The dominant feature of the widening process was shown to be the outward growth of a pair of arms from each side of the central core which contains the twins. This produces, in cross section, an I-beam type of configuration. Freezing between these arms lags in varying degrees behind their outward growth. The places in which dislocation arrays can arise from this peculiar mode of growth were indicated. The role of accretional growth layers in giving the final ribbon-like dendrite with its very smooth surface was briefly discussed.

7890 INITIATION AND GROWTH OF DENDRITES OF DIAMOND-LATTICE MATERIALS by R. G. Seidensticker, J. W. Faust, Jr., H. F. John, and D. R. Hamilton (Westinghouse Res. Labs.); *Bull. Am. Phys. Soc.*, Ser. II, Vol. 5, p. 165 (A), Mar. 21, 1960

The growth of long ribbon-like dendrites of Ge from undercooled melts was discussed. Recent observations indicate that a multi-twin structure is necessary for the propagation of dendrites of diamond-lattice materials. The morphology of the growth button which is formed when a seed crystal is placed in a supercooled melt was described for various twin configurations. The importance of having a twin configuration which is continuous across the width of the seed was indicated. The lack of lateral continuity of the twin structure can prevent extension of dendritic growth into ribbon form.

7891 GROWTH OF ATOMICALLY FLAT SURFACES ON GERMANIUM DENDRITES by R. L. Longini, A. I. Bennett, and W. J. Smith (Westinghouse Res. Labs.); *Bull. Am. Phys. Soc.*, Ser. II, Vol. 5, p. 165 (A), Mar. 21, 1960

A theory of nucleation and growth of atomically flat surfaces on Ge dendrites was discussed. The theory suggests that part of the liquid-solid interface is supercooled. New atomic planes are occasionally nucleated and rapidly grow across the supercooled region. When such a growing layer reaches the melt surface, a step is created on the solid. It was proposed that the meniscus momentarily sticks to the corner of this step. Subsequent planes nucleated during this sticking period result in a step several atomic layers high, in accord with experiment. Elementary estimates of corner energy and amount of meniscus sticking yield results consistent with experiment.

CRYSTAL GROWTH (Cont'd)

7892 LIQUID-SOLID INTERFACE STUDIES IN GERMANIUM DENDRITES by A. I. Bennett and S. O'Hara (Westinghouse Res. Labs.); Bull. Am. Phys. Soc., Ser. II, Vol. 5, p. 165(A), Mar. 21, 1960

The structure of the liquid-solid interface in dendritic growth of Ge was discussed. A device for jerking a growing dendrite suddenly from the melt at high initial velocity and acceleration, estimated to be in excess of 250 cm sec^{-1} and 10^3 gravities, respectively, was constructed. Several dendrites of various twin structures and impurity content, and with growth directions of both $\langle 211 \rangle$ and $\langle 110 \rangle$, were so jerked. Examination of the resulting structures disclosed some features apparently due to the freezing of a film of liquid which adhered to the solid on jerking, and other features apparently characteristic of the liquid-solid interface just prior to jerking. In several cases the flat $\{111\}$ faces of the solid extended some distance below the melt surface; below the boundaries of these flats, the interface was curved, and thus thermally limited in growth. Dendrites grown from very highly doped material show significant differences from pure samples.

7893 DISLOCATIONS IN DENDRITES by J. W. Faust, Jr. and H. F. John (Westinghouse Res. Labs.); Bull. Am. Phys. Soc., Ser. II, Vol. 5, p. 165 (A), Mar. 21, 1960

The introduction of dislocations in Ge dendrites caused by the trapping of molten Ge was discussed. Evidence to support this model was given, and other aspects of dislocations were investigated. The central stripe of dislocations is caused by the entrapment of liquid Ge within the dendrite. The position of these inclusions can be seen as raised hillocks on the unetched surface. The size of the hillocks depends on the size of the included droplets. Upon etching, these hillocks are found to be the sites of stars of dislocations. The stars have a core of very high density of dislocations and arms of shallow surface loops. Dislocations on the edges of the $\{111\}$ faces may be either parallel or inclined to the central twin lamella, but never cross it.

Dendritic Inclusions in AlSb Grown-Junction Diodes - See 8016

Formation of Junctions in SiC by Vapor Doping - See 8018

7894 FORMATION OF PHOSPHOR FILMS BY EVAPORATION by L. R. Koller (GE Res. Lab.); 1960 Spring Mtg. Electrochem. Soc. (A)

Preparation of thin luminescent films of zinc sulfide phosphors by evaporation of powder phosphors in vacuo was discussed. The procedure consists in depositing the film on a heated substrate so that a crystalline rather than amorphous film is formed. This was accomplished by carrying out the evaporation in a container with walls at the same temperature as the substrate. Cathodo-, photo-, and electroluminescent films have been made by this method. Other phosphors have been made by modifications of this procedure.

Growth of (Zn, Hg)S Phosphors - See 7988

Growth of ZnS-In Phosphors - See 7991

7895 FILAMENTARY CRYSTALS GROWN FROM THE SOLID METAL by G. Sines (U. California); J. Phys. Soc. Japan, Vol. 15, pp. 1199-1210, July 1960

Conditions which promote whisker growth from the solid metal are discussed. The elastic strain-energy arising from the anisotropy of thermal expansion is a source of energy for spontaneous whisker growth. Observation of whisker growth on a Bragg bubble raft suggests that the growth mechanism could occur by cooperative repetitive movement of dislocations. The conditions for whisker growth from the solid are presented and fulfilled to produce growths on gold, silver, bismuth, lead, indium, and lead-indium alloys. The crystallographic orientations of several tin whiskers are reported, one of which had a transition between two orientations, although it was straight. The tensile strength of several tin whiskers was measured and observed to be lower than that calculated from bending tests. The high elastic strain of 5 per cent in bending was observed for an indium whisker.

Growth of Ferrites by Pyrolysis - See 7886

7896 MAGNESIUM-CHROMIUM-COPPER FERRITES FOR THE LOWER PART OF THE MICROWAVE BAND [in Russian] by A. S. Khlystov and E. M. Smokotin (SFTI, Tomsk U.); Izv. VUZ. Fizika, No. 2, pp. 157-160, 1960

The influence of admixtures of Cu on the microwave characteristics of the ferrite $MgFe_{1.36}Cr_{0.64}O_4$ is investigated. It is shown that a 20% molar substitution of Mg by Cu diminishes the width of the ferromagnetic resonance curve to 150 oe while retaining the other characteristics of the Mg-Cr ferrite. Ferrites are proposed with a relatively low synthesis temperature (1200°C) and a narrow resonance linewidth suitable for use in the decimeter radiowave range.

7897 ANISOTROPY OF THE COSTA-RIBEIRO EFFECT IN SINGLE CRYSTAL GROWTH OF NAPHTHALENE by S. Mancarenhas and L. G. Freitas (U. San Paulo); Bull. Am. Phys. Soc., Ser. II, Vol. 5, p. 166 (A), Mar. 21, 1960

The difference in the amount of charge trapped in an insulator during solidification as a function of crystal growth characteristics was discussed. It was found that for a single crystal of naphthalene this effect depends also on the crystallographic orientation. The charge value for growth normal to the cleavage plane is 32×10^{-9} coulomb/g, for growth along b , 2.9×10^{-9} coulomb/g, and for growth along a , 2.5×10^{-9} coulomb/g. Thus the growth normal to the cleavage plane gives the highest values. All data were obtained for a material of $3 \times 10^{-11} \text{ v/cm}^2$ residual conductivity at 90°C. An explanation of this effect, which depends upon impurity content, may be the existence of an anisotropic double layer at the solid-liquid interface. A possible dependence of partition coefficients upon the crystal orientation during growth from a melt was proposed.

Growth of Dielectrics by Pyrolysis - See 7886

Chemical Deposition of Thin Ferroelectric Films of $Pb(Ti \cdot Zr \cdot Sn)O_3$ on Platinum - See 7922

Growth of $BaTiO_3$ - See 7920

7898 DIAMOND SYNTHESIS by H. T. Hall (GE); U.S. Pat. 2,947,608, Issued Aug. 2, 1960

The synthesis of diamond from commonly available types of carbon such as coal, coke, charcoal, and graphite is described. A mixture of carbon and a catalyst is subjected to a pressure of at least 75,000 atm and a temperature of from 1200° to 2000°. The reaction chamber incorporates a reaction vessel and a high pressure device for insertion between the platens of a hydraulic press; variations in preparation of the reactant mixture and for

CRYSTAL GROWTH (Cont'd)

of the reaction vessel are suggested. Under the specified operating conditions, incipient conversion to diamond is indicated by a marked change in electrical resistance of the reacting mixture; no direct temperature readings are necessary. The diamonds obtained are indistinguishable from natural diamonds, and may be so utilized.

899 DIAMOND SYNTHESES by H. M. Strong (GE); U. S. Pat. 2,947,609, Issued Aug. 2, 1960

The conversion of common carbonaceous material to diamond, when subjected to pressure of from 50,000 to 115,000 atm, and temperature of from 1200 to 2600°C, is cited. Catalysts consisting of preformed alloys of certain metals are an integral part of the reaction mixture, and apparently permit conversion to diamond at pressures somewhat less than those described in the past. The composition and approximate operating pressure and temperature ranges for several alloys are listed. The structure and operation of the apparatus which accomplishes the synthesis are described, as are methods to determine the pressure and temperature in operation. The diamonds obtained are indistinguishable from natural diamonds, and may be so utilized.

CRYSTAL SURFACES AND PROCESSING

Adsorption and Surface Breakdown of Si Rectifiers - See 8015

7900 PRODUCTION OF ISLANDS AND DICE IN SEMICONDUCTOR SLICES WITH AN ULTRASONIC DRILL by R. D. Knight (Services Electronics Res. Lab.); J. Sci. Instr., Vol. 37, pp. 263-265, Aug. 1960

The production of islands less than 0.002-in in diameter is discussed. The ultrasonic drill used is described, as are the tools and the additions made to the equipment to achieve the degree of accuracy required. A novel feature is a frictionless gauge to indicate depth and rate of cutting. A method of bulk dicing and bulk islanding by the use of laminated tools is also described. Each of these tools has a protruding "pilot-blade" to locate the work so that dicing can be correctly related to islanding and/or to any strip plating markings, etc., put on the slice in earlier operations. A novel self-aligning work table, essential to the bulk islanding process, ensures that the exposed face of the semiconductor slice is in intimate contact with the tool slice.

Preparation of Thin Ge Samples - See 7947

Polishing of Quartz Crystal Surfaces - See 8048

ENVIRONMENTAL EFFECTS (Including Heat Treatment, Stress, and Radiation Effects)

Heat Treatment of PbTe - See 7849

7901 AGING OF A RUTILE CERAMIC [in Russian] by V. Ia. Kunin, Iu. A. Polonskii, and A. N. Tsikin (Leningrad Polytech. Inst.); Izv. VUZ, Fizika, No. 2, pp. 85-89, 1960

The stability of rutile ceramic with respect to prolonged heating, and its aging only under the effect of an electric field are discussed. An increase in the oxygen partial pressure in the roasting zone, as compared with atmospheric pressure did not reduce the intensity of aging, as could be expected on the basis of results in the literature.

Conversion of Conductivity Type in Ge Films by Heating - See 7887

Strain Enhanced Diffusion - See 7859

Effect of Pressure on Diffusion - See 7860

7902 EFFECT OF DEUTERON ENERGY ON IRRADIATION DAMAGE IN W by D. R. Muss and J. R. Townsend (U. Pittsburgh); Bull. Am. Phys. Soc., Ser. II, Vol. 5, p. 277 (A), Apr. 25, 1960

Cyclotron irradiations at 200°K of 0.0016-in diameter W wires previously annealed at 500°C using deuterons having energies of 13.7, 12.0, and 10.3 Mev were reported. The slope of the resistivity versus integrated deuteron flux curve was measured as a function of flux for these energies up to a total resistivity change of about 50 per cent as measured at 200°K. Even though the resistivity change is not a linear function of flux over this large range, the 10.3-Mev slope was found to be a constant multiple of the 13.7-Mev slope up to a resistivity change of 26 per cent; the ratio $(dR/d)_{10.3}/(dR/d)_{13.7}$ was found to be 1.43 ± 0.01 . Assuming a $1/E$ dependence and correcting for the slight nonuniformity of damage due to deuteron energy loss in the sample, the corresponding theoretical slope value is 1.38 ± 0.03 where the uncertainty arises from deuteron energy uncertainties. Thus the rate of production of displacements is very close to the expected $1/E$ dependence. The corresponding experimental ratio for the two energies 12.0 and 13.7 Mev was found to be 1.16 as compared with the corrected $1/E$ ratio of 1.15.

Radiation Induced Point Defects in Quartz - See 7853

Neutron Irradiation Defects in Ge - See 7929

Effect of Radiation on Diffusion - See 7861

SOLID STATE PHYSICS

GENERAL

7903 THE METALLIC STATE by A. H. Cottrell (U. Cambridge); Contemporary Phys., Vol. I, No. 6, pp. 417-432, Aug. 1960

Various theoretical and practical implications of the fact that metals contain free electrons are discussed. Recent views which emphasize ease of ionization, unsaturated metallic bonds, and screening of electrical charges by free electrons as the basis for distinguishing between metals, semiconductors, and insulators, are described. The importance of the free electron bond for crystal structures, cohesive properties and alloying behavior of metals is emphasized, and the principles underlying the engineering strength properties of matter and the design of creep-resistant alloys are briefly discussed in terms of free electrons and dislocations in solids.

GENERAL (Cont'd)

7904 HEXAGONAL FERRIMAGNETIC COMPOUND CONTAINING FLUORINE by E. H. Frei, M. Schieber, and S. S. Shtrikman (Weizmann Inst. Sci., Israel); *Phys. Rev.*, Vol. 118, p. 657, May 1, 1960

A partial substitution of the oxygen ions by fluorine in $\text{BaO} \cdot 6\text{Fe}_2\text{O}_3$ is reported. The new compound with a formula near to $\text{BaF}_2 \cdot 2\text{FeO} \cdot 5\text{Fe}_2\text{O}_3$ has (at room temperature) a magnetization saturation of 72 cgs units/gm compared to 67 cgs units/gm for $\text{BaO} \cdot 6\text{Fe}_2\text{O}_3$. The specific gravity, Curie temperature and unit cell dimensions are practically the same for both compounds.

CRYSTAL PHYSICS

7905 ON THE DIRECTIVITY OF PHYSICAL PROPERTIES IN CRYSTALS, WITH SPECIAL CONSIDERATIONS OF THE GALVANO- AND THERMOMAGNETIC EFFECTS [in German] by H. Bross; *Z. Naturforsch.*, Vol. 15a, pp. 859-874, Oct. 1960

A method to determine the influence of crystal symmetry on the directivity of vector-dependent tensors is discussed. As a point of departure scalar functions invariant in regard to the symmetry operations of the distinct classes of crystals are employed. By suitable differentiation of these scalar functions, tensors of any desired order may be found. For the 32 classes of crystals, the general form of the scalar functions and their frequency are presented. As an example of the tensors calculated by this method, a phenomenologic theory of galvano- and thermomagnetic effects is presented.

Classification of Solids by Metallic Bonds - See 7903

7906 ENERGY BAND CALCULATIONS FOR ALKALIS WITH THE COMPOSITE WAVE REPRESENTATION by H. Schlosser (Carnegie Inst. Tech.) and P. M. Marcus (IBM); *Bull. Am. Phys. Soc.*, Ser. II, Vol. 5, p. 162 (A), Mar. 21, 1960

A new technique for the calculation of electronic energy bands in solids, tested on Li and Na and yielding results of high accuracy for arbitrary points in the Brillouin zone, was developed. The technique utilized a composite wave function expanded in symmetrized plane waves in the outer part of the cellular polyhedron and matched on the inscribed sphere to a spherical wave expansion inside the sphere. A variational principle for wave functions with discontinuities on surfaces in the cell was used to determine the best eigenvalue for a given number of plane waves and gave a generalized secular equation in which the unknown eigenenergy appeared in all matrix elements. An IBM 704 program for the automatic high speed generation of matrix elements and solution of the resulting secular equation was written and applied to 25 points in the Brillouin zone of Li and 15 points in Na, including a number of points without symmetry. Agreement to four significant figures was found with Kohn and Rostoker for Li; close agreement with Ham for Li and Na was also obtained.

Energy Levels in Paramagnetic Crystals - See 7977

7907 ATOMIC RADII ELECTRONEGATIVITIES AND ACTIVATION ENERGIES IN INORGANIC SEMICONDUCTOR COMPOUNDS [in French] by J. P. Suchet (Cie St. Gobain); *J. Phys. Chem. Solids*, Vol. 16, pp. 265-278, Nov. 1960

Atomic and structural results on the value of the energy gap are derived. Empirical formulae, allowing the computation of homopolar and heteropolar contributions are used. The interatomic distances in the Cl , DO_3 , $\text{A}7$, $\text{B}1$, $\text{C}6$, $\text{C}33$, $\text{B}29$, and DO_{18} structures are used to build three tables of covalent atomic radii for bonds with sp^3 , sp^2 , and p^3 orbitals by generalizing Pauling's work on tetrahedral radii. The homopolar contribution is computed from these radii. The heteropolar contribution is then related to the differences of electronegativity between the atoms and to their atomic numbers. It is shown that Pauling's electronegativity table cannot be used here and another table is built in good agreement with experimental results. Tables give the computed energy gaps and their homopolar and heteropolar parts for about one hundred semiconducting binary compounds.

7908 ELECTRON IMPACT IONIZATION. THE PROBABILITY OF OCCUPYING STATES AFTER IONIZATION by M. Miasek (U. Warsaw); *Czech. J. Phys.*, Vol. 10B, No. 8, pp. 584-594, 1960

The probability function of occupying states with a definite energy in the conduction band after collision in the process of electron impact ionization is calculated. The valence band is assumed of finite width. Several cases of the primary energy and the effective mass in the valence band are examined.

Wave Functions and Energies of an Electron in a Deep Trap - See 7930

7909 THEORY OF THE VALENCE BAND STRUCTURE OF GERMANIUM IN AN EXTERNAL MAGNETIC FIELD by R. F. Wallis and H. J. Bowlden (U.S. Naval Res. Lab.); *Phys. Rev.*, Vol. 118, pp. 456-461, Apr. 15, 1960

Calculation of the energies of the magnetic sub-bands associated with the V_1 and V_2 valence bands in germanium as a function of k_z , the propagation constant parallel to the external magnetic field, is presented. Warping of the V_1 and V_2 bands was neglected. Sub-bands belonging to the 1^+ and 2^+ ladders (light holes) have minima at $k_z = 0$ and show quantum effects consisting of a decrease in curvature as the valence band edge is approached. Sub-bands belonging to the 2 -ladder (heavy holes) also have minima at $k_z = 0$, but the curvatures increase near the valence band edge. The 1^- heavy hole sub-bands show very marked quantum effects. The sub-band minima occur at values of k_z different from zero, and local maxima appear at $k_z = 0$. The peculiar nature of the 1^- magnetic sub-bands may lead to observable effects in various magneto-optic phenomena in germanium.

7910 ON THE HOLE COMPONENT OF THE FERMI SURFACE IN BISMUTH by N. B. Brandt (Moscow State U.); *Soviet Phys. JETP*, Vol. 11, pp. 975-976 (L), Oct. 1960

The Fermi surface of a group of holes observed in bismuth at low temperatures is discussed. The Fermi surface has been found to consist of an ellipsoid of rotation, elongated along the trigonal axis. The ellipsoid has the following parameters: Area of the principal sections: perpendicular $S_1 = 6.75 \times 10^{-42} \text{ gm}^2 \text{ cm}^2/\text{sec}^2$ and parallel to the trigonal axis $S_2 = 25.75 \times 10^{-42} \text{ gm}^2 \text{ cm}^2/\text{sec}^2$; hole concentration $n^H = 0.34 \times 10^{16} \text{ cm}^{-3}$; bounding Fermi energy $E_0^H \approx 2.5 \times 10^{-14} \text{ erg}$ ($E_0^H/K \approx 180^\circ\text{K}$); effective mass in the plane perpendicular to the trigonal axis $m_1^H = m_2^H = 0.05 m_0$ (m_0 is the free electron mass) and in the direction of the trigonal axis $m_3^H = 0.7 m_0$. The magnitude of the anisotropy of the hole surface and the effective mass values are in good agreement with

CRYSTAL PHYSICS (Cont'd)

lished data. Since the heat capacity of the holes is small in comparison with the observed linear term in the heat capacity of Bi, at least three groups of carriers must exist.

11 ENERGY SPECTRUM OF HOLES IN DIAMOND-TYPE CRYSTALS by K. Ya. Shtivel'man (Semicon. Inst.); Soviet Phys.-Solid State, Vol. 2, pp. 464-467, Sept. 1960

Calculation of the energy spectrum of both p-type germanium and p-type silicon, beginning with the many-electron Hamiltonian of Pauli, is presented. The calculation is implemented in consideration of the spin-orbital interaction.

12 EFFECT OF DEFORMATION ON THE HOLE ENERGY SPECTRUM OF GERMANIUM AND SILICON by G. E. Pikus and G. L. Bir (Acad. Sci., USSR); Soviet Phys.-Solid State, Vol. 1, pp. 1502-1517, May 1960

general expression for the energy spectrum of the holes in a lattice of germanium type with arbitrary uniform deformation of the crystal is obtained. The effect of deformation on the electrical properties of germanium and silicon in the low-temperature and high-temperature limiting cases are briefly considered.

13 PRESSURE DEPENDENCE OF THE DIRECT ENERGY GAP IN GERMANIUM by M. Cardona and W. Paul (Harvard U.); Phys. Chem. Solids, Vol. 17, pp. 138-142, Dec. 1960

The pressure dependence of the energy gap corresponding to allowed optical transitions in germanium has been measured at room temperature and pressures up to 7000 kg/cm². This direct energy gap is found to increase at a rate of $1.3 \pm 0.1 \times 10^{-5}$ ev²/kg, in agreement with previous approximate determinations and with the pressure coefficient of the same energy gap in group 3-5 compounds.

Energy Gap of GaAs-Ga₂Se₃ - See 7942

14 STATISTICS OF THE OCCUPATION OF DISLOCATION ACCEPTORS (ONE-DIMENSIONAL INTERACTION STATISTICS) by R. M. Broudy and J. W. McClure (Union Carbide); J. Appl. Phys., Vol. 31, pp. 1511-1516, Sept. 1960

Improved statistics which explicitly take into account interactions between nearest-neighbor electrons are derived. It is shown that the results are valid over the complete range of occupation. The statistics are given in terms of two functions occurring in the form of infinite series which have been evaluated over a considerable range of occupation and are tabulated. Techniques for use of the results are presented. Statistics which take into account the proper spin degeneracy of acceptor states are also derived.

Purity Levels in Ge Films - See 7887

15 EFFECT OF PRESSURE ON THE M CENTER IN ALKALI HALIDE CRYSTALS by S. Minomura and H. G. Drickamer (Illinois); J. Chem. Phys., Vol. 33, pp. 290-293, July 1960

The effect of pressure to 52,800 atm, measured on the M band NaCl, KCl, KBr, and KI, and on the R₂ and N bands in Cl is described. In general, the band peak shifts to higher frequency with increasing pressure for all bands. At the phase transition from fcc to sc there is a blue shift in KCl, but a red

shift in KBr and KI. It is suggested that the shift corresponds to a balance between contraction and polarizability effects. From an Ivey-type relation, it seems that the M center is somewhat less compressible than the F center. There is a marked increase in intensity of the M center in the potassium halides in passing through the phase transition from the fcc to the sc lattice.

Excited Levels of Activator Ions in Alkali Halide Crystals - See 7983

Band Structure of Alkali Halide Phosphors - See 7989

Emission Bands in Sn, Pb, and Sb Activated Phosphors - See 7925

1916 CALCULATION OF LATTICE SPECIFIC HEATS IN THE HARMONIC APPROXIMATION by A. F. Stevenson (Wayne State U.); Bull. Am. Phys. Soc., Ser. II, Vol. 5, p. 204 (A), Mar. 21, 1960

A method which permits the explicit expression of the lattice free energy, specific heat, etc., in terms of the polynomial whose roots determine the natural frequencies when periodic boundary conditions are used was presented. In this way, the explicit determination of the frequencies is avoided. For the numerical calculation of specific heats in forms of interaction constants the method is less laborious than the usual approach that uses the frequency distribution function. A numerical example was given.

1917 CENTER LAW OF THE LATTICE VIBRATION SPECTRA by J. N. Plendl (AF Cambridge Res. Ctr.); Phys. Rev., Vol. 119, pp. 1598-1603, Sept. 1, 1960

The frequency of the center of gravity of the infrared spectrum, simply called center frequency, is considered. It is shown that the lattice vibration spectra of a solid as a whole can be characterized by the center frequency. Data on this frequency have been determined for many nonconducting solids from the experimental spectra of lattice vibrations in reflectance as well as in absorption. A striking experimental phenomenon is discovered: the center frequency, whether determined from the reflectance or from the absorption type spectrum, is found to be equivalent and identical with Debye's characteristic frequency. This phenomenon is exhibited for a large variety of nonconducting compounds covering almost the entire range of the vibrational spectra of solids. Moreover, the center frequency remains constant with varying temperature. The equality of the center frequency of the infrared spectrum and the characteristic frequency from specific heat constitutes the center law of lattice vibration spectra.

1918 IMPURITY INDUCED INFRARED LATTICE VIBRATION ABSORPTION by R. F. Wallis (U.S. Naval Res. Lab.) and A. A. Maradudin (U. Maryland); Prog. Theoret. Phys., Vol. 24, pp. 1055-1077, Nov. 1960

The effects of isotopic impurities on the lattice vibrational optical absorption of both monatomic and diatomic linear chains of alternately charged particles are calculated. It is found that even with the harmonic approximation and the use of cyclic boundary conditions, the presence of impurities leads to a broad absorption of the low frequency side of the main maximum. This is in contrast with the delta-function type of absorption at the optical frequency predicted by these models in the absence of impurities. For those cases in which discrete frequencies associated with localized vibrational modes occur, absorption at

CRYSTAL PHYSICS (Cont'd)

these isolated frequencies also occurs. This latter absorption can take place at frequencies higher than that of the main maximum. The results of the calculations and available experimental data are compared.

Phonon Scattering in Nonpolar Crystals - See 7924

ELECTRICAL PROPERTIES

7919 INFLUENCE OF OXYGEN CONTENT ON ELECTRIC AND THERMOELECTRIC PROPERTIES OF TERNARY SYSTEM $\text{Bi}_2\text{Te}_{3-x}\text{Sex}$ by K. Smirous and L. Stourac; Czech. J. Phys., Vol. 10B, p. 659, Sept. 1960

A study of the influence of dissolved oxygen on the electric and thermoelectric properties of the semiconducting system $\text{Bi}_2\text{Te}_{3-x}\text{Sex}$ is reported. It is shown that the addition of oxygen to prepared samples of $\text{Bi}_2\text{Te}_{2.4}\text{Se}_{0.6}$ causes a decrease in electrical conductivity while the thermoelectric force remains unchanged. This influence is connected with a decrease in the mobility of the electrons caused by the presence of oxygen, which does not affect electron concentration. Conclusions as to the influence of oxygen on the efficiency of the conversion of thermal energy into electric energy and vice versa are reached.

7920 THE PROBLEM OF REPLACEMENT OF A TITANIUM ION BY A SILICON ION IN POLYCRYSTALLINE BARIUM TITANATE by L. N. Kamysheva (Voronezh State U.); Soviet Phys. -Solid State, Vol. 2, pp. 909-910, Nov. 1960

The temperature dependence of permittivity of the $\text{Ba}(\text{Ti}, \text{Si})\text{O}_3$ system in a weak one kc field is evaluated. The use of usual ceramic techniques to prepare the samples is stated. A second group of samples was prepared by adding SiO_2 to BaTiO_3 . In both cases, as the Si content increases up to eight to ten per cent, the Curie point of the first phase transition is displaced toward higher temperatures. Replacement of Ti ions by Si ions is indicated. For Si content greater than about ten per cent, the flatness of the permittivity curve prevented detection of the Curie point. The formation of a heterogeneous mixture is indicated.

7921 A DIELECTRIC RESONATOR METHOD OF MEASURING INDUCTIVE CAPACITIES IN THE MILLIMETER RANGE by B. W. Hakki and P. D. Coleman (U. Illinois); IRE Trans., Vol. MTT-8, pp. 402-410, July 1960

A novel technique for the measurement of dielectric and magnetic properties of a homogeneous isotropic medium in the range of approximately 3 to 100 kMc is described. An accuracy of 1 to 0.1 per cent is possible in the determination of permittivity or permeability in those cases where the loss tangent is sufficiently small. The measuring structure is a resonator made up of a right circular cylindrical dielectric rod placed between two parallel conducting plates. For measurement of permittivity two or more resonant TE_{0n1} mode frequencies are determined whereas for the measurement of permeability two or more resonant TM_{0n1} mode frequencies are determined. The dielectric or magnetic properties are computed from the resonance frequencies, structure dimensions, and unloaded Q. Since the loss tangent is inversely proportional to the unloaded Q of the structure, the precision to which Q is measured determines the accuracy of the loss tangent.

7922 THIN FERROELECTRIC FILMS OF $\text{Pb}(\text{Ti-Zr-Sn})\text{O}_3$ by M. S. Lur'e; Soviet Phys.-Doklady, Vol. 4, pp. 1082-1083, Mar. -Apr. 1960

Measurements made on thin ($\sim 2\mu$ thick) films of ferroelectric $\text{Pb}(\text{Ti-Zr-Sn})\text{O}_3$ are discussed. The films were chemically deposited on platinum foil, then were annealed in an atmosphere of lead oxide vapor and a silver electrode was evaporated on the ferroelectric. The films prepared by this process had a homogeneous fine-grain structure. A rectangular hysteresis loop and a large change of charge during switching were measured. The films were found to have a significantly nonlinear dielectric permeability. An unusually large breakdown voltage of 300 kv/cm was found in many specimens at room temperature. This is explained by the presence of volume charge in a surface layer comparable with the overall thickness of the film.

7923 KINEMATIC THEORY OF FERROELECTRIC DOMAIN GROWTH by T. Nakamura (Ochanomizu U.); J. Phys. Soc. Japan, Vol. 15, pp. 1379-1381, Aug. 1960

Sidewise motion of a 180° wall in ferroelectric barium titanate is described. The kinematic wave theory developed by Light-hill-Witham is applied and it is shown that the peculiar shapes of the domain in growing and in shrinking processes, observed by Miller and Husimi, can be derived purely kinematically. The 180° wall is described as an assembly of steps and orientation of the wall is described by step density. There is a part of constant orientation that moves with a constant velocity which is shown to be identical to the kinematic wave velocity. Square-like domain boundaries with convex sides observed in the growing process and straight domain fronts in the shrinking process are fairly well explained as a result of propagation of kinematic waves, assuming a suitable functional relationship between the velocity and the density of the progressing steps. Discontinuity of wall orientation is interpreted as a "kinematic shock wave."

7924 VARIATIONAL TREATMENT OF WARM ELECTRONS IN NONPOLAR CRYSTALS by I. Adawi (RCA); Bull. Am. Phys. Soc., Ser. II, Vol. 5, p. 193 (A), Mar. 21, 1960

Studies of deviations from Ohm's law in n-type Ge over a wider range of temperature than previously reported were presented. Two effective masses were assumed. Both acoustical and optical phonons, and also ionized impurities were included in the scattering. The ionized impurity effect was shown to be important. It was proved that the relative importance of optical phonon scattering is maximum at a temperature which corresponds, approximately, to the optical phonon energy. The low temperature limit was found to be that of acoustical phonons alone, and that of high temperature the same except for a factor of the order of unity. Finally, the convergence of the variational method was established in a limiting case using as representation a set of polynomials which are orthonormal with respect to the collision operator.

7925 ATOMIC WAVE FUNCTIONS OF ACTIVATORS by K. H. Butler (Sylvania); 1960 Spring Mtg. Electrochem. Soc., (A)

The sp configuration which is characteristic of the excited states of many primary activator ions (i.e., Sb^{3+} , Sn^{2+} , TI^{+}) was discussed. Quantum mechanical formulas were used to show that the electron density distribution of this configuration depends strongly on the coupling of the electron spins and on the magnetic quantum number of the combined electrons. The marked difference in the shapes of an ion in the ${}^1\text{P}_1$ and ${}^3\text{P}_1$ states, combined with variations in the coordinator number of

ELECTRICAL PROPERTIES (Cont'd)

the surrounding anions in different crystal structures, provided explanations for such phenomena as the polarization of luminescence in KCl:Tl and the appearance of two emission bands in many tin-activated phosphors as contrasted to the single emission band for most materials activated by lead or antimony.

7926 EFFECT OF CRYSTALLINE FIELDS ON CHARGE DENSITIES AND MAGNETIC FORM FACTORS by A. J. Freeman (Materials Res. Lab. and MIT) and R. E. Watson (MIT); Phys. Rev., Vol. 118, pp. 1168-1172, June 1, 1960

The effects of crystalline fields on 3d charge densities and magnetic form factors for transition metal ions, based on recent theoretical investigations augmented by an analysis of optical absorption data are discussed. It is shown that the crystalline field has two effects on the free ion 3d wave functions and hence on their form factors as well: a differentiation or "splitting" of the two types of cubic 3d functions by an expansion of the t_{2g} (e_g) orbitals and a contraction of the $e_g(t_{2g})$ orbitals resulting in two different radial charge densities, and a net expansion of the charge distribution from the free ion value. The magnetic form factors due to this "splitting" effect when calculated according to the methods of Weiss and Freeman show measurable deviations from the free atom results. A form factor for Mn^{+2} based on optical absorption data shows a large expansion of the 3d charge density, in agreement with the magnetic form factor measurements of Hastings, Elliott, and Corliss. This agreement, based on the use of theoretical $F_k(3d, 3d)$ integrals, indicates that the well-known discrepancy between theoretical and experimental values of these integrals arises from the fact that the quantities obtained experimentally are not true $F_k(3d, 3d)$ integrals. The crystalline potential due to an array of negative ion charge densities is employed to discuss these various effects and their meaning with respect to an essentially molecular treatment.

Carrier Density of AlSb-InSb - See 7938

Carrier Density of GaAs-Ga₂Se₃ - See 7942

Carrier Concentration of Vitreous Materials - See 7949

7927 GENERATION OF FREE CARRIERS IN PHOTOCONDUCTING ANTHRACENE. Part I. by W. Moore (U. North Carolina) and M. Silver (U.S. Army); J. Chem. Phys., Vol. 33, pp. 1671-1676, Dec. 1960

Determination of the source of free carriers in photoconducting anthracene by an investigation of the spatial distribution of trapped electrons is reported. Free carriers are generated in the bulk in addition to electrons that are injected into the anthracene at the negative electrode. The bulk generated carriers cannot come from an intrinsic process, which simultaneous yields a free electron and a free hole. A tentative extrinsic model for the generation of free carriers is proposed in which electrons are injected at the negative electrode, free holes and trapped electrons are generated by the incident radiation in the bulk at impurities or other defects, and free holes are generated by the incident radiation at the positive illuminated electrode. On the basis of these results it is concluded that anthracene is an extrinsic rather than an intrinsic photoconductor.

Field Dependence of Electron-Hole Pair Creation in InSb - See 7934

Measurement of Minority Carrier Lifetime in Transistor Bases - See 8024

7928 INFLUENCE OF DISORDER ON THE LIFETIME OF POSITRONS IN ANTHRACENE by C. Cottini, G. Fabri, E. Gatti, and E. Germagnoli (Lab. Cent. Info. Studio Esperienze, Milan); J. Phys. Chem. Solids, Vol. 17, pp. 65-68, Dec. 1960

The decay features of positrons in anthracene using both single crystals and polycrystals at temperatures ranging between -196°C and 295°C are experimentally investigated. In solid specimens, annihilation lifetime is equal to 3.7×10^{-10} sec independently of the measuring temperature. A notable effect is found near the melting point (218°C), a complex decay appearing at about 210°C. Neutron irradiated specimens show a complex decay even at room temperature.

7929 MONOENERGETIC NEUTRON IRRADIATION OF GERMANIUM by O. L. Curtis, Jr. and J. W. Cleland (Oak Ridge Natl. Lab.); J. Appl. Phys., Vol. 31, pp. 423-427, Feb. 1960

The nature of defects induced in Ge by 14 Mev neutron irradiation, and their comparison with damage produced by neutrons from a fission spectrum are discussed. Measurements of lifetime, Hall effect, and resistivity were made. The electron removal rate in high-resistivity, n-type material is $\sim 8/cm^3$ per incident neutron/cm², measured at 77°K. Lifetime measurements have been made on n- and p-type material. On the basis of simple recombination theory, assuming no variation of capture probabilities with temperature, the results for n-type material indicate that a recombination level is located 0.32 ev above the valence band near the center of the energy gap. Assuming an introduction rate of recombination centers equal to one-half the electron removal rate in n-type material, the following values of recombination capture cross sections are obtained: $\sigma_n = 2.2 \times 10^{-17} \text{ cm}^2$; $\sigma_p = 6 \times 10^{-15} \text{ cm}^2$, the latter value being correct only within about a factor of two. The ratio of the cross sections, σ_p/σ_n , which is independent of the method of determining the number of recombination centers, is ~ 300 , indicating that the recombination centers are negatively charged. The lifetime measurements for p-type germanium are not so readily analyzed. Possible explanations for observed behavior are discussed.

7930 ABSORPTION AND EMISSION SPECTRA OF AN ELECTRON IN A ONE-DIMENSIONAL DEEP TRAP by B. S. Gourary (Johns Hopkins U.) and A. A. Maradudin (U. Maryland); J. Phys. Chem. Solids, Vol. 13, pp. 88-104, May 1960

The wave functions and the energies of the bound states of an electron in a special one-dimensional deep trap are calculated. The only essential approximations made in the course of the treatment are the Born-Oppenheimer approximation for the separation of the electronic and the nuclear motions and the harmonic approximation for the lattice energy. Further approximations are also made, but these are not essential to the calculation and they can be avoided, if necessary. Green's function techniques are employed in the solution of the electronic and the lattice-vibration problems, making possible treatment of both the localized and the extended lattice-vibration modes and their influence on the electronic absorption (emission) spectrum. The first two moments of the absorption and emission spectra are then calculated.

Analysis of Trapping Kinetics of Additively Colored KBr - See 7993

Traps in CdS - See 7951

ELECTRICAL PROPERTIES (Cont'd)

7931 DE HAAS-VAN ALPHEN EFFECT IN GRAPHITE BETWEEN 3 AND 85 KILOGAUSS by W. J. Spry and P. M. Scherer (Nat'l. Carbon); Phys. Rev., Vol. 120, pp. 826-829, Nov. 1, 1960

The de Haas-van Alphen effect in a single crystal of graphite between 3 and 85 kgauss with the c axis of the crystal parallel to the magnetic field is measured. Two periods are observed: 2.05×10^{-5} gauss $^{-1}$ for the electronic component and 1.53×10^{-5} gauss $^{-1}$ for the holes. No new and unexpected oscillations are observed at magnetic fields as large as 100 kgauss.

7932 MEASUREMENT OF MICROWAVE HALL MOBILITIES IN SEMICONDUCTORS by Y. Nishina, S. H. Liu, G. C. Danielson, and R. H. Good, Jr. (Iowa State U.); Bull. Am. Phys. Soc., Ser. II, Vol. 5, pp. 264-265 (A), Apr. 25, 1960

A method of measuring the microwave Hall mobilities in semiconductors was described. This method utilizes a bimodal cavity with a sample attached on a wall. One mode of oscillation is excited externally, and when a steady magnetic field is applied the other mode is induced by the Faraday rotation inside the sample. The relative intensity of the two modes determines the Hall mobility. Theoretical calculations were carried out to obtain the power ratio of the two modes in terms of the Hall mobility, the magnetic field and the dimensions of the cavity and the sample. Measurements were made on n- and p-type Ge samples at X-band frequencies between 29° and 300°K in weak fields ($B\mu \ll 1$). At room temperature the power ratio of the n-type samples followed the field and geometrical dependencies given by the calculations. The p-type samples exhibited the same type of dependence of Hall mobility on magnetic field as found by Willardson et al.

7933 THE CHANGE IN ELECTRON MOBILITY IN INDIUM ANTIMONIDE AT LOW ELECTRIC FIELD by Y. Kanai (Electrical Commun. Lab., Tokyo); J. Phys. Soc. Japan, Vol. 15, pp. 830-835, May 1960

The change in electron mobility in indium antimonide at low electric field, measured by the bridge method at 77°, 201°, and 297°K, is described. At 77°K the electron mobility in high purity indium antimonide decreases with increasing electric field, but increases in impure indium antimonide. At 201° and 298°K the change in electron mobility is too small to be detected. The effect of transverse magnetic field upon the change in electron mobility is also measured. In a transverse magnetic field, the electron mobility in indium antimonide increases with increasing electric field at 77°K, while it decreases at 201°K. At 297°K, the change in electron mobility in a transverse magnetic field is also too small to be measured. To explain the experimental results mentioned above, some considerations of the scattering mechanism of conduction electrons in indium antimonide are applied. It is then concluded that polar scattering in indium antimonide is most important from 77° to about 300°K, that impurity scattering is important at 77°K, and that acoustic scattering takes place at 201°K.

Mobility of Vitreous Materials - See 7949

Mobility of AlSb-InSb - See 7938

Mobility of GaAs-Ga₂Se₃ - See 7942

Phonon Scattering in Nonpolar Crystals - See 7924

Carrier Diffusion in p-n Junctions - See 8008

7934 PROPERTIES OF P-TYPE InSb IN PULSED HIGH ELECTRIC FIELDS by M. C. Steele and M. Glicksman (RCA Labs.); Phys. Rev., Vol. 118, pp. 474-477, Apr. 15, 1960

The results of high electric field experiments on p-type InSb at 77°K are discussed. It is shown that electron-hole pair creation occurs at electric fields greater than 700 v/cm. When a sufficient number of pairs are created the Hall coefficient changes from positive to negative. The question of whether holes or possibly injected electrons initiate the pair creation is examined in detail. An incipient negative resistance effect in transverse magnetic fields and the absence of any self-pinching effects are also discussed.

CONDUCTIVITY

7935 THERMALLY STIMULATED CONDUCTIVITY IN SEMICONDUCTORS by I. I. Boiko, E. I. Rashba, and A. P. Trofimienko (Phys. Inst. UkrSSR, Kiev); Soviet Phys.-Solid State, Vol. 2, pp. 99-107, July 1960

A theory of thermally stimulated conductivity, constructed on the basis of a quite general model of a semiconductor, is presented. It is shown that an analysis of plots of thermally stimulated conductivity for various heating rates allows for the determination of the depth of localized levels. A preliminary comparison of theory and experiment is made.

7936 THE TEMPERATURE DEPENDENCE OF THE CONDUCTIVITY OF DRY CELLULOSE by E. J. Murphy (Rockefeller Inst.); J. Phys. Chem. Solids, Vol. 15, pp. 66-71, Aug. 1960

An experimental investigation of the conductivity of dry cellulose is described. It leads to the following expression for the conductivity: $\sigma = 4.50 \times 10^2 \exp(-30.7 \times 10^3 / RT + 3.55 \times 10^{-10} \exp(-10.6 \times 10^3 / RT)$ where σ is the conductivity in $(\Omega \text{ cm})^{-1}$, R the gas constant, and T the absolute temperature. This has the form usual in the theory of ionic conduction in crystals. From the coefficient of the first term the lattice constant for conduction can be calculated, the value obtained being 5.4 Å. The observed energy in the Boltzmann factor for the first term can be regarded as splitting into a sum of two terms, a dissociation energy of 40.2 kcal/mole and an activation energy for mobility of 10.6 kcal/mole; this gives $(40.2/2) + 10.6 = 30.7$, the observed value. The second term which is due to impurity conduction of some kind, has an activation energy for mobility of 10.6 kcal/mole. This agrees approximately with the activation energy for conduction in ice consequently the second term is regarded as due to conduction in adsorbed water. The first term is regarded as representing volume conduction in which dissociation requires 40.2 kcal/mole, but mobility is governed by the breaking of two hydrogen bonds. The ratio $3.55 \times 10^{-10} / 4.50 \times 10^2 (= 0.79 \times 10^{-12})$ is proportional to the concentration of impurities and is unusually small.

Effect of Oxygen on Conductivity of Bi₂Te_{3-x}Se_x - See 7919

Effects of Impurities in Diodes Upon Rectification - See 8016

7937 INFLUENCE OF THE ELECTRIC FIELD ON THE ELECTRICAL CONDUCTIVITY, HALL COEFFICIENT, AND MAGNETORESISTANCE OF N-TYPE InSb AT LOW TEMPERATURES by L. Chih-ch'ao and D. N. Nasledov (Physicotech. Inst.);

CONDUCTIVITY (Cont'd)

Soviet Phys.-Solid State, Vol. 2, pp. 729-733, Nov. 1960

Deviations from Ohm's law of the electrical conductivity, σ , and the dependence of the Hall coefficient, R , and magneto-resistance, $\Delta\rho/\rho_0$, of n-type InSb on the electric field are discussed. The investigation was conducted at temperatures in the liquid helium range. Transition of electrons from the impurity band to the conduction band, occurring under the influence of the electric field, may explain the observed deviations. On that basis, expressions for σ and R are derived, incorporating an observed temperature dependence.

7938 SOME ELECTRICAL PROPERTIES OF THE AlSb-InSb SYSTEM by Ya. Agaev and D. N. Nasledov (Physicotech. Inst.); Soviet Phys.-Solid State, Vol. 2, pp. 758-760, Nov. 1960

The Hall constant, electrical conductivity, and changes in electrical resistance in a transverse magnetic field for three compositions in the system AlSb-InSb are evaluated. The study was made over a temperature range from approximately 80° to 1000°K. At low temperature, electrical conductivity is practically independent of temperature, while at high temperature, the transition to intrinsic conduction produces a marked increase in conductivity. As the amount of AlSb increases, the transition to intrinsic conduction is displaced toward higher temperatures. The same relationship between the AlSb content and the temperature at which the Hall constant changes from positive to negative was noted. Carrier mobility and density are recorded.

7939 THE ELECTRICAL CONDUCTIVITY OF SODIUM ALUMINOSILICATE GLASSES by G. I. Khvostenko and V. A. Ioffe (Inst. for Chem. of Silicates); Soviet Phys.-Solid State, Vol. 2, pp. 475-481, Sept. 1960

Electrical conductivity of glasses of the system $\text{Na}_2\text{O} \cdot x \text{Al}_2\text{O}_3 \cdot (y - x) \text{SiO}_2$, where x ranges from zero to 1.1 while y is 2, 3, 4, or 6 over the temperature range from 15 to 240°C is discussed. The electrical conductivity depends on the ratio of Al to Si atoms existing in the glass. The hypothesis that a combination of ionic and electronic conduction exists in such glasses is formulated. As the ratio Al/Si increases, the contribution of ions to the conduction decreases while the contribution of electrons increases.

Conductivity Decay in Doped Quenched KCl Crystals - See 7868

Conductivity Type Dependence on Composition in PbTe - See 7849

7940 SPATIAL CORRELATION OF LOW-FREQUENCY CONDUCTIVITY FLUCTUATIONS IN GERMANIUM by D. N. Mirlin (Semicon. Inst.); Soviet Phys.-Solid State, Vol. 2, pp. 927-928, Nov. 1960

Spatial correlation in n-type Ge at low frequency (80 cps) and also at relatively high frequency (4 kc) is discussed. The derivation and application of the correlation coefficient, k , are described. At both frequencies, the value of k was approximately the same. Since correlation at high frequency is due to minority carrier drift, it is assumed that correlation at low frequency is also due to that factor. For one sample subjected to variation in surface treatment, the values of k obtained at two different field intensities are listed.

7941 INVESTIGATION OF THE LOW-FREQUENCY CONDUCTIVITY FLUCTUATIONS IN GERMANIUM WHICH APPEAR ON ILLUMINATION by M. I. Kornfel'd and D. N. Mirlin (Semicon. Inst.); Soviet Phys.-Solid State, Vol. 2, pp. 929-931, Nov. 1960

The nature of, and causes of low-frequency conductivity fluctuations in n-type Ge are discussed. Variations of the rate of both generation and recombination in minority carriers produce the fluctuations usually observed. Compensation of these rates at equilibrium reduces fluctuation to a relatively low intensity. Intensity is increased, however, upon application of an external field. Illumination does not produce low-frequency fluctuation. The need for further study of the mechanism which varies the generation and recombination rates is indicated.

7942 ELECTRICAL CONDUCTIVITY OF GALLIUM ARSENIDE-SELENIDES AT HIGH TEMPERATURES by D. N. Nasledov and I. A. Feltin'sh (Physicotech. Inst.); Soviet Phys.-Solid State, Vol. 2, pp. 755-757, Nov. 1960

The electrical conductivity of six compositions in the system GaAs-Ga₂Se₃ at temperatures ranging from approximately 300 to 1000°K is discussed. The energy gap for each composition was determined from the temperature dependence of the Hall constant. In pure gallium selenide (Ga₂Se₃), the temperature dependences of the thermoelectric power and the Hall effect indicate p-type conduction is prominent; intrinsic conduction begins at 750°K. The temperature dependence of mobility and carrier density in Ga₂Se₃ are discussed.

7943 LOW-TEMPERATURE IMPURITY CONDUCTION IN N-TYPE SILICON by K. R. Atkins, R. Donovan, and R. H. Walmsley (U. Pennsylvania); Phys. Rev., Vol. 118, pp. 411-414, Apr. 15, 1960

Measurement of Hall coefficients and electrical resistivities down to liquid helium temperatures for silicon specimens containing about 10¹⁷ phosphorus impurities per cm³ and about 10¹⁵ boron impurities per cm³ is reported. The density of minority impurities was determined during the preparation of the ingots, rather than deduced from the electrical measurements themselves. The results, extremely sensitive to the density of minority impurities, are discussed in relationship to the theories of Conwell, Mott, and Price.

7944 ELECTRICAL CONDUCTIVITY OF HIGH VANADIUM PHOSPHATE GLASS by M. Munakata (Electrotech. Lab., Tokyo); Solid-State Electronics, Vol. 1, pp. 159-163, July 1960

The electrical conductivity of high vanadium phosphate glass as a function of composition is discussed. The conductivity varies with the concentration of V⁴⁺ if the concentration of total vanadium is kept constant and has a maximum for a certain critical value of V⁴⁺/V_{total}. These results indicate that the conduction is due to valence-electron exchange between V⁴⁺ and V⁵⁺. When basic metal oxide (the third component of the glass) is varied, a simple relation between the maximum conductivity of the glass and the "cationic field strength" of the metal is found. By this means, it is possible to obtain semiconducting glass with a room-temperature resistivity of the order of 10³ Ω-cm.

Conductivity of Pyrographite - See 7948

7945 THERMAL AND ELECTRODYNAMIC ASPECTS OF THE SUPERCONDUCTIVE TRANSITION PROCESS by W. H. Cherry and J. I. Gittleman (RCA Labs.); Solid-State Electronics,

CONDUCTIVITY (Cont'd)

Vol. 1, pp. 287-305, Sept. 1960

Derivations of the formulas describing the velocity of propagation of the superconductive transition process and of the relations between current, bath temperature and the quenching characteristics of thin wires and films are outlined and necessary approximations are indicated. In many cases, such as expulsion of or quenching by an external magnetic field or in certain extreme conditions of current quenching and recovery, the chief aspects of the process are electrodynamic. While the London equations and boundary conditions give a complete characterization of the electrodynamic properties of the superconductor, they are shown not to apply to the transition process itself. Some considerations for an appropriate generalization of these equations and of those of more recent theories are given. A few simple, heuristic models are used to suggest specific equations.

7946 CRITICAL FIELD FOR SUPERCONDUCTIVITY IN NIOBIUM-TIN by R. M. Bozorth, A. J. Williams, and D. D. Davis (Bell Labs.); Phys. Rev. Lett., Vol. 5, p. 148 (L), Aug. 15, 1960

Measurement of the magnetization of Nb_3Sn at 4.2°K as a function of applied magnetic field is discussed. The magnetic moment per gram of the sample (a rod about 2 cm long and 4 mm in diameter with rounded ends) is measured by pulling the specimen from one search coil to another in a constant field, the two search coils being connected in series opposition to a ballistic galvanometer. Measurements are made in both increasing and decreasing fields. In the former, the general shape of the magnetization curve is that observed in a hard superconductor. The critical field necessary for the suppression of all superconductivity is about 70,000 oersteds.

OTHER ELECTRICAL PROPERTIES

7947 OBSERVATIONS OF SURFACE TRANSVERSE MAGNETORESISTANCE EFFECTS ON N-TYPE GERMANIUM by W. A. Albers, Jr. and J. E. Thomas, Jr. (Wayne State U.); J. Phys. Chem. Solids, Vol. 14, pp. 181-185, July 1960

New techniques of preparing thin semiconductor samples of uniform thickness which allow for high sensitivity in the measurement of surface effects are described. Measurements of the surface transverse magnetoresistance effect first reported by Zemel and Petritz are extended to lower resistivity n-type material of different crystallographic orientation. Data are obtained for directions of the magnetic field both in and perpendicular to the plane of the thin films. Large swings in surface potential are accomplished by employing an HF rinse prior to ambient cycling. Observations of surface transverse magnetoresistance effects as a function of surface potential at fixed magnetic field strengths, and as a function of magnetic field strength at fixed surface potentials are reported. The analysis of the data requires a general solution of Poisson's equation which does not employ the semi-infinite geometry in order to ascertain values of the electric field at the surface of a semiconductor. This general solution is presented for several special cases of sample thickness and resistivity and the deviations from the semi-infinite geometry solutions are delineated. Finally, the observations of the surface transverse magnetoresistance effect are discussed in view of the present theoretical model of the surface.

Magnetoresistance of InSb - See 7937

7948 GALVANOMAGNETIC PROPERTIES OF PYROGRAPHITE by C. A. Klein (Raytheon); Bull. Am. Phys. Soc., Ser. II, Vol. 5, pp. 187-188 (A), Mar. 21, 1960

Galvanomagnetic data taken on specimens of pyrographite deposited at temperatures ranging from 1700° to 2600°C were reported. At room temperature, the ratio of conductivities in the (a,b) and (c) directions of the better samples exceeded 2000, with a resistivity in the hard direction of $0.5 \text{ ohm}\cdot\text{cm}$. The temperature coefficients appeared to be negative in the investigated temperature range of 50°K to 1250°K . Room temperature magneto-resistivities were measured with applied transverse magnetic fields of 2 to 25 kgauss. A rather pronounced magnetoresistance effect of the type $\Delta\rho/\rho = CH^x$, with $1 < x < 2$, occurred in the basal plane and provided indications on the carrier mobilities. Hall effect of specimens deposited at or above 2500°C appeared to be n-type. In all other cases, it seemed that the conduction process in the basal plane is determined by holes with concentrations of the order of 10^{19} cm^{-3} .

Galvanoelectric Effect in Crystals - See 7905

7949 HALL EFFECT IN VITREOUS MATERIALS OF THE $\text{TiSe}-\text{As}_2(\text{Se},\text{Te})_3$ SYSTEM. Part II. by B. T. Kolomiets and T. F. Nazarova (Leningrad Inst. of Phys. Tech.); Soviet Phys.-Solid State, Vol. 2, pp. 369-370, Sept. 1960

Values for the concentration and mobility of current carriers at room temperature, for compositions within the system, are presented. The mobility did not vary with composition. The data was obtained by extrapolation from measurements of the temperature dependence of the Hall effect. The Hall effect was measured at room temperature on the three lowest resistance compositions of the system. The sign of the Hall effect indicated conduction was by electrons; thermo-emf measurements, however, indicated conduction was by holes.

Hall Effect in AlSb-InSb - See 7938

Hall Coefficient of InSb - See 7937

Measurement of Low Temperature Hall Coefficient in Si - See 7943

7950 ENTROPY AND CROSS-RELAXATION IN SPIN SYSTEMS by A. E. Siegman (Stanford U.); Phys. Rev., Vol. 119, pp. 562-563, July 15, 1960

The fact that if cross-relaxation and harmonic cross-relaxation between nuclear and electronic magnetic resonance transitions can be described in thermodynamic terms using spin temperatures and that the results can be predicted in a simple fashion by maximizing the spin entropy is discussed. Heretofore, the appropriate cross-relaxation rate equations have generally been invoked to predict the result observed. A simple approximation for the entropy of a multilevel spin system in terms of the population differences Δ_{ij} is derived and applied to a typical cross-relaxation problem.

7951 CADMIUM SULFIDE SURFACE NOISE by J. J. Brophy (Armour Res. Found.); Bull. Am. Phys. Soc., Ser. II, Vol. 5, p. 186 (A), Mar. 21, 1960

Previous measurements of current noise and photoconductivity of CdS single crystals to determine the frequency factor and energy distribution of shallow traps were extended. 4400 A illumination was used to obtain results characteristic of the crystal surface. The noise data determined the depth to which

OTHER ELECTRICAL PROPERTIES (Cont'd)

electron-hole pairs diffuse as 30 microns, which is in good agreement with the ambipolar diffusion length recently reported, and established that the energy depth of the discrete traps below the conduction band is the same in this surface region as in the bulk of the crystal. The current noise spectrum was observed to follow an $f^{-3/2}$ diffusion law until retrapping noise became dominant at about 550 cps. Experimentally determined transition frequencies were noted to be in good agreement with those predicted from the photoconductive time constants. Trap densities in the surface regions were an order of magnitude greater than those in bulk and the frequency factors were observed to be in the range 10^8 to 10^9 sec^{-1} .

Thermal Noise of Semiconductor Hall Generators - See 8034

MAGNETIC PROPERTIES

1952 ADIABATIC DEMAGNETIZATION AND SPECIFIC HEAT IN FERRIMAGNETS by J. E. Kunzler, L. R. Walker, and J. K. Galt (Bell Labs.); Phys. Rev., Vol. 119, pp. 1609-1614, Sept. 1, 1960

The specific heat of yttrium iron garnet (YIG) at 1.45°K as a function of magnetic field from zero to 18 kilo-oersteds is measured. It is found to drop about 30 per cent over this field range as the field is increased. Adiabatic temperature changes, ΔT , were observed during magnetic cycles over various field intervals in the range from 3 to 18 kilo-oersteds, and at various temperatures between 1 and 4°K. The experimental values of ΔT and the specific heat fit the predictions of spin-wave theory to within experimental error. The data are sufficiently extensive to provide a useful test of spin-wave theory as well as checks on the consistency of the data itself between the two types of observations. Values of various parameters which characterize the thermal and magnetic properties of YIG are determined from this investigation to have the following values: Landau-Lifshitz exchange constant $A = 4.3 \times 10^{-7} \text{ erg/cm}^2$; Debye temperature $\theta = 510^\circ\text{K}$. The serious effect of magnetic impurities on investigations of this sort is pointed out.

1953 SENSITIVE FLUX MEASUREMENT OF THIN MAGNETIC FILMS by H. J. Oguey (IBM); Rev. Sci. Instr., Vol. 31, pp. 701-709, July 1960

A study of the flux distribution around a thin magnetic film specimen, permitting determination of the merits of various pickup coil configurations as well as the form which optimizes the signal-to-noise ratio is reported. The various disturbing voltages and ways to eliminate them are examined. Optimization of the amplifier noise figure, proper choice of the integration network, dc restoration, and hum synchronization for reduction of output noise after integration and amplification. Two instruments built according to these principles are described. The first has a single wire pickup and is well suited for measurement of the flux distribution around a thin magnetic film and for experiments in vacuum at elevated temperatures; the second is more flexible and sensitive. By using different pickup coils covering a frequency range from 50 cps to 10 kc its sensitivity is sufficient to measure flux values of $2 \times 10^{-12} \text{ v-sec}$ at a frequency of 500 cps.

Domain Structure of MnBi Films During Heat Treatment - See 7873

7954 THE SIZE EFFECT OF FERRITE SPHERES by W. Hauser and L. Brown (Lincoln Lab.); Quart. J. Mech. Appl. Math., Vol. 13, pp. 257-271, Aug. 1960

An integral equation technique to obtain an approximate formula for the apparent susceptibility of a small ferrite sphere of radius "a" within a microwave cavity is described. The first-order effect of a plane wall is also considered using the quasi-stationary approximation that the fields within the sphere are uniform. It is shown that for spheres at a distance of the order of one wavelength λ away from the cavity wall, the wall contributes to the apparent susceptibility of the sphere terms of the order of $(ka)^3$ and higher, where $k = 2\pi/\lambda$, justifying to order $(ka)^3$ the use of free space calculations in cavity problems to estimate the fields within the sphere.

Measurement of Permeability in Millimeter Range - See 7921

7955 MAGNETIZATION OF A DILUTE SUSPENSION OF A MULTIDOMAIN FERROMAGNETIC by C. P. Bean and I. S. Jacobs (GE Res. Lab.); J. Appl. Phys., Vol. 31, pp. 1228-1233, July 1960

The similarity between the observed magnetization curve of a dilute suspension of carbonyl iron powder, type E, and that which one would derive from consideration of a dilute assembly of randomly oriented, single-crystal, multidomain spheres is discussed. The deviations are in the directions expected from the effects of stress and nonspherical clumping. The effects of packing and the applicability of various laws of approach to saturation are discussed.

Theory of Elastic Switching in Square Loop Materials - See 8039

Thermomagnetic Effect in Crystals - See 7905

7956 MAGNETIC ANISOTROPY IN SINGLE-CRYSTAL THIN FILMS by E. L. Boyd (IBM); IBM J. Res. and Dev., Vol. 4, pp. 116-129, Apr. 1960

The growing of thin single-crystal films of Ni, Fe, Ni-Fe and Ni-Co by vacuum deposition onto heated rock salt is described. The cubic crystalline anisotropy constant K_1 of these films has been measured at room temperature by a torque method. In the case of the Ni-Fe alloys, K_1 is found to be the same for thin films as for bulk materials of the same composition. The measured anisotropy in the Ni-Co films differs quantitatively but has the same qualitative variation with composition as is reported for bulk crystals. The results of one magnetic annealing experiment on a 75 per cent Ni - 25 per cent Fe film lends support to the short-range ordering model of uniaxial anisotropy in alloys. Pure nickel films exhibit a pronounced uniaxial anisotropy superimposed on the crystalline anisotropy. This uniaxial term disappears after the film is removed from the substrate, indicating that its origin is in an anisotropic stress in the deposited film.

7957 THE THICKNESS DEPENDENCE OF THE DOMAIN STRUCTURE OF MAGNETOPLUMBITE by J. Kaczer and R. Gemperle (Czech. Acad. Sci.); Czech. J. Phys., Vol. 10B, No. 7, pp. 505-510, 1960

The changes in domain structure as a function of crystal thickness in artificial magnetoplumbite crystals are studied. The thickness dependence of the width of the domains follows the theoretical half-power law up to thicknesses of about 10μ . Above 10μ the exponent is 0.633. The energy density of the Bloch walls $\gamma = 4.82 \text{ erg cm}^{-2}$ and the exchange constant

MAGNETIC PROPERTIES (Cont'd)

$A = 0.66 \times 10^{-6}$ erg cm⁻¹ are calculated on the basis of the above measurements.

7958 SIDEWISE MOTION OF "c" DOMAIN NUCLEATION CENTERS IN BaTiO₃ by G. L. Link (Bell Labs.); Bull. Am. Phys. Soc., Ser. II, Vol. 5, p. 202 (A), Mar. 21, 1960

A new effect, observed when a biased square wave field was applied to a "c" domain crystal of BaTiO₃ containing a few "a" domains, was reported. When the field was applied and the sample was viewed with a polarizing microscope, there appeared a large number of small "c" domains which moved horizontally in well-defined paths. The motion occurred only above "a" domains and was in straight line paths perpendicular to the "a" domain edges. The sidewise velocity of the "c" domains above a given "a" domain varied directly as the field's frequency and exponentially as the reciprocal of the field-on-the-low-field-pulse. A model invoking a novel displacement which a spike-shaped "c" domain undergoes when it penetrates an "a" domain, thus accounting for these observations, was proposed. The effect was used to estimate the velocity of propagation in the forward direction of nucleated steps on the sides of the "c" domains. This velocity was found to be on the order of 1 cm/sec at room temperature and is believed to be independent of field.

7959 FERROMAGNETIC RESONANCE IN POLYCRYSTALLINE FERRITES USING CIRCULARLY POLARIZED RADIATION by R. J. Zeender and E. Schloemann (Raytheon); J. Appl. Phys., Vol. 31, pp. 1112-1116, June 1960

Evidence showing that the use of circularly polarized radiation facilitates a clear identification of the peaks of resonance curves observed in polycrystalline ferrites is presented. In cubic materials the central peak, arising from grains which have a [110] direction aligned with the dc field, is partially excited by both senses of circular polarization, whereas the two outer peaks are excited only by the positive sense of circular polarization. Experimental results obtained in the compensation region of the nickel ferrite-aluminate system agree well with theoretical predictions. These results rule out the possibility that the additional absorption peaks are due to an exchange resonance.

7960 SINGLE CRYSTALS OF MAGNESIUM-MANGANESE FERRITES WITH A NARROW FERROMAGNETIC RESONANCE ABSORPTION CURVE by K. P. Belov, V. F. Belov, and A. A. Popova (Inst. Cryst.); Soviet Phys.-JETP, Vol. 2, pp. 1372-1373 (L), Dec. 1960

Measurements of resonance absorption linewidth in a group of single crystal magnesium-manganese ferrites is discussed. The crystals were grown by the Verneil method and machined into spheres 0.8 - 1 mm in diameter. The surfaces of the spheres were polished and the measurements were made in a short-circuited waveguide section of 9470 Mc. The linewidth ΔH varied between 12 to 18 oe, with the narrowest linewidth found in a ferrite having the composition (by weight) 8.4 MgO, 23.9 MnO, and 67.5 Fe₂O₃. The anisotropy of ΔH was measured at room temperature in the [110] plane in a ferrite with the composition 6.9 MgO, 37.3 MnO, and 55.9 Fe₂O₃. A maximum in ΔH was observed along [111] (axis of easy magnetization) and a minimum in ΔH was observed along [100] (axis of difficult magnetization). The measured anisotropy of ΔH corresponds to the phenomenological calculation of Skrotzkii and Kurbatov.

Line-Width Narrowing in Microwave Ferrites - See 7896

7961 MECHANISM OF ANTFERROMAGNETISM IN DILUTE ALLOYS by A. W. Overhauser (Ford Motor); J. Phys. Chem. Solids, Vol. 13, pp. 71-80, May 1960

A mechanism for the antiferromagnetic ordering of a dilute paramagnetic solute in a metal is proposed and its relation to the phenomena that occur in copper-manganese alloys is discussed. Long-range antiferromagnetic order results from a static spin-density wave in the electron gas of the metal. This new state of the gas is dynamically self-sustaining as a result of the exchange potentials arising from the spin-density distribution. The paramagnetic solute atoms are then oriented by their exchange interaction with the spin-density wave. The resulting interaction energy more than compensates the increase in energy associated with the formation of the spin-density wave. The theory predicts correctly the magnitude and concentration-dependence of the critical temperature, the anomalous low-temperature specific heat and the anomalous electrical and magnetic properties of the alloys.

Theory of Antiferromagnetism - See 7998

7962 THE ANTIFERROMAGNETIC SUSCEPTIBILITY AT MODERATE FIELDS by J. van den Broek and C. J. Gorter (Kamerlingh Onnes Lab.); Physica, Vol. 26, pp. 638-646, Aug. 1961

Calculation of the isothermal differential susceptibility of an antiferromagnetic substance in a moderately strong magnetic field of arbitrary direction using the molecular field model as given by Gorter and van Peski-Tinbergen is presented. The results are compared with the formulae of Nagamiya and Yosida and with experimental results on hydrated copper and manganese chlorides.

7963 THE SPECIFIC HEATS OF TWO POLYMORPHIC FORMS OF MANGANOUS SULPHIDE, AND THE INFERRRED POSSIBILITY OF ANTIFERROMAGNETIC ORDERING IN STACKING FAULTS by W. S. Carter (Central Electricity Generating Board, England); Proc. Phys. Soc., Vol. 76, pp. 969-978, Dec. 1960

The results of the measurement of the specific heats of two samples of manganous sulfide in the range 76°K to 250°K are reported. The samples used in the measurements were zincblende and wurtzite structures. The large anomaly in the specific heat of one sample confirms the onset of antiferromagnetic ordering in the zincblende structure at 100°K. The absence of a similar large anomaly in the second specimen above 76°K shows that the wurtzite structure remains unorderd at this temperature, but there is a small anomaly at 110°K. A study of the x-ray powder photographs and the calculation of Madelung's constant for several possible types of stacking faults show that this anomaly in the specific heat is consistent with magnetic ordering within stacking faults. The possibility that the presence of ordered stacking faults may depress and smooth out the Néel temperature of the rest of the sample is also considered, and is suggested as a possible explanation for the absence of a Néel temperature above 76°K in the second specimen.

Antiferromagnetic Interaction Shift in Mn-ZnF₂ Crystals - See 7980

7964 STUDY OF MAGNETIC AFTER-EFFECT IN MAGNESIUM MANGANESE FERRITES by S. Krupicka (Inst. Tech. Phys., Prague); Czech. J. Phys., Vol. 10B, No. 11, pp. 782-810, 1960

An investigation of the magnetic after-effect caused by the

MAGNETIC PROPERTIES (Cont'd)

diffusion of electrons in MnMg ferrites of the series $Mg_xMn_{1.15-x}Fe_{1.85}O_4+y$ is reported. Measurements are also carried out on a sample of $MgFe_2O_4+y$ ($\gamma < 0$). By combining two methods, i.e., (a) investigation of the disaccommodation of initial permeability at different temperatures and (b) measurement of the displacement of the maximum of the temperature dependence of $\tan \delta$ with frequency, it is possible to study the relaxation processes whose time constants are between 0.5 sec and several hours, or between 10^{-4} and 10^{-7} sec. It is found that the processes taking place at low temperatures and studied by method (a) differ from those observed at high temperatures by method (b) particularly in the lower activation energies and greater dispersion of the time constants. In addition to these two main relaxation processes, a weak relaxation superposed over the main disaccommodation is found in ferrites with non-zero manganese content. An analysis of the intensity of different relaxation effects reveals participation of Mn ions in these relaxation effects and it is found that both main relaxations are probably equivalent as regards the final steady state, to the creation of which they lead; they differ, however, in the mechanism of electron diffusion by which this state is realized. The main features of the different diffusion mechanisms are discussed.

7965 CROSS RELAXATION AND MASER PUMPING BY A FOUR SPIN FLIP MECHANISM by P. Sorokin, G. J. Lasher, and I. L. Gelles (IBM); Quantum Electronics, Columbia U. Press, New York, 1960, pp. 293-297

The four spin flip mechanism is discussed. The paramagnetic resonance of nitrogen centers in diamond was studied to determine the existence of this process. For such a mechanism to exist, when T_{21} is much less than the relaxation times of the system, the application of the pump to the center line of the nitrogen spectrum should make the absorption at either satellite drop to zero. If the pump is applied to one of the satellites, the center line absorption should reduce to $3/5$ its thermal equilibrium value and the absorption at the other satellite should increase by a factor of $6/5$. This behavior was observed at liquid helium temperatures in diamonds containing the largest concentration of nitrogen centers. It is pointed out that the four spin flip transition can be used in special cases to establish cw maser operation by inverting the population of one of the satellite lines.

7966 EXCHANGE INTERACTION AND CUBIC CRYSTAL FIELD SPLITTING PARAMETER OF Fe^{3+} IN SPINEL STRUCTURE by Y. Sugiura (Electrotech. Lab.); J. Phys. Soc. Japan, Vol. 15, pp. 1217-1222, July 1960

Measurement of the line widths of paramagnetic resonance absorption of Fe^{3+} ions in $MgAl_2O_4$ and $ZnAl_2O_4$ polycrystals and of Mn^{2+} ions in $ZnAl_2O_4$, having the same spinel crystal structure as ferrite, as a function of concentration is reported. The cubic crystal field splitting parameters α of the Fe^{3+} ion at A- and B-sites are determined from the line widths extrapolated to zero concentrations: $\alpha_A = 1.0 \times 10^{-2} \text{ cm}^{-1}$ and $\alpha_B = 3.1 \times 10^{-2} \text{ cm}^{-1}$. On the other hand, the magnitudes of the exchange integrals between Fe^{3+} ions in A- and B-sites or in B- and B-sites are estimated from the decrease of line width due to exchange narrowing as the concentration increases, namely, $J_{AB}/g\beta = 1.32 \times 10^5 \text{ oe}$ and $J_{BB}/g\beta = 1.90 \times 10^3 \text{ oe}$. The Curie temperatures obtained from the exchange integral are in agreement with the Curie temperatures of Mg-ferrite and Zn-ferrite.

7967 NUCLEAR QUADRUPOLE SPIN-LATTICE RELAXATION IN ALKALI HALIDES by E. G. Wikner, W. E. Blumberg, and E. L. Hahn (U. California); Phys. Rev., Vol. 118, pp. 631-639, May 1, 1960

Measurement of nuclear quadrupole spin-lattice relaxation times in alkali halide crystals by the pulsed magnetic resonance technique is reported. Measurements were made on Na^{23} in $NaCl$, $NaBr$, and NaI ; Cl^{35} in $NaCl$ and KCl ; $Br^{79,81}$ in $NaBr$, KBr , $RbBr$, and $CsBr$; Rb^{87} in $RbCl$ and $RbBr$; and I^{127} in NaI , KI , and CsI . Over the temperature range of 298° to $195^\circ K$ the relaxation times are inversely proportional to the square of the absolute temperature. The data are compared to relaxation times calculated from an ionic crystal model of Van Kranendonk and a covalent model of Yosida and Moriya. The ionic model is modified to include the interaction between the nuclear quadrupole moment and the electric field gradient due to electric dipole moments associated with optical modes of vibration. Neither of these models alone predicts the experimental relaxation times for all cases; rather, a combination of the two effects is required. The modified ionic model applies reasonably well to crystals which contain the lighter ions.

7968 SPIN-LATTICE RELAXATION IN NEODYMIUM ETHYL-SULPHATE AT LIQUID HELIUM TEMPERATURES by J. J. Daniels and K. E. Rieckhoff (U. Brit. Columbia); Can. J. Phys., Vol. 38, pp. 604-615, May 1960

Use of the optical Faraday effect to measure instantaneous magnetization in neodymium ethylsulphate is reported. The spin populations are disturbed by pulses of microwave power and by adiabatic magnetization and demagnetization and the approach to equilibrium is studied. The relaxation is found to be exponential and spin lattice relaxation times are measured for temperatures between $1.3^\circ K$ and $4.2^\circ K$ and for magnetic fields between 80 and 6000 oersteds. The relaxation time is found to decrease with increasing magnetic field and to vary with temperature approximately as $1/T^3$. No dependence of relaxation time on pulse length is found.

7969 SPIN-LATTICE RELAXATION TIMES IN RUBY AT 34.6 Gc by J. H. Pace, D. F. Sampson, and J. S. Thorp (Roy. Radar Estab.); Proc. Phys. Soc., Vol. 76, pp. 697-704, Nov. 1960

Measurements of spin-lattice relaxation time in ruby at 34.6 Gc by a pulse saturation method at temperatures from 1.4° to $90^\circ K$ are reported. With weak concentrations the values for the first-order transitions (e.g. 22 msec at $4.2^\circ K$) are of the same order of magnitude as those reported at lower frequencies, and the variation of relaxation time with temperature is in fair agreement with theory. A successive increase in relaxation time with the order of the transition, pronounced at $1.4^\circ K$, decreases with increasing temperature, and at about $77^\circ K$ a common value of about 44 μ sec is obtained for all transitions. The main effects of increasing concentration are to reduce the relaxation time and to alter its temperature dependence.

7970 SPIN RELAXATION IN RUBY by R. A. Armstrong and A. Szabo (Natl. Res. Coun., Ottawa); Bull. Am. Phys. Soc., Ser. II, Vol. 5, p. 344 (A), June 15, 1960

Measurements of spin relaxation in ruby (0.05 per cent nominal chromium concentration) near 3 kMc, made by observing the increase of susceptibility with time following saturation by a single pulse, were reported. In the nitrogen range the relaxation was described by a single exponential; the relaxation varies with temperature as T^{-7} and is independent of θ , the angle be-

MAGNETIC PROPERTIES (Cont'd)

tween the crystal axis and the magnetic field. Measurements made at 4.2°K and 1.6°K for the ($+\frac{1}{2} \leftrightarrow -\frac{1}{2}$) transition as a function of θ were also given. In this temperature range harmonic coupling is a predominant feature, pure spin-lattice relaxation being observed only for limited ranges of θ . Coupling was observed for ratios of the harmonic frequency to signal frequency of 2, 3/2, and 1/2. At harmonic points very long time constants were observed in addition to the spin-lattice relaxation time and the harmonic energy sharing time.

7971 SOME MEASUREMENTS OF THE DECAY OF PARAMAGNETIC SATURATION IN SYNTHETIC RUBY by J. C. Gill (Roy. Radar Estab.); *Quantum Electronics*, Columbia U. Press, New York, 1960, pp. 333-336

Measurement of the decay of paramagnetic saturation in synthetic ruby by observing the return of resonance absorption after the application of a "saturating" pulse of microwave energy is discussed. The measurements were made on seven samples of ruby containing Cr concentrations between 0.014 per cent and 0.89 per cent at liquid nitrogen temperature. The decay curves were found to have the form $A = A_0 (1 - \exp -t/T)$, where A is the absorption at a time t after the end of the saturating pulse, A_0 is the absorption when the recovery from the pulse is complete, and T is the relaxation time. No dependence of T on the length of the saturating pulse was found for pulses up to the maximum available length of 5 msec. The relaxation times were measured for the $-\frac{1}{2} \rightarrow +\frac{1}{2}$ transition and for the $-3/2 \rightarrow -\frac{1}{2}$ transition at liquid nitrogen temperature and for the $-\frac{1}{2} \rightarrow +\frac{1}{2}$ transition in ruby containing approximately 0.04 per cent Cr at 5 different temperatures.

7972 NUCLEAR MAGNETIC RESONANCE IN ALKALI ALLOY SYSTEMS NaK AND NaRb by L. Rimal and N. Bloembergen (Harvard U.); *J. Phys. Chem. Solids*, Vol. 13, pp. 257-270, June 1960

The Knight shift K in liquid NaK and NaRb systems, shown to be a linear function of the relative Na-concentration $1-C$, is considered. The relative variation K^{-1} ($\partial K / \partial C$) = 0.361 for Na^{23} in NaK, = 0.518 for Na^{23} in NaRb and = 0.270 for Rb^{87} in NaRb. An interpretation in terms of the scattering theory of conduction electrons is given. The line width of the Na^{23} and Rb^{87} resonances is a nonlinear function of C . It is 5 times larger in the Rb-rich alloys than in the Na-rich alloys. This result can be explained by the electron-coupled spin exchange interaction between different nuclei. The fact that these spin-spin interactions do not average to a small value in the liquid metal necessitates the postulate of a long range character for the electron-coupled interaction. The Knight shift and line width in solid terminal solutions have also been observed and compared with theory. The experiments show that nuclear magnetic resonance is particularly well suited to determine phase diagrams of alkali alloy systems.

7973 KNIGHT SHIFT IN TANTALUM METAL by L. H. Bennett (Nat'l. Bu. Stand.) and J. I. Budnick (IBM Watson Lab.); *Bull. Am. Phys. Soc.*, Ser. II, Vol. 5, p. 242 (A), Apr. 25, 1960

Observations of the nuclear magnetic resonance of Ta^{181} in tantalum metal at 6.092 Mc in a magnetic field of 11,820 gauss were reported. The Knight shift, relative to KTaO_3 , was 1.1 per cent. The measurements were made at the National Bureau of Standards with a Varian wide line spectrometer at room temperatures. The sample consisted of a stack of foils of tantalum metal prepared by heating in vacuum at 2500° to

2800°C. The interaction between the very large electric quadrupole moment of Ta^{181} and random internal electric field gradients arising from various crystal defects, notably interstitial impurities, probably account for the fact that the nuclear magnetic resonance was previously observed in the bcc structure of tantalum metal. The use of foils permitted annealing and degassing at higher temperatures than are possible with powdered specimens in which sintering may occur.

7974 DEPENDENCE UPON VOLUME OF NUCLEAR QUADRUPOLE INTERACTIONS IN CRYSTALS by R. A. Bernheim and H. S. Gutowsky (U. Illinois); *J. Chem. Phys.*, Vol. 32, pp. 1072-1082, Apr. 1960

The electric quadrupole splitting of Na^{23} nuclear magnetic resonance measured in single crystals as a function of pressure and temperature for NaNO_3 , and as a function of temperature for NaBrO_3 is reported. It is found that the electric field gradient at the sodium nuclei varies as $V^{-3.8}$ in NaNO_3 and as $V^{-2.0}$ in NaBrO_3 . These results, together with the previously reported $V^{-1.9}$ dependence for Na^{23} in NaClO_3 , are compared with theoretical values computed from point charge models for the crystal lattices. It is concluded that the large volume dependence in NaNO_3 arises from the anisotropic thermal expansion and compressibility of the hexagonal crystal plus the retention of size and configuration of the NO_3^- group. The experimental results for NaClO_3 can be explained in the same manner assuming a rigid ClO_3^- group; however, this model does not account for the V^2 dependence of the Na^{23} quadrupole coupling observed in NaBrO_3 . The assumed rigidity of the ClO_3^- group is supported by the small volume dependence, $V^{-0.10}$, found for the Cl^{35} quadrupole coupling in NaClO_3 , and also by calculations of the interionic contribution to the field gradient at the chlorine nuclei in NaClO_3 and KClO_3 .

7975 PARAMAGNETIC RESONANCE OF V^{4+} IN TiO_2 by H. J. Gerritsen and H. R. Lewis (RCA Labs.); *Phys. Rev.*, Vol. 119, pp. 1010-1012, Aug. 1, 1960

The paramagnetic spectrum of vanadium in TiO_2 observed at 10.14 and 22.68 kMc/sec is discussed. An analysis of the data indicates that the spectrum is due to single d electrons of tetravalent vanadium ions located at titania sites in the lattice. The calculated values of the components of the g tensor and the hyperfine interaction constant are: $g_x = 1.915$, $g_y = 1.912^5$, $g_z = 1.956^5$, $A_x = 0.00315 \text{ cm}^{-1}$, $A_y = 0.0043 \text{ cm}^{-1}$ and $A_z = 0.0142 \text{ cm}^{-1}$. The axes of the magnetic coordinate system of the two non-equivalent ions per unit cell are: $\{\bar{1}, 1, 0\}$, $\{0, 0, 1\}$, $\{1, 1, 0\}$, $\{0, 0, 1\}$, $\{\bar{1}, 1, 0\}$.

7976 PARAMAGNETIC AND OPTICAL SPECTRA OF YTTERBIUM IN THE CUBIC FIELD OF CALCIUM FLUORIDE by W. Low (Hebrew U.); *Phys. Rev.*, Vol. 118, pp. 1608-1609, June 15, 1960

A paramagnetic resonance spectrum of Yb^{3+} in CaF_2 at 20°K and 3 cm wavelength is reported. The spectrum is described by a cubic spin Hamiltonian $\mathcal{H} = g\beta\mathbf{H}\cdot\mathbf{S} + AS\cdot\mathbf{I}$ with $g = 3.426 \pm 0.001$, $S = \frac{1}{2}$, $A^{171} = (886.5 \pm 1.5) \times 10^{-4} \text{ cm}^{-1}$, $A^{173} = (243.2 \pm 0.4) \times 10^{-4} \text{ cm}^{-1}$, $I^{171} = \frac{1}{2}$, $I^{173} = \frac{5}{2}$. The ratio of magnetic moments is $\mu^{173}/\mu^{171} = 1.374 \pm 0.005$. The optical spectrum shows lines at 9774A, 9770A, 9763A, and more diffuse and unresolved bands at 9080 and 12730A. The paramagnetic spectrum is explained as arising from the Γ_7 doublet. The other levels are removed by at least a few cm^{-1} leading to an isotropic g value of 3 Λ or 24/7 for the lowest Γ_7 level.

OPTICAL PROPERTIES

Polarized Light Determination of Optical Constants of Se Crystals - See 7997

7977 OPTICAL PROPERTIES OF PARAMAGNETIC SOLIDS by W. Low (Hebrew U.); Quantum Electronics, Columbia U. Press, New York, 1960, pp. 410-427

The spectra of the iron and rare earth groups in different crystallographic symmetries are discussed. The main methods and the results of energy level calculations are summarized and the intensity and linewidth of many of these transitions are discussed.

Magneto-Optic Effect in Ge - See 7909

Optical Absorption Method in Measurement of Charge Densities - See 7926

7978 SPECTRUM OF Yb^{3+} IN YTTRIUM GALLIUM GARNET by R. Pappalardo and D. L. Wood (Bell Labs.); J. Chem. Phys., Vol. 33, pp. 1734-1742, Dec. 1960

The optical absorption at various temperatures of an ytterbium-doped yttrium gallium garnet is reported. The effect of a cubic and rhombic crystal field on the splitting of the free-ion levels is calculated. A tentative interpretation of the fine details of the spectrum is given.

7979 ABSORPTION LINES OF Cr^{3+} IN RUBY by W. Low (Hebrew U.); J. Chem. Phys., Vol. 33, pp. 1162-1163, Oct. 1960

The line spectrum of chromium in ruby is investigated. New lines are found at 14,795, 14,950, and 15,178 cm^{-1} . These lines are identified as belonging to the $2F_1$ triplet. Similarly, a line at 21,352 cm^{-1} is assigned to the $2F_2$ triplet. It is shown that these levels originate from the $2G$ and $2D$ levels, respectively, with considerable admixture from the $2H$ level.

7980 THE OPTICAL ABSORPTION IN MANGANESE ZINC FLUORIDE SINGLE CRYSTALS NEAR THE NÉEL TEMPERATURE by D. M. Finlayson, I. S. Robertson, T. Smith, and R. W. H. Stevenson (U. Aberdeen); Proc. Phys. Soc., Vol. 76, pp. 355-368, Sept. 1960

Measurements of the visible and ultra-violet absorption spectra of single crystals of manganese fluoride and of two manganese zinc fluoride mixtures down to 62°K, are presented. The sharp lines arising from the level complexes $\{^4E_g\ ^4A_{1g}\} (^4G)$ and $^4E_g (^4D)$, which are insensitive to the magnitude of the crystalline electrostatic field show a nonlinear shift with temperature which varies with composition and is correlated with the temperatures at which long-range antiferromagnetic order becomes appreciable. A separation of the exchange interaction effect from that due to the thermal expansion of the lattice can be made with some certainty in material of medium dilution, except in the immediate neighborhood of the ordering temperature where effects due to the lattice expansion anomaly may be appreciable. The magnitude of the antiferromagnetic interaction shift aids the identification of the transitions, and is interpreted as giving a measure of the variation of short-range spin order with temperature. Measurements of line width and oscillator strength have been made for several absorption lines, and the data for magnetically dilute materials can be interpreted on simple vibrational models. These models seem less satisfactory for pure manganese fluoride.

Effect of Pressure on Color Centers in Ag Doped Silver Halides - See 7854

Optical Spectrum of Ytterbium in the Cubic Field of CaF_2 - See 7976

7981 LUMINESCENCE DECAY IN AgCl CRYSTALS by K. Vacek (Charles U.); Czech. J. Phys., Vol. 10B, No. 6, pp. 468-474, 1960

The kinetics of luminescence decay of single crystal plates of AgCl at liquid nitrogen temperatures is measured. Luminescence decay first takes place (for $t \leq 2.5 \times 10^{-3}$ sec) hyperbolically and then exponentially. The constants a and a' of the hyperbolic and τ of the exponential dependence are measured for different intensities of the exciting radiation in normal and deformed samples and in samples irradiated with β -particles during measurement.

7982 ON THE FIELD AMPLIFICATION IN $\text{ZnCdS}-\text{Mn-PHOSPHORS}$ [in German] by G. Wendel; Z. Naturforsch., Vol. 15a, pp. 1010-1011, Nov. 1960

An investigation based on the results of Destriau, who observed a field amplification of approximately $\rho = B/B_0 = 2$ to 3 in $\text{ZnCdS}-\text{Mn-phosphor}$ in powder form, when excited by x-rays, and succeeded in obtaining an amplification of 6 by activating the phosphor with gold in gold chloride form is presented. It is shown that the amplification is not a direct result of gold activation, as similar amplifications were observed in preparations without gold. An amplification of 6-10 was observed, independent of x-ray frequency. The ac frequency exciting the screen on which the powder is deposited has a marked effect on ρ .

7983 THE KINETICS OF THE SHORT-LIVED PHOTOLUMINESCENCE OF SOME ACTIVATED ALKALI HALIDE CRYSTALS by I. K. Vitol and I. K. Plyavin; Optics and Spectrosc., Vol. 9, pp. 189-191, Sept. 1960

The influence of the two lowest excited levels of the activator ions Ga^+ , In^+ , and Tl^+ on the kinetics of the short-lived photoluminescence of crystals of KI-Ga , KI-In , and KI-Tl is investigated. Good agreement is obtained between the calculated and experimental results, confirming the validity of the initial assumptions of the calculation and permitting the determination of certain of the parameters of the luminescence centers.

7984 ELECTROLUMINESCENCE OF INSULATED PARTICLES. Part II. by K. Maeda (Matsuda Res. Lab.); J. Phys. Soc. Japan, Vol. 15, pp. 2051-2053, Nov. 1960

Using a new model, Lehmann's experimental results on the emission intensity of a single electroluminescent phosphor particle embedded in an insulating dielectric as a function of the applied voltage are analyzed. The local field enhancement is attributed to the disturbance of the applied field due to the conducting phase of the phosphor particle. The results are reasonable and the validity of the model is confirmed.

7985 VERY LOW FREQUENCY EXCITATION OF ELECTROLUMINESCENCE by W. J. Fredericks (Stanford Res. Inst.); Bull. Am. Phys. Soc., Ser. II, Vol. 5, p. 187 (A), Mar. 21, 1960

Electroluminescence brightness waves produced by very low frequency excitation were studied. A symmetrical sawtooth voltage was applied to electroluminescence cells of a ZnS ,

OPTICAL PROPERTIES (Cont'd)

ZnO, Cu, Ag, Cl phosphor. Measurements of the brightness waveforms and phase as a function of excitation frequency in the range from 0.02 cps to several hundred cps, and in temperature range from 273° to 450°K were made on cells. These cells had the phosphor embedded in a slightly conducting medium so that the average field across the phosphor was approximately equal to and in phase with the average field applied to the cell. At low excitation frequencies the emission of this phosphor was predominantly in a green band at 5200 Å. At room temperature with low frequency excitation the maximum in the brightness wave occurred before the voltage maximum. As the excitation frequency was increased the brightness wave maximum occurred later with respect to the excitation voltage, and finally followed the voltage maximum. As the temperature was increased the brightness wave maximum occurred earlier.

7986 ON THE ROLE OF A STIMULATING ACTION OF EXCITING LIGHT IN THE LUMINESCENCE KINETICS OF THE CRYSTALLINE PHOSPHOR ZnS-Cu by L. A. Vinokurov and M. V. Fock (P. N. Lebedev Phys. Inst.); 1960 Spring Mtg. Electrochem. Soc.

An experiment showing that the release of electrons from traps in a ZnS-Cu phosphor by an exciting light leading to a decrease of the electron concentration in deep traps with increase of excitation intensity is reported. After removing the excitation, the distribution of electrons over traps gradually approached equilibrium distribution. A flash under the action of an infrared light was shown to be determined mainly by release of electrons from deep levels. Therefore it was concluded that the above effects may be detected by measuring the value of the flash under different intensities of afterglow and at various stages of decay.

7987 LUMINESCENCE IN SEMICONDUCTING DIAMOND by J. B. Krumme and W. J. Leivo (Oklahoma State U.); Bull. Am. Phys. Soc., Ser. II, Vol. 5, p. 187 (A), Mar. 21, 1960

Investigation of various forms of luminescence in semiconducting diamond, conducted to correlate the results with other known properties of the same specimens, was reported. Ultraviolet-light-induced blue luminescence was observed in the investigated temperature range of 90° to 430°K, and the spectrum extended from 375 m μ to 615 m μ with a maximum at 480 m μ at 300°K. The temperature dependence of the luminescent intensity indicated that the luminescence is a phosphorescence rather than a slow fluorescence. One specimen had a blue region and a clear region, and in the former the luminescence was considerably more intense, the electrical conductivity much higher and the photoconductive response different from that in the clear region. Both regions are p-type semiconductors. Electroluminescence and triboluminescence were observed in all specimens. An unusual red luminescence with a longer lifetime than the blue luminescence was found in two of the samples. The red luminescent intensity which is quite low at room temperature increased with increasing temperature, being already quite apparent at 360°K and thus implying a phosphorescent process.

7988 (Zn,Hg)S AND (Zn,Cd,Hg)S ELECTROLUMINESCENT PHOSPHORS by A. Wachtel (Westinghouse); J. Electrochem. Soc., Vol. 107, pp. 682-688, Aug. 1960

The preparation of cubic structure solid solutions of (Zn,Hg)S by firing in sealed silica tubes is reported. With suitable ad-

ditions of Cu and a coactivator, photoluminescence and electroluminescence are obtained. The coactivators used were halides, Ga, or In. The red electroluminescence consists of two emission bands which do not appear to be analogous to the blue and green emission bands of Cu, Cl in ZnS. The quantum efficiency is of the same order of magnitude as that of ZnS: Cu, Cl, but the emission bandwidth is about twice as large and the red electroluminescence consists of emission located to a large extent in the infrared. HgS tends to retain the cubic structure of ternary (Zn, Cd, Hg)S systems provided that the Cd/Hg ratio does not exceed certain limits. The introduction of Cd causes increased electroluminescence until these limits are attained.

7989 CRYSTAL STRUCTURE AND SPECTRA OF ALKALI HALIDE PHOSPHORS by F. D. Klement (Acad. Sci. Estonian SSR); 1960 Spring Mtg. Electrochem. Soc.

Luminescence studies in crystals undergoing polymorphic transitions induced by temperature and pressure were discussed. The effect of hydrostatic pressure on luminescent spectra was also investigated. Vacancies formed in alkali halides activated by divalent impurities were found to associate with the activator ions and give rise to characteristic emission bands. Luminescence in mixed crystals was studied and indications of decomposition of the solid solutions under certain treatments were obtained. These studies also showed that there are preferential sites for the activator impurity in the lattice.

7990 P-N LUMINESCENCE AND PHOTOVOLTAIC EFFECTS IN GaP by H. G. Grimmeiss and H. Koelmans (Philips); Philips Res. Rep., Vol. 15, pp. 290-304, June 1960

Preparation of GaP crystals from the constituent elements is reported. Crystals made at low phosphorus pressure show primarily n-conductivity with an activation energy of 0.07 ev. Crystals with p-conductivity are obtained by heating at high phosphorus pressure (activation energy 0.19 ev) or by doping with Zn. The non-doped crystals show electroluminescence in bands at 6250 Å and 5650 Å. The electroluminescence is shown to be due to the recombination of charge carriers within p-n junctions via levels within the forbidden gap. A level scheme for undoped GaP is proposed. The crystals show point-contact rectification and photovoltaic effects. On measuring the photovoltage as a function of wavelength, excitation bands are found at 4200 Å and 5600 Å in non-doped crystals and at 4200 and 6000 Å in Zn-doped crystals. The long-wave excitation peaks of the photovoltage are explained with a two-step optical and thermal mechanism.

7991 ASSOCIATION AND DISSOCIATION OF CENTRES IN LUMINESCENT ZnS-In by H. Koelmans (Philips Res. Labs.); J. Phys. Chem. Solids, Vol. 17, pp. 69-79, Dec. 1960

Preparation of ZnS-In phosphors which are efficient upon excitation with $\lambda = 3650$ Å by firing in H₂S at 1200°C and quick cooling to room temperature is reported. The emission spectrum depends on the In concentration and consists of three bands at 6200 Å, 5350 Å and 4700 Å. X-ray analysis shows that the maximum amount of In incorporated is about 10⁻² gram-atoms In per mole ZnS. Refiring the phosphors at 600°C kills the luminescence at room temperature, an effect shown to be due to association. The trivalent In is compensated in the lattice by V'Zn. On the basis of the experimental evidence the 6200 Å band is ascribed to In_{Zn}, the 5350 Å band to the associate InZnV'Zn and the 4700 Å band to V''Zn. The low-temperature phosphorescence of the ZnS-In phosphors is strongly stimulated by irradiation into bands at 1.8 μ and < 1.2 μ.

OPTICAL PROPERTIES (Cont'd)

Anisotropy Effects in Photoconductivity of Pyrographite - See 7996

7992 ELECTRICAL PROPERTIES OF ORGANIC SOLIDS. Part I. KINETICS AND MECHANISM OF CONDUCTIVITY OF METAL-FREE PHTHALOCYANINE by G. Tollin, D. R. Kearns, and M. Calvin (U. California); *J. Chem. Phys.*, Vol. 32, pp. 1013-1019, Apr. 1960

Experimental investigations of the kinetics of photoconductivity in metal-free films of phthalocyanine are discussed. These experiments, in conjunction with measurements of steady-state photoconductivity, are consistent with the following scheme: The principal route for the formation of charge carriers is via the first excited singlet state, although the lowest triplet state can, to some extent, contribute to charge carrier production. The mobility of the carriers is low and is concentration-dependent, being lower at higher carrier concentrations. The decay of the photocurrent is the result of a diffusion-limited bimolecular recombination with a capture radius of approximately one molecular diameter. The experiments indicate that carriers produced thermally in the dark do not interact with light-produced carriers.

7993 PULSE PHOTOCONDUCTIVITY OF ADDITIVELY COLORED KBr by M. Onuki and H. Ohkura (Osaka City U.); *J. Phys. Soc. Japan*, Vol. 15, pp. 1862-1871, Oct. 1960

Investigations, by repeated pulsive illumination and by applying the dc and ac electric fields, of the space charge effect in the measurement of a photocurrent in additively colored KBr are reported. The space charge polarization may arise from the accumulation of electrons trapped in surface states, the depth of which is about 0.3 ev. The condition for the absence of space charge is realized by using the ac field and the pulsive illumination synchronized with plus and minus peaks of the ac field. The temperature-dependence of pulse photocurrent is measured. The time constants of current decay after switching-off of illumination are also observed. Three kinds of electron traps are found, one corresponding to F centers and the other two to unknown centers. Activation energies for releasing the electrons trapped in these centers are estimated to be 0.44, 0.35 and 0.43 ev respectively. The growth and bleaching of optical absorption bands are investigated in relation to the above electron traps. A detailed analysis for the trapping kinetics applying to additively colored KBr crystals is made.

Extrinsic Model for Free Carrier Generation in Photoconducting Anthracene - See 7927

Photoconductivity of CdS - See 7951

Photovoltaic Effects in GaP - See 7990

7994 THE TEMPERATURE DEPENDENCE OF THE REFRACTIVE INDEX OF GERMANIUM by F. Lukes (Brno U.); *Czech. J. Phys.*, Vol. 10B, pp. 742-748, Oct. 1960

For three samples of single crystal germanium having different concentrations of impurities, the temperature dependence of the refractive index of germanium in the wave-length region of $1.8\mu - 5.5\mu$ and the temperature region of $100^{\circ}\text{K} - 530^{\circ}\text{K}$ is given. The dependence is found to be nonlinear, and the results are compared with those of other authors. An attempt to interpret the observed dependence theoretically is also made.

7995 DECAY OF PERSISTENT POLARIZATION IN DIAMOND by J. A. Elmgren and D. E. Hudson (Iowa State U.); *Bull. Am. Phys. Soc.*, Ser. II, Vol. 5, p. 187 (A), Mar. 21, 1960

A study of the decay of the internal field created by trapped charges in partially type I diamond by utilization of the counting rate as a probe of the internal field with no applied external applied field was reported. The decays induced by thermal excitation and by photons of seven energies in the range from 2.14 to 3.40 ev were investigated. The effect of photon flux density was determined at each photon energy. The observed dark decay appeared to be a result of two energy levels at thermal depths of approximately 0.5 and 0.6 ev. An optical band around 3 ev was found to be very active in decay, with an estimated charge liberation cross section of the order of 10^{-14} cm^2 . This same band was found in the absorption spectrum of type I diamond. The large cross section tends to support the aggregate vacancy model of this system as proposed by Champion.

7996 OPTICAL PROPERTIES OF PYROGRAPHITE by G. Ruprecht (Raytheon); *Bull. Am. Phys. Soc.*, Ser. II, Vol. 5, p. 188 (A), Mar. 21, 1960

The manner in which the high anisotropy of structural and electrical properties of pyrographite causes an anisotropy of the optical absorption was explained. In the hard direction, the crystallographic c axis, the optical transmission was measured on thin samples which were prepared in such a way that the plane exposed to the incident light contained the a axis and the c axis. In the infrared range from 3μ to 15μ the absorption was explained in terms of free carrier absorption. The absorption coefficient was tentatively calculated from the conductivity σ on the basis of a free carrier conductivity model. It appeared that the conductivity obtained by optical measurements is in satisfactory agreement with the results of dc measurements. Since the conductivity in the basal plane exceeds the conductivity in the hard direction by a factor of 10^3 , it is obvious that pyrographite provides a new and effective means of polarizing infrared light.

7997 THE OPTICAL CONSTANTS OF SINGLE CRYSTALS OF HEXAGONAL SELENIUM by V. Prosser (Charles U.); *Czech. J. Phys.*, Vol. 10B, No. 4, pp. 306-316, 1960

The optical constants of single crystals of hexagonal selenium in the region of the intrinsic absorption edge in polarized light are investigated. The absorption edge for light polarized normal to the optical axis of the crystal is displaced towards longer wavelengths. The absorption maximum of hexagonal selenium for a wavelength of 0.6μ is interpreted as the maximum corresponding to interaction between neighboring chains and in connection with this the position of the absorption edge of different modifications of selenium is discussed.

THERMAL PROPERTIES

7998 SPECIFIC HEAT OF DILUTE ALLOYS by W. Marshall (Atomic Energy Res. Estab.); *Phys. Rev.*, Vol. 118, pp. 1519-1523, June 15, 1960

Use of the Ruderman-Kittel-Yosida theory of spin-spin coupling via conduction electrons to explain the fact that the addition of Mn to Cu produces a large contribution to the specific heat which, at low temperatures, is linear in temperature and in-

THERMAL PROPERTIES (Cont'd)

dependent of Mn concentration is reported. It is noted that the specific heat results of Beck et al. on FeV and FeCr alloys are probably of essentially the same origin as those which Zimmermann made on CuMn. Serious objections to the mechanisms of antiferromagnetism postulated by Overhauser and used by him to explain the specific heat results are pointed out.

Specific Heat of YIG - See 7952

Specific Heats of Polymorphic Forms of Manganese Sulfide - See 7963

Harmonic Approximation Calculation of Lattice Specific Heat and Free Energy - See 7916

7999 RESISTANCE ANISOTROPY AT LOW TEMPERATURES by S. Simons (Queen Mary Coll., London); Proc. Phys. Soc., Vol. 76, pp. 458-464, Oct. 1960

A variation principle-based theoretical treatment of the thermal conductivity tensor of dielectrics at low temperatures, where N-processes predominate, is given. The general expression in the case where U-processes are the only ones not conserving wave number is developed, and the ratio of components of the conductivity tensor at very low temperatures is shown to depend only on the geometry of the lattice unit cell. The results are applied to different crystal structures and a comparison is made with the available experimental data on quartz and sapphire.

8000 DETERMINATION OF THE COEFFICIENT OF THERMAL CONDUCTIVITY FOR METALS IN THE HIGH TEMPERATURE RANGE by V. V. Lebedev (Physico-Tech. Inst.); Phys. Metals Metallog., Vol. 10, No. 2, pp. 31-34, 1960

A method for the determination at high temperatures (above 800 to 900°C) of the coefficient of thermal conductivity of metals and alloys is described. Figures for the specific electrical resistivity, coefficient of thermal conductivity, and Wiedemann-Franz ratio of molybdenum rod at various temperatures in the range 900 to 2200°C are given.

8001 MEASUREMENT OF THERMAL CONDUCTIVITY IN SEMICONDUCTORS by R. Nii (Nippon Tel. and Tel.); Rev. Elect. Commun. Lab., NTT, Vol. 8, pp. 99-104, Mar.-Apr. 1960

Measurements of the thermal conductivity of Bi_2Te_3 , PbTe and InSb, determined by a modified Angstrom method in the temperature range of 100°-600°K are reported. A heat source whose temperature varies sinusoidally with time is used. The samples used are all single crystals, with dimensions $0.3 \times 0.3 \text{ cm}^2$ in cross section and 0.2 - 0.8 cm in length. The samples are soldered to the heat source. A sinusoidal temperature wave travels through them and is reflected at their ends. Two values of thermal conductivity are determined, one from the amplitude ratio and the other from the phase difference at both ends of the sample. These two values agree very well. The results obtained by this method differ from those determined by Joffe and Devyat'kova for PbTe.

8002 ON THE EXPERIMENTAL DETERMINATION OF THE THERMOELECTRIC EFFICIENCY OF SEMICONDUCTORS [in German] by U. Birkhol (Siemens AG); Solid State Electronics, Vol. 1, pp. 34-38, Mar. 1960

A method for measuring the parameters determining the thermoelectric figure of merit z using a single piece of apparatus is described. By definition, $z = \sigma^2 \sigma / \kappa$, where σ is absolute thermo electric power, σ is electrical conductivity, and κ is thermal conductivity of a given sample. Errors in measurement of the parameters caused by heat radiation and sample inhomogeneity are discussed.

8003 DEPENDENCE OF THE VOLUME PELTIER EFFECT ON RESISTIVITY GRADIENTS by P. I. Baranski and P. M. Kurilo (Kiev Inst. Phys.); Soviet Phys. - Solid State, Vol. 2, pp. 424-428, Sept. 1960

The dependence of the volume Peltier effect (E_p) on the value of resistivity (ρ) gradients within single crystals of Ge is established. A simple experimental method used Cu-Constantan thermocouples to study $d\rho/dx$. The relation $E_p = \text{const. } 1/\rho d\rho/dx$ and ($I = \text{const.}$) was verified experimentally for seven pairs of specimens of n-type Ge. The origin of E_p is demonstrated to be characterized by the presence of inhomogeneities of the resistivity.

Oxygen Influence on Thermoelectric Energy Conversion in $\text{Bi}_2\text{Te}_{3-x}\text{Se}_x$ - See 7919

MECHANICAL PROPERTIES

8004 ELASTIC CONSTANTS OF HEXAGONAL CADMIUM SULFIDE by D. I. Bolef, N. T. Melamed, and M. Menes (Westinghouse); J. Phys. Chem. Solids, Vol. 17, pp. 143-148, Dec. 1960

The adiabatic elastic constants of a single crystal of hexagonal cadmium sulfide measured at 27°C are presented. Measurements are made at 10 Mc by means of an ultrasonic cw mechanical resonance technique. The elastic stiffness constants, in units of 10^{11} dynes/cm², are: $c_{11} = 8.432$, $c_{33} = 9.397$, $c_{44} = 1.489$, $c_{12} = 5.212$, $c_{13} = 4.638$. Single crystal CdS has very low anisotropy, as indicated by the ratios $c_{11} - c_{12}/2c_{44} = 1.08$ and $c_{33}/c_{11} = 1.11$.

8005 THE INTERNAL FRICTION OF LONGITUDINAL OSCILLATIONS IN FERROMAGNETIC MATERIALS by L. Spacek (Tech. Coll. Trans. Engrg.); Czech. J. Phys., Vol. 10B, No. 6, pp. 439-451, 1960

The theory of a new magnetomechanical phenomenon in an alternating field is discussed. The internal friction of longitudinal oscillations of a ferromagnetic material in the shape of a wire in a constant magnetic field is considered. It is assumed that the medium in which the sample oscillates is conducting and has a certain permeability. Equations defining the magnetic field in the oscillating material are derived from the basic thermodynamic relations. The term describing the non-conservative force component in a complex formulation is used to determine the internal friction. A general relation between the internal friction and the magnetic field is derived, as well as other expressions which are a simplification of it. Internal friction in an alternating field is also considered. It is shown that the solution can be transformed to the sum of the internal frictions of the different harmonic oscillations, which are obtained as a partial solution of the problem on the assumption that the elastic oscillations in interaction with the field oscillations are separated into their harmonic components. The calculation then becomes that of the internal friction previously

MECHANICAL PROPERTIES (Cont'd)

considered. In this case the internal friction significantly depends on the field amplitude. The functional dependence of the internal friction peak on the frequency of the mechanical oscillations is also calculated. Agreement of theory with experiment is satisfactory.

stress Compensation for Frequency Changes in Quartz Crystals
See 8047

SOLID STATE DEVICES

DIODES

006 THE P-I-N MODULATOR, AN ELECTRICALLY CONTROLLED ATTENUATOR FOR MM AND SUB-MM WAVES by J. C. de Ronde, H. J. G. Meyer, and O. W. Memelink (Philips Res. Labs.); *IRE Trans.*, Vol. MTT-8, pp. 325-327, May 1960

The construction and performance of a millimeter wave modulator are described. The main part of the modulator consists of p-i-n germanium structure inserted into a rectangular waveguide. A modulation depth of 11 db could be obtained at frequencies up to 5 kc, this modulation being caused primarily by attenuation.

007 THE NONLINEAR BARRIER CAPACITANCE OF SILVER BONDED DIODES by S. Kita and K. Sugiyama (Nippon Tel. and Tel.); *Rev. Elect. Commun. Lab. NTT*, Vol. 8, pp. 112-18, Mar.-Apr. 1960

The design and construction of a silver bonded diode suitable for use as a parametric amplifier are described. The diode consists of a silver-gallium whisker bonded to an n-type Ge wafer. The cutoff frequency of the diode is more than 400 kMc and its carrier capacitance variation factor, C_1/C_0 , is four times greater than that of other point contact diodes. A 6 kMc parametric amplifier using a silver bonded diode was constructed. The bandwidth is 40 Mc at 20 db gain and the noise figure is about 5 db.

008 MEASUREMENT OF MINORITY CARRIER DIFFUSION LENGTHS IN P-N JUNCTIONS BY ANALYZING PHOTOVOLTAIC SPECTRAL RESPONSE CURVES by J. J. Loferski and J. J. Wysocki (RCA Labs.); *Bull. Am. Phys. Soc.*, Ser. II, Vol. 5, p. 265 (A), Apr. 25, 1960

The application of photovoltaic response in measuring minority carrier diffusion lengths in p-n junctions was discussed. If the absolute value of absorption constant a of a semiconductor is known as a function of photon energy, $h\nu$, the shape of the spectral response of a photovoltaic cell with a specified geometry, minority carrier diffusion lengths (L_n and L_p), and surface recombination velocity may be calculated. Consequently, by establishing the position of the p-n junction by some independent means, an estimate of L_n and L_p is possible from the shape of the spectral response curve of the junction. Representative

theoretical curves of response versus λ for various plausible combinations of semiconductor parameters were calculated. Experimental photovoltaic spectral response curves of diffused germanium and silicon p-n junction photocells were used to verify the theory. Similar curves taken on GaAs cells with different junction depths were used to estimate L_n and L_p .

8009 ESAKI OR TUNNEL DIODES by W. W. Gaertner (USASRDL); *Semicon. Prod.*, Vol. 3, pp. 31-38, May 1960; pp. 36-38, June 1960

The design and construction of tunnel diodes are discussed. The physical effects which produce the electrical characteristics are indicated, and the characteristics realized thus far are reviewed. The potentialities of tunnel diodes are listed, and diagrams and design equations for dc bias, oscillator, amplifier, and switching circuits are given.

8010 A SURVEY OF TUNNEL DIODES by G. C. Messenger, W. Steiger, and C. E. Todd (Hughes Aircraft); *Solid State J.*, Vol. 1, pp. 35-43, July-Aug. 1960

The design and applications of tunnel diodes are reviewed. Basic tunnel effect theory is presented along with circuit characterization and idealized models used to represent the actual device. Examples of tunnel diode applications in switching circuits, oscillators, amplifiers and other circuits are also given. Many references on tunnel diodes are listed.

8011 PRESSURE DEPENDENCE OF THE REVERSE CHARACTERISTIC OF A GERMANIUM ESAKI DIODE by M. I. Nathan, S. L. Miller (IBM), and L. Finegold (Harvard U.); *Bull. Am. Phys. Soc.*, Ser. II, Vol. 5, p. 265 (A), Apr. 25, 1960

The pressure dependence of the reverse I-V characteristic of a Ge Esaki diode at room temperature was measured. The pressure ranged up to 28,000 kg/cm². The diode was alloyed with an InGa dot on an Sb-doped substrate. The peak current density was ≈ 0.04 a/cm². At atmospheric pressure the I-V curve at 4.2°K indicated that almost all tunnelling in the forward direction is phonon assisted. The "Morgan-Kane kink," which indicates the onset of direct tunnelling between the (000) edges of the valence and conduction bands, was observed at 4.2°K and at 77°K, but not at room temperature. The pressure coefficients for the energies of the (000) and the (111) conduction band minima relative to the valence band are known. Since these coefficients are different, the pressure changes of the phonon-assisted and the direct-tunnelling currents will be different. Hence it is possible to observe the presence of direct tunnelling at room temperature from the pressure dependence of the I-V curve. The Morgan-Kane prediction was confirmed by the pressure data. The data indicated that direct-tunnelling current was in the range of 3 to 8 times phonon-assisted current at atmospheric pressure, for $-V \geq 0.2$ v.

8012 THE CHARACTERISTICS OF AN ESAKI-DIODE AT MICROWAVE FREQUENCIES [in Japanese] by H. Fukui (Sony); *J. Inst. Elect. Commun. Engrs. Japan*, Vol. 43, pp. 1351-1356, Nov. 1960

An equivalent circuit to determine the characteristics of Esaki diodes at microwave frequencies is discussed. The accuracy of the circuit is shown by comparison of actual and calculated values of diode properties, indicating that the circuit may be confidently employed from low to microwave frequencies. The diode admittance was measured in the frequency range from 0.3 to 4.6 Gc, utilizing the standing wave method and avoiding parasitic oscillations caused by operation in the negative conductance region.

DIODES (Cont'd)

8013 AN INVESTIGATION OF P-N JUNCTIONS AT HIGH CURRENT DENSITIES by Yu. K. Barsukov (Acad. Sci., USSR); Soviet Phys. -Solid State, Vol. 1, pp. 1518-1524, May 1960

The transition blocking process, the diffusion voltage, and the conductivity of the low-impurity region in relation to the forward current value in fused In-Ge p-n junctions are investigated. The dynamic test conditions include current densities from approximately 10 to 1000 a/cm². It is established that the inertia of the p-n junction decreases with increase in the forward current preceding the transition blocking process. The dependence of the diffusion voltage on the forward current indicates the presence of an antibarrier layer in the vicinity of the second electrode. It is shown that the decrease in inertia is due to the reduced rate of increase of the excess carrier density with current. The approximate calculations are in good qualitative agreement with the experimental data.

8014 TWO-CARRIER THEORY OF P-N JUNCTIONS by Y. F. Chang (Purdue U.); Bull. Am. Phys. Soc., Ser. II, Vol. 5, p. 265 (A), Apr. 25, 1960

Application of the two-carrier theory to explain the actual behavior of p-n junctions in the forward direction was made. The two-carrier theory takes into consideration the space-charge voltage due to the difference in electron and hole mobilities, and the IR-drop voltage across the bulk semiconductor material. The junction relations derived by Fletcher and the boundary condition derived by this author from the basis for this study.

8015 CUTOFF CHARACTERISTICS OF SILICON p-Sp-n RECTIFIERS AT BREAKDOWN [in German] by O. Jaentsch (Siemens AG); Z. Naturforsch., Vol. 15a, pp. 302-307, Apr. 1960

Evidence that negative acid ions, ozone, and oxygen adsorbed by p-Sp-n rectifiers cause surface breakdown is reported. Reduced reverse current for small voltages and reduction of breakdown voltage are found to be characteristic effects of breakdown. The former effect is explained by decreased surface recombination and a resulting decrease of carrier generation in the space charge region. It is also stated that several days of storing the unprotected rectifier in high temperature ambient nitrogen or oxygen leads to surface breakdown and that breakdown may be reversibly compensated by adsorption of positive water ions.

8016 DENDRITIC INCLUSIONS IN AlSb GROWN-JUNCTION DIODES by H. C. Gorton (Battelle Mem. Inst.); J. Electrochem. Soc., Vol. 107, pp. 248-249, Mar. 1960

The adverse effect of dendritic inclusions on the electrical properties of AlSb grown-junction diodes is discussed. The lack of rectification and the anomalously low reverse voltages of seven diodes are attributed to the inclusion of Al₃Ta filaments during crystal growth from a melt initially containing 0.5 atomic per cent Ta impurity [see abstract 2382]. The long filaments, about 1-5 μ in diameter, are oriented parallel with the direction of growth, penetrate the junction, and exhibit a radial symmetry in the plane perpendicular to the direction of growth. On the other hand, two diodes which exhibited rectification were fabricated from material near the edge of the crystal where the filament concentration was low. The similarity between dendritic inclusions and arrays of etch pits observed in other semiconducting materials is pointed out. The possibility of a similar mechanism for such anomalous behavior in other semiconducting devices is also suggested.

8017 SEMICONDUCTIVE DEVICE AND METHOD by W. Shockley; U.S. Pat. 2,937,114, Issued May 17, 1960

The fabrication of transistors and diodes of the diffused junction type, featuring small size and high impurity concentration is described. The double diffusion oxide masking technique is employed in material containing a single dislocation. The junctions form along the dislocation since diffusion takes place preferentially along them. The devices fabricated by this method are useful at microwave frequencies.

Formation of Diffused Junctions in Si - See 7858

8018 THE FABRICATION OF SILICON CARBIDE JUNCTION by K. M. Hergenrother (Transitron); U.S. Gov. Res. Rep., Vol. 33, p. 510 (A), May 13, 1960 PB 144 974

The growth of p-n junctions in SiC by depositing a single crystal film from the vapor phase onto a silicon carbide seed is discussed. The junction is made by adding impurities to the ambient gas in the furnace during the crystal growth. These p-n junctions are suitable for fabricating diodes and other junction devices which will operate at 500°C and have relatively good resistance to high energy radiation.

Junctions in SiC - See 8030

8019 PROTECTIVE TREATMENT FOR SEMICONDUCTOR DEVICES by H. F. John (Westinghouse); U.S. Pat. 2,937,110, Issued May 17, 1960

A surface treatment for Ge and Si diodes and transistors before the device is encapsulated in a resin or hermetically sealed in a container is described. Finely divided particles of lead tetroxide or mercuric oxide are thoroughly mixed in an elastomer silicone resin in the ratio of 0.6 to 2.0 parts by weight metal oxide to 1 part by weight of resin. A layer of the mixture is then applied to the entire device or to selected regions of it and the coating is cured by heating it at a temperature and for a time sufficient to convert the resin to a tough elastomer. The improvement which results from the technique is illustrated by several examples. Other coatings are also considered and reverse current-voltage characteristics are measured.

TRANSISTORS

8020 TRANSISTOR RATINGS AND RELIABILITY by I. R. Stevenson (Stand. Telephones Cables); Proc. IRE, Austl., Vol. 21, pp. 138-141, Mar. 1960

The factors which affect transistor life expectancy are described. It is emphasized that properly manufactured transistors are capable of extreme reliability and long life. The precautions which the user must take in order to take advantage of these capabilities are indicated.

8021 TEST CIRCUITS FOR THE MEASUREMENT OF TRANSISTOR CURRENT-GAIN IN THE 0.1 - TO 200-Mc FREQUENCY RANGE by G. N. Kambouris and E. Hirschmann (Diamond Ord. Fuze Labs.); U.S. Gov. Res. Rep., Vol. 33, p. 377 (A), Apr. 15, 1960 PB 144 665

The design and construction of test sets that permit accurate measurement of transistor current gain are discussed. Both the common-emitter and common-base configurations over an extended frequency range (up to 200 Mc) and at various bias

TRANSISTORS (Cont'd)

conditions are included. Components and techniques used and problems encountered are described.

8022 DYNAMIC DETERMINATION OF THE CHARACTERISTICS OF LOW-POWER p-n-p TRANSISTORS [in Italian] by D. Brini and A. Drioli; *Alta Frequenza*, Vol. 29-2, pp. 251-256, Apr. 1960

A circuit which facilitates evaluation of p-n-p transistors by displaying their characteristics on the screen of an oscilloscope is presented. The device makes it possible to obtain either a single characteristic for a predetermined value of the base current or an entire family of characteristics.

Transistor Switching Circuit Design Using Charge-Control Parameters - See 8091

8023 SEMICONDUCTOR DEVICES by R. J. Zelinka (Minn.-Honeywell); U.S. Pat. 2,923,870, Issued Feb. 2, 1960

Fabrication of a double tetrode transistor having gain in both its input and output circuits is described. Two tetrode transistors with a common bias base electrode are fabricated on a single chip having a resistivity gradient. In one design, the chip is circular with a higher resistivity at its center, the input tetrode. Three ohmic bases are alloyed as annular rings on one side of the chip and two emitters are alloyed between them, opposed on the other side by two collectors. In the other design, the chip is square and the rings are replaced by bars. Again, the low resistivity part of the chip is at the edges which form the output tetrode.

8024 THE EXPERIMENTAL DETERMINATION OF BASIC TRANSISTOR PROPERTIES BY THE MEASUREMENT OF MINORITY CARRIER CHARGE IN THE BASE by V. I. Shveikin (Lomonosov State U., USSR); *Radio Engrg. Electronics*, Vol. 5, No. 7, pp. 192-201, 1960

A pulse method for measuring the minority carrier charge injected into a transistor base is described. The base charge measurements permit the determination of the transistor α -cutoff frequency and the effective lifetime of minority carriers in the base. Measurements by the technique have been made on alloy and drift transistors. Good results were obtained with alloy transistors whereas experimental difficulties were encountered in measurements on drift transistors.

8025 TRANSISTOR AVALANCHE VOLTAGE by L. van Biljon (U. Pretoria); *Electronic Tech.*, Vol. 37, pp. 72-76, Feb. 1960

An expression for the collector avalanche voltage in an alloyed junction transistor as a function of base resistance is developed. This expression may be used to predict the voltage where avalanche breakdown will occur for any value of base resistance, once the breakdown voltage at a particular value of base resistance, including $R_b = 0$ and $R_b = \infty$, is known. It is further shown that the avalanche voltage is a function of both forward and reverse-current amplification factors but that, at high values of base resistance, the reverse amplification factor is not important. It is concluded from experiment that it is not the base resistance itself which determines the avalanche voltage but rather the emitter-base voltage as set up by the current through this resistance.

8026 CHARACTERISTICS OF GERMANIUM P-N JUNCTION WITH IRREGULAR STRUCTURE by M. Tomono (Hitachi); *J.*

Phys. Soc. Japan, Vol. 15, pp. 1223-1236, July 1960

The dynamic characteristics of a transistor having an imperfect emitter junction and a comparatively perfect collector junction are evaluated. The imperfect emitter junction is produced by applying a very thin In layer on an n-type Ge pellet. The current into the imperfect emitter is divided into various components and the voltage-current characteristics of each component are studied. Particular attention is given to the electron current component which flows through the minute area of the m-n junction existing at the irregular part of the p-n junction. The phenomena of the voltage-current characteristics of the emitter as determined from these studies differ greatly from those described by the Shockley equation. The abnormally strong current dependency of the current amplification factor of the transistor, and the floating-potential of the emitter are explained.

8027 JUNCTION TRANSISTOR OPERATING CHARACTERISTICS WITH SINUSOIDAL INPUT AND OUTPUT VOLTAGES by L. D. Zarkhi; *Radio Engrg. Electronics*, Vol. 5, No. 7, pp. 172-191, 1960

A method for measuring the mean parameters of the equivalent "hybrid- π " circuit of a junction transistor is described. Analytical expressions approximating the dependence of mean parameters of the equivalent hybrid- π circuit on the signal level and supply voltages are developed.

Thermal Drift in Junction Transistors - See 8055

8028 CONDITIONS FOR OBTAINING GERMANIUM TRANSISTORS BY DOUBLE DIFFUSION [in French] by R. Deschamps (Lab. Magnetisme Phys. Solide, Bellevue); *Comptes Rendus*, Vol. 250, pp. 3137-3139, May 9, 1960

The conditions necessary for producing an n-p-n structure in n-type Ge by successive diffusions of n- and p-type impurities are derived. The structure can also be produced by the diffusion-evaporation process. The parameter formulas for both methods are derived, and are very similar. It is also shown that the conditions necessary for fabricating an n-p-n structure by simultaneous double diffusion are not fulfilled in n-type germanium.

8029 METHOD OF MAKING SEMICONDUCTOR DEVICE by J. R. A. Beale (Philips); U.S. Pat. 2,964,430, Issued Dec. 13, 1960

The fabrication of Ge transistors with controllable base widths by diffusion and etching techniques is described. A thick n-layer is formed upon a p-type Ge wafer by the diffusion of Sb. By etching a cavity through this diffused layer, inserting a dot of Pb-Sb-Ga, and heating the assembly, a p-n-p transistor structure is obtained. Antimony from the dot diffuses at a faster rate than Ga and forms a thin n-type base layer which unites with the thicker diffused layer; the Ga recrystallizes to form a p-type emitter above the base. Etching of unnecessary areas and alloying base and collector contacts completes the transistor structure. Reference is also made to a field-effect transistor employing the above fabrication techniques.

Double Diffused Junctions in Transistors - See 8017

Fabrication of Ge Transistor with Imperfect Emitter Junction - See 8026

TRANSISTORS (Cont'd)

8030 RESEARCH ON SILICON CARBIDE TRANSISTORS (Westinghouse); U.S. Gov. Res. Rep., Vol. 33, p. 511 (A), May 13, 1960 PB 144 975

The use of boron-tin-platinum alloy for formation of p-n junctions in n-type SiC is investigated. The results obtained are encouraging. The rectification ratios for the fused junctions are higher for higher fusion temperature and greater temperature gradient normal to the regrowth layer.

Ultrasonic Dicing of Semiconductor Slices - See 7900

Protective Treatment for Transistors - See 8019

8031 INTRODUCTION TO THE THEORY OF THE TECNETRON [in French] by A. V. J. Martin (Carnegie Inst. Tech.); *J. Phys. Radium*, Vol. 21, Suppl. to No. 3, pp. 24A-36A, Mar. 1960

The approximate fundamental theory and the principal characteristics of the tecnetron are discussed. The tecnetron is a semiconductor amplifying device which uses the centripetal striction produced by the field effect in a cylindrical structure. The secondary effects and their bearing on the fundamental theory and the practical design of the device are also investigated.

8032 THE TECNETRON AS A CIRCUIT ELEMENT [in French] by A. V. J. Martin (Carnegie Inst. Tech.); *J. Phys. Radium*, Vol. 21, Suppl. to No. 7, pp. 113A-122A, July 1960

The tecnetron is considered as a circuit element in relation with external electronic circuits. Representative equivalent circuits are established, under certain simplifying assumptions. The frequency dependence of interesting parameters is examined. Other frequency characteristics are also described.

Fabrication of Field Effect Transistors - See 8029

MAGNETOELECTRIC DEVICES

8033 HALL-EFFECT MULTIPLIERS by W. A. Scanga, A. R. Hilbinger, and C. M. Barrack (Aircraft Arms); *Electronics*, Vol. 33, pp. 64-67, July 15, 1960

A semiconductor Hall generator with a bandwidth of several kc and an accuracy of 0.1 to 1 per cent is discussed. Equations are developed to show that the output is proportional to the product of the inputs. A comparison of Si, Ge, InAs, and InSb as the multiplying element is made. Junction transistors are used in the product and input amplifiers. Separate grounds are required unless a chopper amplifier is used as the product amplifier. Direct coupled amplifiers with feedback stabilization are required. Ferrite is used as the magnet core material to achieve wide-band operation. With 300 ma, control current and 100 ma field current through 300 turns, the output is 70 mv.

8034 ON THE MEASUREMENT OF MAGNETIC FIELDS WITH HALL GENERATORS [in German] by H. Weiss (Siemens AG); *Solid-State Electronics*, Vol. 1, pp. 225-233, July 1960

The thermal noise of the internal resistance of the semiconductor as a sensitivity-limiting factor of InAs Hall generators is discussed. The generators are utilized for low frequency magnetic field measurements. For the smallest detectable field the

Hall power is equal to the noise power $kTdf$. For constant magnetic fields the sensitivity is smaller by two to three orders of magnitude. Experiments over a period of 8 months showed a reproducibility of $\pm 2 \times 10^{-5}$ for the Hall voltage of a generator made of InAs. For InSb and InAs with $N_D = 6 \times 10^{16}/\text{cm}^3$ no dependence of the Hall coefficient on magnetic induction below 10^4 gauss was found.

InSb Magnetoresistive Voltage Regulator - See 8143

PHOTODEVICES

8035 CONSTRUCTION AND PERFORMANCE OF A POSITION-SENSITIVE PHOTO-TRANSISTOR by L. R. Baker (BSIRA); *Optica Acta*, Vol. 7, pp. 191-198, Apr. 1960

The construction of a photocell by modification of a phototransistor is described. A three-terminal model sensitive to movement in only one direction is considered. A five-terminal device sensitive to motion in two directions can also be fabricated. Test results which indicate the mechanical, optical, and electrical stability of the device are given.

Photoresponse of p-n Junctions - See 8008

THERMAL DEVICES

8036 LOW FREQUENCY WAVE FILTERS EMPLOYING THERMISTORS by R. A. Rasmussen (U. California); *Rev. Sci. Instr.*, Vol. 31, pp. 747-751, July 1960

The general properties of thermistors are reviewed and their small signal characteristics are analyzed. Measurements of their ac properties and response curves obtained for the simplest filter circuit configurations are described and analyzed.

FERRITE DEVICES

8037 FREE ELECTROMAGNETIC OSCILLATIONS OF A SPHERICAL RESONATOR WITH MAGNETIZED FERRITE SPHERE IN THE CENTRE by A. A. Pistol'kovs and S. Ian'-Shen; *Radio Engrg. Electronics*, Vol. 5, No. 7, pp. 77-87, 1960

A theoretical investigation of free electromagnetic oscillations of a spherical resonator with a small ferrite sphere at the center is discussed. The condition of tuning the entire system to resonance is investigated and expressions for the decremental attenuation of the oscillations in dependence on the half-width of the ferromagnetic resonance curve, ΔH , are derived. The effect of wall losses in the resonator is estimated.

Faraday Rotator Circulator Employed in Radar Duplexing - See 8114

8038 FERROMAGNETIC AMPLIFIERS by A. F. H. Thomson (Services Electronics Res. Lab.); *Proc. IRE*, Vol. 48, p. 259 (L), Feb. 1960

The absorption of power at microwave frequencies by magnetized yttrium garnet spheres is discussed. It is reported that when

FERRITE DEVICES (Cont'd)

A sphere is placed in a microwave field which has its H component parallel to the magnetization and its frequency approximately twice that corresponding to the magnetization, an absorption of microwave power occurs when the amplitude of the field exceeds a threshold value. The threshold value is about 0.5 oe and varies little with either orientation or shape of the sample. It is suggested that the absorption is caused by parametric excitation of pairs of spin wave modes of the material. Experiments indicate that the mode numbers are so high that there is negligible coupling of the excited modes to the surroundings. The spin wave excitation mechanism is compared with that suggested by Suhl.

Ferromagnetic Parametric Amplifiers - See 8072 and 8073

8039 ELASTIC SWITCHING PROPERTIES OF SOME SQUARE LOOP MATERIALS IN TOROIDAL STRUCTURES by W. C. Seelbach and J. R. Kiseda (IBM Res. Lab.); *J. Appl. Phys.*, Suppl. to Vol. 31, No. 5, pp. 1355-1365, May 1960

Elastic switching properties of some square loop materials are presented and the concept of an elastic switching constant $S_w(r)$ is introduced. The plot of applied "turn over" field strength vs the inverse of the drive width indicates that the inelastic switching constant for a given material is four to five times greater than the elastic switching constant $S_w(r)$. The "turn over" field strength is defined to be that value of field strength at which inelastic switching just starts and therefore is considered to be the upper limiting field strength for elastic switching. To a first-order approximation, the ratio of $S_w(r)$ to S_w is shown to be equal to the percentage of the total flux capacity of the core that can be switched in an elastic mode of operation. $S_w(r)$ values for Molybdenum Permalloy range from 0.0374 oe- μ sec for 1/8-mil tapes to 0.0913 oe- μ sec for 1/2-mil tape.

Microwave Frequency Doubling and Mixing in Ferrites - See 8100

8040 THE SCANSOR, A NEW MULTI-APERTURE RECTANGULAR-LOOP FERRITE DEVICE by S. Duinker and B. Van Ommeren (Philips); *Solid-State Electronics*, Vol. 1, pp. 176-182, July 1960

The properties, characteristics, and applications of scanners are discussed. The scanner consists of a multi-aperture plate of rectangular-loop ferrite which is provided with a large number of separate output windings. Consecutive output pulses can be developed across the windings by driving the plate from one remanence position into the other by triangularly shaped pulses. The various output pulses are of rather uniform height but mutually delayed. Depending on the geometry of the scanner and on the slope of the driving current, the delay between pulses corresponding to any two adjacent single-turn output windings can be varied from 0.05 to 2 μ sec with corresponding pulse heights of 10 to 0.2 v, respectively. Experiments which indicate that the response of certain output windings can be either suppressed or shifted in time by applying appropriate additional pulses are described. A few possible applications of scanners such as rapid scanning devices and code converters, are briefly discussed.

8041 BROADBAND NONRECIPROCAL TRANSMISSION DEVICE by H. Boyet and S. Weisbaum (Bell Labs.); U.S. Pat.

2,923,899, Issued Feb. 2, 1960

The design and characteristics of a broadband nonreciprocal transmission device are discussed. To produce uniform nonreciprocal performance over a range of frequencies or temperatures or other operating conditions, two slabs of ferrite are mounted in parallel in a longitudinal section of waveguide. The two ferrites differ in length, thickness, or magnetic properties, and use externally-applied magnetic fields that may differ in magnitude. Thus, the combined use of the two ferrites results in a differential effect which compensates for frequency or temperature variations.

8042 NONRECIPROCAL ELECTROMAGNETIC WAVE MEDIUM by A. G. Fox (Bell Labs.); U.S. Pat. 2,923,903, Issued Feb. 2, 1960

A waveguide which produces nonreciprocal rotation of the plane of polarization of a linearly polarized electromagnetic wave is described. A section of the waveguide has a varying cross section and a tapered rod of gyromagnetic material along its axis. The phase constants in the guide and the gyromagnetic coupling between vertically and horizontally polarized wave components are chosen to produce a nonreciprocal normal mode transfer of power between the two polarizations. The transfer of power, which resembles a polarization rotation of ninety degrees, is of broadband type.

MASERS

8043 AN INTRODUCTION TO THE THEORY OF SOLID-STATE MASERS WITH PARTICULAR REFERENCE TO THE TRAVELLING WAVE MASER by P. N. Butcher (Roy. Radar Estab.); *Proc. IEE*, Vol. 107B, pp. 341-351, 352-353, July 1960

An introduction to the theory of solid-state masers with particular reference to the travelling-wave maser is presented. The relevant properties of paramagnetic ions are described and the quantum theory of maser action is outlined qualitatively. A semi-classical treatment based on the classical equation of motion of a magnetic dipole is developed, and used to evaluate the engineering characteristics of a travelling-wave maser which employs the comb type of slow-wave guide.

CW Maser Operation by a Four Spin Flip Mechanism - See 7965

8044 PACKAGED TUNABLE L-BAND MASER SYSTEM by F. R. Arams and S. Okwit (Airborne Instr. Lab.); *Proc. IRE*, pp. 866-874, May 1960

A low-noise tunable L-band maser system is described. The maser uses a pink ruby crystal oriented at 90° and is tunable from 850 to 2000 Mc. The voltage-gain bandwidth product is as high as 37.5 Mc at a liquid helium bath temperature of 1.5°K. An L-band circulator has been developed for use with the maser. It has an insertion loss of 0.3 db, operates over a 200 Mc frequency range at L-band, and determines the usable tuning range of the circulator-maser system. The maser and circulator have been packaged into an operational unit that includes all auxiliary components, and has a system noise factor of 0.5 db (35°K). Electrical and mechanical features of the system are described and performance data are given.

MASERS (Cont'd)

8045 A TUNABLE X-BAND RUBY MASER by P. D. Gianino and F. J. Dominick (Ewen Knight); Proc. IRE, Vol. 48, p. 260 (L), Feb. 1960

A tunable ruby maser which has been operated at X-band frequencies with constant 20 db gain and 10 Mc bandwidth over a continuous tuning range of 205 Mc (from 9405 to 9610 Mc) was described. Voltage-gain bandwidth products up to 230 Mc have been achieved even though all parameters have not been fully optimized. The tuning mechanism for the cavity, consisting of only two external controls mounted on the maser superstructure, was also described. The magnetic field orientation is fixed at about 54° to the ruby c-axis and no external pump tuning mechanism is required because the large piece of ruby crystal with its high dielectric constant causes many more modes to appear in the pump circuit, resulting in many pump resonances.

8046 MASERS OR PARAMETRIC AMPLIFIERS? by D. C. Laine' (Glass Dev.); Electronic Tech., Vol. 37, pp. 174-185, May 1960

Two important developments in low-noise microwave amplification, the maser and the parametric amplifier, are described. A brief discussion of the principles of operation and a brief outline of the various types of amplifier in each of these two groups are given. The noise arising in these devices is contrasted with that originating outside the amplifier itself, such as may be found in a practical receiver system. Finally, the choice of a low-noise amplifier for a specific application is discussed on the basis of both practical and important electrical considerations.

OTHER SOLID STATE DEVICES

Ferroelectric Parametric Amplifiers - See 8074 and 8075

Dielectric Resonator for Inductive Capacity Measurement - See 7921

8047 REDUCTION OF FREQUENCY-TEMPERATURE SHIFT OF PIEZOELECTRIC CRYSTALS BY APPLICATION OF TEMPERATURE-DEPENDENT PRESSURE by E. A. Gerber (USASRDL); Proc. IRE, Vol. 48, pp. 244-245 (L), Feb. 1960

The use of temperature-dependent stress to compensate for temperature-induced frequency changes in AT quartz crystal resonators was discussed. The stress is applied by means of bimetal strips at selected spots on the circumference of the crystal plate. One or more bimetal strips may be used, depending on the temperature range over which compensation is desired. Lower power consumption, reduced aging, and greater miniaturization are possible by this technique than by the use of crystal ovens.

8048 VHF CRYSTAL POLISHING AND THE NATURE OF POLISHED QUARTZ SURFACES by I. Ida and Y. Arai (Nippon Tel. and Tel.); Rev. Elect. Commun. Lab. NTT, Vol. 8, pp. 119-174, Mar.-Apr. 1960

The finishing and polishing of quartz crystal surfaces to produce crystals with frequencies up to 140 Mc are described. The nature of skin stress, stages of worked layers, and depths of mechanical disturbances are explained. With the results thus ob-

tained, a mechanism of polishing quartz that is explained as the aggregation of micro-scratches by points of abrasives in the process of polishing is described. A model of the polished layer, by which mechanical factors having influence on the vibration loss may be suggested, is shown.

8049 METHODS OF REDUCING THE ENERGY DISSIPATED IN THE SURFACE LAYERS OF QUARTZ by A. G. Smagin (All Union Physicotech. Electronic Meas. Res. Inst.); Soviet Phys. Cryst., Vol. 4, pp. 818-821, June 1960

Methods for reducing energy loss in the surface of quartz crystals used to stabilize standard-frequency sources or in precision frequency meters are described. The Q can be increased to $5-20 \times 10^6$ by the methods. The steps involve grinding the crystals with abrasives used in an appropriate sequence, each successive grinding removing the surface damage caused by the previous grinding. Finally, the crystal is polished until the asymptotic value of Q is attained.

Piezoelectric Microphones in Acoustical Firing Indicator - See 8105

Magnetic Delay Line - See 8124

BASIC SOLID STATE DEVICE CIRCUITS

GENERAL

8050 NETWORK SYNTHESIS WITH NEGATIVE RESISTORS by H. J. Carlin and D. C. Youla (Polytech. Inst. Brooklyn); Proc. IRE, Vol. 49, Part 1, pp. 907-920, May 1960

A consideration of the negative resistor as an additional basic circuit element in linear network analysis and synthesis is presented. This work was stimulated by the development of new solid-state active elements, such as variable-capacitor diodes and tunnel diodes. It is first shown that if the negative resistor is added to the usual set of lumped passive building blocks, then it is possible to represent as a network any linear relation between n-port voltages and currents prescribed in terms of real, rational functions of a complex-frequency variable. This leads to the synthesis of some novel pathologic circuits which have neither admittance nor scattering representations, such as a one-port, which is simultaneously an open circuit and a short circuit ($v = i = 0$, the "nullator"), and the linear network in which voltages and currents at the ports are completely arbitrary (the "norator," the unique, linear nonreciprocal, one-port). These elements are shown to be basic linear circuit building blocks. The second part of the paper considers the synthesis in the frequency domain of a real, rational $n \times n$ admittance matrix in which pole locations and pole multiplicities are completely arbitrary. It is shown that such a matrix can always be realized with lossless elements and at most n positive and n negative resistors.

8051 ELECTRONICALLY-VARIABLE PHASE SHIFTERS UTILIZING VARIABLE CAPACITANCE DIODES by R. H. Hardin, E. J. Downey, and J. Munushian (Hughes Aircraft); Proc. IRE, Vol. 48, pp. 944-945 (L), May 1960

Variable Capacitance diode phase shifters are discussed. In

GENERAL (Cont'd)

the device, a transmission line is terminated in a pure reactance (the capacitance of the reverse biased diode). Energy incident on the termination is reflected with a phase shift which is a function of the diode capacitance. Practical devices have utilized two variable capacitance diode terminations with hybrid rings, hybrid junctions, and certain types of 3-db couplers. Phase shifts of over 180° at 1 kMc, 110° at 6 kMc, and 41° at 9 kMc have been obtained in single unit phase shifters. Maximum insertion loss varied from 1.2 db at 1 kMc to 3.9 db at 9 kMc. At present these phase shifters are useful only at lower power levels and they have a limited phase shift-bandwidth product.

8052 METHODS OF ANALYZING ELECTRIC CIRCUITS WITH MULTITERMINAL NETWORK ELEMENTS [in Russian] by V. P. Sigorskii; Izv. VUZ, Radiotekh., Vol. 3, No. 1, p. 123, 1960

A systematic theory of linear electric circuits with lumped constants is derived. Methods of analyzing linear electric circuits with multiterminal network elements (called generalized methods of contour currents and nodal voltages by the author), based on the replacement of the whole circuit by matrices of equivalent conductivities or equivalent resistivities are shown. The application of the generalized methods to analyze circuits consisting of two-terminal networks, circuits with inductive coupling and circuits with vacuum tubes plus semiconducting triodes is analyzed. Various methods of analyzing electric circuits including methods based on the replacement of the multiterminal network elements by equivalent circuits are compared as are methods based on the splitting of complex circuits into multiterminal network sub-circuits. Special attention is paid to a criticism of the matrix-tensor analysis of G. Kron.

8053 ON NETWORK SYNTHESIS WITH NEGATIVE RESISTANCE by F. T. Boesch and M. R. Wohlers (Polytech. Inst. Brooklyn); Proc. IRE, Vol. 48, pp. 1656-1657 (L), Sept. 1960

A synthesis procedure which permits the synthesis of arbitrary real coefficient rational functions as driving point or transfer impedances utilizing positive resistors, inductors, capacitors, and two-negative resistors is described. The procedure, in each case, results in networks that are realizable with lossy elements arranged in Foster forms.

8054 BIASING METHODS FOR TUNNEL DIODES by R. P. Murray (U.S. Navy School); Electronics, Vol. 33, pp. 82-83, June 3, 1960

The correct circuit impedances and bias to operate the tunnel diode as a switch, amplifier, or oscillator are derived. The total series resistance of the circuit determines the mode of operation. A high resistance is required for operation in the switching mode. The requirements for operation as an oscillator or amplifier are presented and formulas developed.

8055 JUNCTION TRANSISTOR CIRCUITS by J. J. Ward (Rank Cintel); Electronic Tech., Vol. 37, pp. 109-115, Mar. 1960; pp. 143-145, Apr. 1960

A method of calculating current drift due to changes of junction temperature in a direct-coupled transistor circuit with series negative feedback is presented. A brief comparison between this circuit and circuits using parallel feedback is made. Although only a limited number of configurations are analyzed, the treatment is in general terms which are applicable to a

large number of other arrangements. The information derived should enable the design of drift-compensating circuits to be undertaken by less empirical means than are usually adopted; some methods of drift cancellation which suggest themselves from the analysis are discussed. A design example is given together with results obtained from measurements on a practical circuit using silicon transistors.

8056 ON DUAL CONVERSION OF A GYRATOR [in Russian] by Ia. K. Trokhimenko (Kiev Polytech. Inst.); Izv. VUZ, Radiotekh., Vol. 3, No. 6, pp. 661-662, 1960

The representation of gyrators by substitution circuits with dependent generators to permit dual conversion by the simplest means is discussed. The equivalent circuits presented make the physical meaning of the gyrator more graphic because of the use of conventional linear circuit elements.

AMPLIFIERS

8057 POWER GAIN AND STABILITY OF MULTISTAGE, NARROW-BAND AMPLIFIERS EMPLOYING NONUNILATERAL ELECTRON DEVICES by M. Lim (Far Eastern U., Manila); IRE Trans., Vol. CT-7, pp. 158-166, June 1960

An analysis of the gain and stability of a multistage, narrow-band amplifier employing nonunilateral active two-port devices is presented, and some fundamental considerations in the design of such an amplifier are discussed. The amplifier is assumed to consist of n identical stages with input and output terminations. The transducer gain of the amplifier is studied as a function of the interstage and the terminating network parameters. The gain is expressed in terms of a design parameter λ , which is directly related to the terminating conductances of the amplifier. For an amplifier employing inherently stable active devices, there is a value of λ which gives maximum transducer power gain; for an amplifier employing potentially unstable active devices, the optimum transducer power gain of the amplifier usually will be a monotonically decreasing function of λ . In any case the prescribed value of λ determines the maximum gain obtainable from the amplifier.

8058 SIMPLIFICATIONS OF TRANSISTORS SPECIFICATIONS by F. J. Potter and G. Sager (Genl. Dynamics); Proc. IRE, Vol. 48, pp. 2040-2041 (L), Dec. 1960

The practical difficulties involved in the design of high frequency amplifiers by means of the h parameters usually used to specify the small signal characteristics of transistors are discussed. It is suggested that the forward transconductance g_m is a more practical parameter than the input parameter h_i . The simplifications of the common emitter high frequency amplifier design technique of Martin and Schreiber which utilizes only parameters h_{fe} and g_{me} and their respective cutoff frequencies are shown to be realistic.

8059 D-C AMPLIFIER WITH BALANCED CHOPPER by S. Gennon and H. Kembadjian (Mullard); Mullard Tech. Commun., Vol. 5, pp. 97-103, Apr. 1960

A junction transistor balanced chopper which can measure voltages on the order of 100 μ V from low-impedance sources of different impedances and which operates to 45°C is described. Two transistors in a symmetrical circuit reduce error voltage and temperature sensitivity. The design of a dc amplifier which

AMPLIFIERS (Cont'd)

provides 750 mv output for 400 μ v input is presented. The amplifier output is practically a linear function of the input voltage. Chopper response is down 6 db at 50 cps.

8060 SOME RESULTS ON DIODE PARAMETRIC AMPLIFIERS by I. Goldstein and J. Zorzy (Raytheon); Proc. IRE, Vol. 48, pp. 1783 (L), Oct. 1960

Measurements made at room temperature on both S- and X-band parametric amplifiers are discussed. In the S-band amplifier with a signal frequency of 3 kMc, a pump frequency of 11.9 kMc, and a pump power of 10 mw, a gain, bandwidth, and noise figure of 17 db, 50 Mc, and 1.6 ± 0.2 db, respectively were measured. A noise figure of 1.74 db was calculated by the noise figure relation of Penfield. In the X-band amplifier with a signal frequency of 9.9 kMc, a pump frequency of 19.8 kMc and a pump power of 120 mw, gain, bandwidth, and a double sideband noise figure of 20 db, 25 Mc, and 1.2 ± 0.5 db, respectively, were obtained. A noise figure of 1.2 db was calculated.

8061 THE DIODE-LOADED HELIX AS A MICROWAVE AMPLIFIER by G. Conrad, K. K. N. Chang, and R. Hughes (RCA); Proc. IRE, Vol. 48, pp. 939-940 (L), May 1960

An experimental microwave amplifier consisting of an S-band helix loaded with alloyed-diffused germanium diodes is discussed. The helix of 20 mil diameter silver-plated tungsten wire was 6 in long, had an 0.276 in mean diameter and approximately 13 turns per in. The diodes, in ceramic cylinders about 0.1 in in diameter, were mounted between turns of the coil. It was found that the position of each diode on the helix, the pump power, and the pump frequency were critical. No general relations among pump frequency, signal frequency, and diode position and characteristics were found. Typical operating data for an amplifier with two diodes are: signal frequency 2800 Mc, pump frequency 3800 Mc, pump power 60 mw, unloaded helix insertion loss -6 db, net power gain 26 db, voltage gain-bandwidth 30 Mc, and noise figure 5-7 db.

8062 ON THE APPLICATION OF NON-NEUTRALIZED TRANSISTORS IN THE STAGES OF MEDIUM FREQUENCY AMPLIFIERS by M. E. Movshovich and D. N. Shapiro; Telecommun., No. 9, pp. 995-1003, 1960

Certain questions of the theory and calculation of intermediate frequency amplifiers with active non-neutralized four-pole circuits are considered. All of the investigations have reference to semiconductor techniques. An example of the calculation of an actual circuit is given. The relations obtained have been experimentally verified.

8063 TUNNEL DIODE AS AN INTERSTAGE GAIN DEVICE by L. A. LoSasso (Airborne Instr. Lab.); Proc. IRE, Vol. 48, pp. 793-794 (L), Apr. 1960

The use of tunnel diodes to provide impedance transformation and power gain between the stages of a cascade of common base transistor amplifiers is discussed. The gain equations are presented and it is pointed out that the desired gain and stability can be easily obtained since the negative resistance values of presently available tunnel diodes are in the same range as R_{in} in typical transistors. A three stage IF amplifier utilizing tunnel diode coupling has been built. An over-all gain of 60 db was obtained for a bandwidth of 300 kc centered at 10 Mc. The diodes had a negative conductance of -0.02 mho,

a shunt capacitance of 500 pf when operated in the tunnel region, and each diode exhibited a gain of 10 db. The gain per transistor was also 10 db.

Transistorized Video Amplifier - See 8106 and 8107

Super-Regenerative Tunnel Diode Amplifier - See 8096

8064 SEMI-CONDUCTOR SIGNAL AMPLIFIER CIRCUIT by C. J. Wheatley (RCA); U.S. Pat. 2,955,258, Issued Oct. 4, 1960

A more efficient signal amplifier employing opposite conductivity type transistors for push-pull operation is described. Limitation in output voltage capabilities in prior amplifiers has been caused by the need of relatively high dc voltages at the transistor driver stage output to handle voltage variations without clipping. By operating both the driver stage and the push-pull output stage in the common emitter mode and preventing signal output at the load from appearing at the output of the driver stage this limitation has been overcome. Output peak-to-peak voltage equaling battery supply voltage has been attained.

Carrier System Feedback Amplifiers - See 8111

8065 MICROWAVE PARAMETRIC AMPLIFIERS AND CONVERTERS by G. Wade and H. Heffner (Stanford U.); Solid State Phys. Electronics and Telecommun., Academic Press Inc. New York, London, 1960, Vol. 3, pp. 317-321

The use of parametric excitation in amplifiers and frequency converters is discussed. The basic parametric circuit is considered and it is shown that it can operate both as an amplifier and as a frequency converter. The circuit is analyzed to show its gain and noise figure characteristics. Solid state parametric amplifiers and converters, including a converter which utilizes a ladder network to produce an output frequency greater than the pumping frequency, are described.

Microwave Parametric Amplifiers - See 8060

8066 ASPECTS OF WIDE-BAND PARAMETRIC TRAVELLING-WAVE AMPLIFIERS by B. T. Henoch (Res. Inst. Natl. Defence, Stockholm); Ericsson Technics, Vol. 16, No. 1, pp. 77-135, 1960

The interaction between signal and idling waves in a filter ladder containing non-maser reactances and exposed to a pump wave is investigated theoretically. The cases of homogeneous lines and circuits with concentrated elements are considered. Satisfaction of certain phase and dispersion conditions leads to wide-band parametric amplification. The properties of such systems are determined. From the theoretical results filter structures applicable to parametric amplification can be derived. Various filter structures of low-pass and band-pass types which are suitable for different frequency ranges are treated. Finally, the influence of losses and generation of noise are determined. Different measures to minimize the noise figure are discussed.

Bandwidth of Lower Sideband Parametric Amplifiers - See 8102

8067 SUMMARY OF MEASUREMENT TECHNIQUES OF PARAMETRIC AMPLIFIER AND MIXER NOISE FIGURE by R. D. Haun, Jr. (Westinghouse); IRE Trans., Vol. MTT-8, pp. 410-415, July 1960

Expressions for the noise factor of a frequency mixing circuit

AMPLIFIERS (Cont'd)

under two different operating conditions are derived. The conditions are single-sideband operation with input only in a band of frequencies at ω_1 , and double-sideband radiometer operation with incoherent inputs in the bands both at frequency ω_1 and at $\omega_2 = \omega_3 - \omega_1$. In both cases, the output is taken only at ω_1 . It is shown that the noise figure for radiometer double-sideband operation is not always 3 db less than for single-sideband operation. It is also shown that it is possible to obtain an output signal-to-noise ratio which is greater than the input signal-to-noise ratio for coherent double-sideband operation. Methods for measuring the effective noise temperature of this circuit by using a broadband noise source are analyzed.

3068 OPTIMUM NOISE PERFORMANCE OF PARAMETRIC AMPLIFIERS by K. L. Kotzebue (Texas Instr.); Proc. IRE, Vol. 48, pp. 1324-1325 (L), July 1960

The results of an analysis of the noise performance of negative resistance and up-converter parametric amplifiers are presented. It is shown that under optimum conditions the same minimum noise figure can be obtained at room temperature in both amplifiers. Expressions for the source and load resistance required to achieve this minimum noise figure are given. The case of maximum gain, rather than minimum noise figure, in the up-converter is also considered. It is shown that an optimum degenerate parametric amplifier in single sideband operation will have a somewhat higher operating noise temperature than the corresponding optimum negative resistance three-frequency amplifier.

Analysis of Parametric Amplifiers - See 8046

8069 X-BAND SUPER-REGENERATIVE PARAMETRIC AMPLIFIER by B. B. Bossard, E. Frost, and W. Fishbein (USASRDL); Proc. IRE, Vol. 48, pp. 1329-1330 (L), July 1960

An X-band super-regenerative parametric amplifier which utilizes a varactor diode with a cutoff frequency of 41 kMc was described. The amplifier had a gain of greater than 50 db at a bandwidth of 2.4 Mc. The signal and pump frequencies were 8.514 kMc and 10.15 kMc, respectively. The noise figure of the amplifier was 13 db and no appreciable decrease in noise figure could be achieved by increasing the diode Q. This indicates that the major noise contribution is not the spreading resistance of the diode. Varactors with several cutoff frequencies were used but no oscillations were observed with varactors having cutoff frequencies lower than 41 kMc. The experimental results indicate that a super-regenerative parametric amplifier can operate at K-band with presently available varactors.

8070 ON STABILIZING THE GAIN OF VARACTOR AMPLIFIERS by B. J. Robinson, C. L. Seeger, K. J. van Damme, and J. T. de Jager (Leiden Observatory); Proc. IRE, Vol. 48, p. 1648 (L), Sept. 1960

The stabilization of power gain of regenerative varactor amplifiers is discussed. The gain can be made independent of pump power level if the amplitude of the pump voltage is close to the value of the bias voltage. The degree of saturation depends on the tuning of the signal and pump circuits. The gain stability can be further increased by utilizing the varactor dc current to control the pump level. A circuit for controlling pump power is presented. Ambient temperature variations have not influenced the gain stability of amplifiers utilizing this stabilization scheme. The instability of a 400 Mc amplifier at

gain settings of 20 - 25 db has been found to be of the order of, or less than, one part in a thousand over periods of 1/2 hr or more.

8071 17.35 AND 30-kMc PARAMETRIC AMPLIFIERS by B. C. DeLoach (Bell Labs.); Proc. IRE, Vol. 48, p. 1323 (L), July 1960

Measurements made on two parametric amplifiers are discussed. A 17.35 kMc amplifier which utilized GaAs point contact diode has a double sideband noise figure of less than 6 db. Amplification and oscillations were also obtained with another type of GaAs point contact diode and with small area n- and p-type silicon p-n junction diodes. In a 30 kMc amplifier specially designed diodes were built into the waveguide circuit and a new traveling wave amplifier tube was used to supply the 60 kMc pump power. Gain and subharmonic oscillations were obtained with GaAs point contact diodes and with p- and n-type silicon diodes. Subharmonic oscillations were obtained with as little as 28 mw of pump power.

8072 A FERROMAGNETIC AMPLIFIER USING LONGITUDINAL PUMPING by R. T. Denton (Bell Labs. and U. Michigan); Proc. IRE, Vol. 48, pp. 937-938 (L), May 1960

A ferromagnetic amplifier which utilizes longitudinal pumping (RF magnetic field parallel to the dc magnetic field) is described. A sphere of single crystal yttrium iron garnet 0.043 in diameter was mounted in a half-wave X-band cavity at a point of maximum RF magnetic field and spaced 0.075 in from the cavity wall. A loop of wire was threaded through holes in the cavity wall and around the sphere, which had a linewidth of 0.40 oe in a plane containing the dc and RF magnetic fields to provide coupling from a coaxial line into the sample. CW pump excitation of the cavity at 9196 Mc was then applied at a power level of 500 mw. The dc field was adjusted to single out one pair of modes and the pump power was reduced to obtain amplification. Amplification with modes at 4626 Mc and 4570 Mc is discussed. Gain of 25 db with a signal frequency in the 4000 Mc range has been obtained.

8073 A FERROMAGNETIC AMPLIFIER USING DIELECTRIC LOADING by H. Gruenberg (Syracuse U.); Proc. IRE, Vol. 48, pp. 1779-1780 (L), Oct. 1960

The use of dielectric loading to reduce the pumping power required by a ferromagnetic parametric amplifier is discussed. A single crystal disc of yttrium iron garnet 0.132 in diameter and 0.027 in thick was located at a point of maximum pump and signal fields in a cavity with internal dimensions 0.618 x 0.384 x 0.210 in and the remainder of the cavity was filled with Stycast Hy K dielectric, which has a dielectric constant of 10. The cavity was designed to be resonant in the TE_{012} mode at pump frequency of ~ 9300 Mc and in the TE_{101} mode at the signal frequency of 5900 Mc. A dc magnetic field was applied parallel to the RF signal field at the sample. Amplification has been observed at dc fields of 700 and 1600 oe. Pumping powers of a few watts peak were required but theoretical estimates indicate that an improvement by at least a factor of ten is possible.

8074 PROPOSED PARAMETRIC AMPLIFIER UTILIZING FERRO-ELECTRIC SUBSTANCE by Y. Aoki (Osaka City U.); IRE Trans., Vol. MTT-8, pp. 465-466 (L), July 1960

The use of ferroelectric materials in microwave parametric amplifiers is discussed. To reduce reflections the length of the ferroelectric material must be an integer multiple of the half

AMPLIFIERS (Cont'd)

wavelength of the signal, idling, and pumping frequencies in the material. The opposite faces of the material must be exactly parallel to each other and the surface roughness must be minimized. The dielectric constant of the material should not vary with frequency and the device should operate with a low pumping power, particularly at high frequencies. The characteristics of amplifiers utilizing two different ferroelectric materials are presented.

8075 INTERACTION OF TWO MICROWAVE SIGNALS IN A FERROELECTRIC MATERIAL by I. Goldstein (Raytheon); Proc. IRE, Vol. 48, p. 1665 (L), Sept. 1960

Some observations made in a degenerate mode parametric amplifier utilizing polycrystalline barium titanate operated at room temperature are discussed. It was found that there was an exchange of energy from the pump frequency to the signal frequency in the ferroelectric material via the idler frequency. No gain was obtained at 1200 Mc and 820 Mc since there was too much loss in the system. The permittivity of the material can be varied at microwave frequencies making it useful in a ferroelectric parametric amplifier.

Parametric Amplifiers with Silver Bonded Diodes - See 8007

8076 NOTE ON THE NOISE FIGURE OF NEGATIVE CONDUCTANCE AMPLIFIERS by A. van der Ziel and J. Tamiya (U. Minnesota); Proc. IRE, Vol. 48, p. 796 (L), Apr. 1960

The coupling of a negative conductance amplifier such as a tunnel diode or parametric amplifier to a receiver is analyzed. Two situations, connecting the amplifier directly to the receiver and connecting the amplifier by means of a lossless step-down transformer of suitably chosen turn ratio, are considered. In both cases it is shown that the coupling can be achieved without a significant increase in the noise figure of the amplifier.

Tunnel Diode Amplifiers - See 8009 and 8010

8077 ABSOLUTELY STABLE HYBRID COUPLED TUNNEL-DIODE AMPLIFIER by J. J. Sie (RCA); Proc. IRE, Vol. 48, p. 1321 (L), July 1960; p. 1783, Oct. 1960

A hybrid coupled tunnel diode amplifier constructed with two matched germanium tunnel diodes and a quarter wave stripline coupled hybrid is discussed. The amplifier has reasonable gain (8.2 ± 0.6 db), extremely wide bandwidth (210 - 625 Mc), low noise (noise figure measured at 365 Mc is 1.93 ± 0.4 db), and is both open- and short-circuit stable at the input without any nonreciprocal device.

8078 TRANSISTOR CIRCUITS WITH ELEVATED INPUT RESISTANCE [in Russian] by V. I. Lebedev (Engrg.-Phys. Inst., Moscow); Izv. VUZ, Radiotekh., Vol. 3, No. 3, pp. 386-393, 1960

An analysis of some circuit means of increasing the input resistance of transistor amplifiers is presented. These means are: (1) a simple emitter follower, (2) a composite emitter follower, and (3) the connection of a resistor in the base loop of a circuit with a common emitter. The maximum value of the input resistance obtained in practice is 15 megohms. The possibility is discussed of producing an R_{in} of several tens of megohms, which is significantly larger than the value of r_c (the differential resistance of the collector junction). The temperature stability

and frequency dependence of the input resistance are analyzed.

8079 TUNNEL (ESAKI) DIODE AMPLIFIERS WITH UNUSUALLY LARGE BANDWIDTHS by E. W. Sard (Airborne Inst. Lab.); Proc. IRE, Vol. 48, pp. 357-358, Mar. 1960

The design and performance of three connections of negative conductance amplifiers operated with lumped-constant filters that give an over-all maximally-flat response are discussed. In the reflection type connection the generator and load are located at one port of the filter and the negative conductance at the other port. A second connection is the reflection type operated with a circulator to isolate the generator and load. The third connection, the transmission type, has the generator and negative conductance located at one port of the filter and the load at the other port. In general the transmission type connection has less bandwidth than the reflection type.

8080 TRANSISTOR CLASS B SIGNAL AMPLIFIER CIRCUIT by J. E. Lindsay (RCA); U.S. Pat. 2,955,257, Issued Oct. 4, 1960

A reliable class B transistor amplifier, stabilized to variations in temperature and to the interchanging of transistors without effecting a decrease in gain or an increase in circuit components, is described. Pairs of opposite conductivity type transistors are employed in the driver and output stages of the amplifier. During positive half cycles the n-p-n driver and output transistors provide the amplification path; during negative half cycles the p-n-p driver and output transistors function. A low resistance voltage divider network fixes the operating points of the transistors and provides circuit stabilization.

Magnetic Equivalent Class "A", "B", and "C" Amplifiers - See 8093

OSCILLATORS

8081 HIGH FREQUENCY TRANSISTOR POLYPHASE OSCILLATOR by T. Takagi and K. Mano (Tohoku U.); Rep. Res. Inst. Elect. Commun., Tohoku U., Ser. B, Vol. 12, No. 1, pp. 1-25, 1960

The condition for oscillation of a transistor polyphase oscillator is discussed. The transistor oscillator is better suited for a high frequency oscillator than conventional types. The device has many oscillation modes and the number of phases can be selected freely so as to satisfy the optimum condition for oscillation.

8082 TRANSISTOR OSCILLATOR CIRCUITS by R. B. Jackson (Natl. Res. Dev., London); U.S. Pat. 2,960,665, Issued Nov. 15, 1960

A transistor oscillator capable of giving sinusoidal output with frequencies from 500 cycles per second to 170 kilocycles per second is described. A series connected R-C circuit between collector output and emitter input serves as a feedback path. Shape of output waveform is set by the resistance and variation in the capacity provides the frequency control for the circuit.

Microwave Generator - See 8087

Voltage Tuning in Microwave Oscillators - See 8089

Millimeter Wave Generator - See 8088 and 8090

OSCILLATORS (Cont'd)

8083 COMPLEMENTARY TRANSISTOR MULTIVIBRATOR by C. Huang; U.S. Pat. 2,956,241, Issued Oct. 11, 1960

A free-running multivibrator comprising a pair of complementary transistors arranged in a symmetrical circuit with mutual feedback paths is described. The transistors are turned on and off simultaneously rather than alternately by direct current bias. Duty cycle is a function of the time constants in the mutual feedback circuits and can be adjusted by varying values of circuit elements.

8084 ANALYSIS OF A SEMICONDUCTOR MULTIVIBRATOR WITH Emitter CAPACITANCE [in Russian] by E. F. Doronkin (Kiev Polytech. Inst.); Izv. VUZ, Radiotekh., Vol. 3, No. 1, pp. 106-111, 1960

Multivibrators with timing condensers connected in the triode emitter loops that are stable at elevated temperatures are discussed. An analysis is made of a multivibrator with emitter capacitance; computational formulas are derived and results of an experimental investigation are presented.

8085 SWEEP CIRCUIT by R. M. Willett; U.S. Pat. 2,923,837, Issued Feb. 2, 1960

A transistorized, triggered, linear sweep circuit is described. The circuit employs two Ge or Si transistors to control the alternate charging and discharging of a capacitor from a constant current source. Triggering for the sweep circuit is provided by a one shot multivibrator. The unit is designed for use with cathode ray oscilloscopes where a high degree of linearity is desired.

8086 A HIGH FIELD EFFECT TWO-TERMINAL OSCILLATOR by R. W. Lade and T. R. Schlax (Marquette U.); Proc. IRE, Vol. 48, pp. 940-941 (L), May 1960

The use in oscillators of the negative resistance associated with avalanche multiplication in reverse biased junctions is discussed. The minimum and maximum negative resistances required for oscillation are derived. An oscillator was constructed utilizing the collector-base junction of a 2N147 transistor. Very low signal distortion was obtained with this circuit. The large quiescent currents which flow in the narrow base region when the junction is biased in the negative resistance region, however, cause the junction temperature to rise and the performance of the oscillator is deteriorate.

8087 A PARAMETRIC SUBHARMONIC OSCILLATOR PUMPED AT 34.3 kMc by A. H. Soloman and F. Sterzer (RCA); Proc. IRE, Vol. 48, pp. 1322-1323 (L), July 1960

A very high frequency parametric subharmonic oscillator using a specially packaged variable capacitance germanium junction diode in a ridged waveguide circuit is described. The device requires less than 4 mw of 34.3 kMc pump power to produce oscillations at the subharmonic frequency of 17.15 kMc and has a maximum conversion efficiency of about 7 per cent. It operates at considerably higher frequency and requires considerably less pump than previously reported subharmonic oscillators.

8088 MILLIMETER WAVE GENERATION BY PARAMETRIC METHODS by G. H. Heilmeier (RCA); Proc. IRE, Vol. 48, pp. 1326-1327 (L), July 1960

The generation of millimeter waves by means of the nonlinear

capacitance of reverse-biased point contact GaAs diodes is discussed. The n-type diode was mounted, flush with the bottom of the harmonic guide, at the junction of a K-band fundamental guide (18-26 kMc) and an RG98U harmonic guide (45-75 kMc). The harmonic generator also included an RF by-pass so that dc bias can be used, a differential screw on top of the guide so that very low pressure contacts can be made to the crystal, and shorting plungers behind the crystal in both guides for matching purposes. An output of 48 kMc was obtained from an input of 24 kMc with a conversion loss of 9 db and zero bias. An explanation of the superior characteristics of GaAs nonlinear capacitance diodes over Ge diodes in millimeter wave generation is presented.

8089 VOLTAGE TUNING IN TUNNEL DIODE OSCILLATORS by J. K. Pulfer (Nat'l. Res. Counc., Ottawa); Proc. IRE, Vol. 48, p. 1155 (L), June 1960

Voltage tuning ranges of experimental microwave tunnel diode oscillators are discussed. In one oscillator the diode was mounted at one end of a low impedance coaxial line and the other end of the line was terminated in a matched load. The operating voltage was applied across the matched load. Voltage tuning ranges of up to 12 per cent have been obtained by varying the operating bias of the oscillator. The power output was approximately -30 dbm. When a quarter wave re-entrant cavity was added in the center conductor of the coaxial line a voltage tuning range of about 1.3 per cent at 1500 Mc was obtained. The power output of this oscillator was -15 dbm. Both oscillators could be tuned mechanically over a 30 per cent bandwidth with little change in output.

8090 MILLIMETER WAVE ESAKI DIODE OSCILLATORS by C. A. Burrus (Bell Labs.); Proc. IRE, Vol. 48, p. 2024 (L), Dec. 1960

Esaki diode oscillators which exhibit fundamental oscillations up to 103 kMc (2.9 mm wavelength) are discussed. The diodes, made by electrically "forming" a point contact between zinc and heavily doped n-type gallium arsenide, have peak currents ranging from a few hundred pa to several ma and peak-to-valley ratios of 3 to 1 or better. The diodes were built into reduced height rectangular waveguides with a movable shorting piston behind the diode. The diode was followed by an attenuator, cavity wavemeter, and video detector diode. The rectified output of the detector was fed directly to an oscilloscope preamplifier and bias for the oscillator was supplied from low impedance dc or 60 cps ac sources. It was found that the frequency of oscillation depended upon both the waveguide size and the diode and that both "strong" and "weak" oscillations occurred. The frequency of oscillation could generally be varied 10 to 15 per cent by movement of the waveguide piston and oscillation was completely suppressed at regular intervals of the piston position. The maximum power output was 25 μ w at 50 kMc. At 90 kMc the power output was about 2 μ w and at 100 kMc a few tenths of a microwatt.

Tunnel Diode Oscillators - See 8009 and 8109

SWITCHING CIRCUITS

Design of Magnetic Matrix Switch - See 8121

SWITCHING CIRCUITS (Cont'd)

8091 TRANSISTOR SWITCHING-CIRCUIT DESIGN USING THE CHARGE-CONTROL PARAMETERS by R. Beaufoy (Brit. Telecommun. Res. Ltd.); ATE J., Vol. 16, pp. 141-152, Oct. 1960

Charge-control parameters considering the operations of switching on, holding on and switching off a transistor, and a simple figure of merit for a switching transistor are derived. Expressions are derived for the switching times and switching currents to provide the changes of charge required to switch a given current, and approximate expressions which clearly reveal the effects on performance of the various parameters are presented. Some examples of circuit design in terms of a typical transistor specification are then given. Following the design of an Eccles-Jordan circuit, the ability of the circuit to control a number of compatible gate circuits is discussed. Recommendations on the form of specification for the various parameters are made.

High Speed Magnetic Switch - See 8119

Gate Circuits for Digital Computers - See 8122

8092 SEMICONDUCTOR SPEECH-PATH SWITCHES SUITABLE FOR DIRECT-COUPLED CONNECTION by I. Endo and S. Yoshida (Nippon Tel. and Tel.); Rev. Elect. Commun. Lab. NTT, Vol. 8, pp. 105-111, Mar.-Apr. 1960

Three types of bilateral speech-path switches for all-electronic telephone exchange systems are described. Elementary semiconductor speech-path circuits which can be connected with each other directly, without using coupling circuits such as transformers or capacitors between stages are obtained. This feature is desirable for multistage connection in a large scale exchange system. The first circuit uses a diode bridge, the second circuit uses grounded base p-n-p and n-p-n transistors connected alternately, and the third circuit uses a compound p-n-p-n transistor made up of one n-p-n transistor and one p-n-p transistor. For practical use, the last circuit seems to be the most promising.

Tunnel Diode Switches - See 8009 and 8010

8093 TRANSFER CIRCUITS FOR ELECTRIC SIGNALS by J. Albin (Soc. d'Electronique et d'Automatisme); U.S. Pat. 2,956,266, Issued Oct. 11, 1960

An improved magnetic transfer circuit employed to register two-level or rectangular signals upon recording media is described. The elementary transfer circuit comprises a pair of magnetic cores with associated activation, routing, and transfer windings. A selective routing transfer device utilizing a plurality of elementary circuits is discussed and its equivalence to "Class-A," "Class-B," and "Class-C" vacuum tube amplifiers is cited.

8094 SHIELDED SUPERCONDUCTOR CIRCUITS by J. J. Lentz (IBM); U.S. Pat. 2,966,647, Issued Dec. 27, 1960

Gating circuits employing thin films of superconducting material are described. The cryotron devices cited are fabricated by successively evaporating, under high vacuum, layers of insulating, "hard," and "soft" superconductive materials upon a substrate. Induced deleterious circulating currents are eliminated in the devices by employing the superconductor shields as return paths for the current in the circuits.

SIGNAL CONVERTERS

8095 A NEW USE OF THE JUNCTION TRANSISTOR AS A PULSE-WIDTH MODULATOR by I. Tagoshima (Japan Broadcastg Proc. IRE, Vol. 48, p. 1663 (L), Sept. 1960

A technique for modulating the output pulse width of junction transistors in the common emitter configuration is described. The transistors are operated in the saturation region and the amplitude of the input base current is modulated at audio frequencies. The output amplitude remains constant because the collector load resistance and collector bias supply voltage are fixed. A circuit for modulating pulse widths by this technique is presented. The pulse width modulation circuit can be used as a pulse-delaying element in pulse and logic circuits.

Germanium p-i-n Millimeter Modulator - See 8006

8096 ESAKI DIODES AS SUPER-REGENERATIVE DETECTORS by A. G. Jordan and R. Elco (Carnegie Inst. Tech.); Proc. IRE, Vol. 48, p. 1902 (L), Nov. 1960

The operation of a super-regenerative amplifier is described, and a schematic diagram of a super-regenerative detector using an Esaki diode is presented. The diode is biased in the negative resistance region and the amplitude of the quench voltage is of such a value that the operating point moves beyond the valley to a positive resistance, causing the oscillations to decay. Oscillograms of oscillations for different signal levels using a sinusoidal quench and oscillations obtained using a modulated signal for different carrier frequencies in the vicinity of the oscillator frequency are presented.

8097 PARAMETRIC DIODES IN A MASER PHASE-LOCKED FREQUENCY DIVIDER by M. L. Stich, N. O. Robinson (Hughes Aircraft), and W. Silvey (Aeroneutronic Systems); IRE Trans., Vol. MTT-8, pp. 218-221, Mar. 1960

The use of an ammonia-beam maser in a portable frequency standard requires a frequency divider which can be transistorized. A divider which uses no microwave tubes and hence one that can be transistorized is described. An ammonia-maser controlled signal generator used to tune up the divider is also described. It is found that the use of a parametric diode frequency multiplier substantially improves the lock-in performance of the divider. Data are given for comparing the performance of the maser frequency divider with and without the parametric diode frequency multiplier.

8098 APPLICATION OF THE HALL EFFECT IN FREQUENCY DIVIDERS by V. S. Andreyev, M. E. Mazurov, and I. N. Prudnikov; Telecommun., No. 9, pp. 958-970, 1960

A number of regenerative frequency divider circuits which utilize semiconductor Hall generators as frequency converters are described. Circuits which divide the frequency by two are discussed in detail and experimental results are given.

8099 UHF HARMONIC GENERATION WITH SILICON DIODES by D. Leenov and J. W. Rood (Bell Labs.); Proc. IRE, Vol. 48, p. 1335 (L), July 1960

The use of a diffused junction silicon diode with a large breakdown voltage in a harmonic generator to achieve high harmonic power output with high efficiency is discussed. Generators have given 1.1 watts of second harmonic power at 800 Mc with an efficiency of 48 per cent, 166 mw of fourth harmonic power at 160 Mc with 17 per cent efficiency and 2 mw of X-band

SIGNAL CONVERTERS (Cont'd)

power with 0.6 per cent efficiency by multiplying an 1800 Mc input. The relation between power handling ability and breakdown voltage was investigated by measurements on a 7 volt breakdown voltage diode and on a 41 volt breakdown voltage diode. For some input power levels the seven volt diode gave efficiencies of over 50 per cent for doubling 400 Mc. The output began to saturate at 10 mw. The 41 volt diode also gave efficiencies of over 50 per cent for this conversion, with a wider range of input power levels, and the output began to saturate at about 1.1 watts.

3100 MICROWAVE FREQUENCY DOUBLING AND MIXING IN FERRITES by W. P. Ayres, J. L. Melcher, and P. H. Vartanian, Jr. (Sylvania); U. S. Pat. 2,922,876, Issued Jan. 26, 1960

The use of ferrites as frequency doublers at microwave frequencies is discussed. Frequency doubling occurs when a dc magnetic field applied to the ferrite in a waveguide is parallel to the E-vector of the signal to be doubled. An arrangement for converting X-band to K-band frequencies is described. Using this arrangement a conversion efficiency of -6 db has been obtained for a 32 kw peak input at 9 kMc with a semicircular ferrite disk mounted with the flat side against one narrow wall of the guide at an equal distance from both of the wide walls of the guide. Other geometries and configurations of the ferrites are also discussed. The arrangement can also be used to mix two signals of different frequencies provided that the magnetic field components of the two signals are perpendicular to the internal magnetic field of the ferrite.

8101 SOLID-STATE MICROWAVE POWER SOURCES USING HARMONIC GENERATION by R. Lowell and M. J. Kiss (Bell Labs.); Proc. IRE, Vol. 48, pp. 1334-1335 (L), July 1960

An harmonic generator for converting VHF power to X-band power is described. The generator consists of three sections, viz., a single transistor oscillator which operates at 218 Mc, a varactor diode fifth harmonic generator that converts the 218 power to 1090 Mc power, and a varactor diode eighth harmonic generator that converts the 1090 Mc power to 8720 Mc power. The transistor, a developmental n-p-i-n transistor, is connected in a common base circuit with pi-network load coupling. Two different diodes are used, a high breakdown, moderate Q diode in the fifth harmonic circuit and a high Q low breakdown diode in the eighth harmonic circuit. This combination of diodes results in an efficient two step conversion of power. With a dc input power of 4 w, 2 mw and 160 mw of power have been obtained at 8720 Mc and 1090 Mc, respectively.

8102 BANDWIDTH OF LOWER SIDEBAND PARAMETRIC UP-CONVERTERS AND PARAMETRIC AMPLIFIERS by S. T. Fisher (Philco); Proc. IRE, Vol. 48, p. 946 (L), May 1960

A simplified expression for the gain of a lower-sideband up-converter as a function of a stability factor α and a frequency factor x is given. The expression allows the bandwidth to be expressed directly as a function of α . The bandwidth and $(\text{gain})^{\frac{1}{2}}$ — bandwidth product can then be evaluated directly for any value of gain from zero to infinity. It has been found that the simplified expression is identical to the more complex expression desired by Rowe.

Parametric Converters - See 8065 and 8122

WAVE GENERATORS

Microwave Generator - See 8087

Millimeter Wave Generator - See 8088 and 8090

8103 A LOW-LEVEL PULSE-HEIGHT STANDARD by T. E. Lomasson and W. W. Grannemann (U. New Mexico); Proc. IRE, Vol. 48, p. 361 (L), Mar. 1960

A circuit which can produce calibrated low level pulses in the range 0 - 2v with an accuracy better than one half per cent of full range is described. The accuracy is limited on short pulses by the overshoot of the transistor. The use of new high frequency transistors can, however, overcome this limitation. A 2N502 transistor can be used to obtain pulses down to 0.2 μ sec with rise and fall times of 0.08 μ sec.

Transistor Linear Sweep Circuit - See 8085

APPLICATIONS OF SOLID STATE DEVICES

MEDICAL AND MILITARY

8104 DETECTING MUSCLE POTENTIAL IN UNANESTHESIZED ANIMALS by S. Bagno (Kidde Ultra. and Det. Alarms), F. Lieberman, and F. Cosenza (New York U.); Electronics, Vol. 33, pp. 58-59, Oct. 7, 1960

An instrument for detecting muscle activity in an unanesthetized animal is described. The instrument consists of a part implanted in the animal which is inductively coupled to a part exterior to the animal. The interior part includes a pair of electrodes placed in the muscle; and a transistor amplifier, a coil, and a rectifier all implanted in neighboring tissue. A voltage is induced in the implanted coil by the external coil driven by an oscillator. The induced voltage is rectified by the diode to provide power for the transistor. The potential generated by muscular activity is applied to the base of the transistor, causing the collector current to change. The collector current flowing through the implanted coil, acts as a partial short or load across the external coil and its magnetic field intensity varies with the muscle potential. A voltage induced in a second external coil is rectified and applied to the base of a transistor which provides an output that follows the muscle potential.

8105 ACOUSTICAL FIRING INDICATOR by J. I. Mattei, J. Blaise, and R. Manganne (Off. Natl. d'Etudes et de Recherches Aero.); U.S. Pat. 2,925,582, Issued Feb. 16, 1960

A system for determining the distance and direction of miss of supersonic bullets fired at a target, during target practice, from a fighter plane is described. Microphones which utilize square plates of piezoelectric ammonium dihydrogen phosphate are placed about the target. The microphones detect the leading and trailing edges of the ballistic N wave. The signal is transmitted to a receiver which computes the target-trajectory distance and direction.

TELEVISION

8106 TV SIGNAL AMPLIFIERS USING DRIFT TRANSISTORS by I. G. McInnes (Radio); Proc. IRE, Austl., Vol. 21, pp. 265-270, Apr. 1960

A four-stage TV IF strip, video amplifier and intercarrier sound unit using drift transistors is described. The IF conforms to Australian Broadcasting Control Board recommendations. The single stage video amplifier is capable of 80 volt peak-to-peak output, sufficient to drive a conventional picture tube. A 5.5 Mc intercarrier IF ratio detector and audio amplifier using transistors completes the sound channel.

8107 HIGH-FREQUENCY CORRECTION IN TRANSISTOR VIDEO AMPLIFIERS USING RC COUNTER-COUPLING IN THE Emitter LOOP [in Russian] by I. N. Pustynskii (Tomsk Polytech. Inst.); Izv. VUZ, Radiotekh., Vol. 3, No. 5, pp. 502-508, 1960

An analysis of a single stage video amplifier which employs a planar transistor in a circuit with a common emitter is presented. The high-frequency correction, with RC-counter-coupling taking account of the inertia of the transistor and the capacitance in the collector loop, is considered. Formulas and graphs are presented for an engineering computation of the correction elements. The computational results are verified experimentally.

8108 WIDE-BAND TRANSISTORIZED VIDEO AMPLIFIER by E. Naess (Diamond Ord. Fuze Labs.); U.S. Gov. Res. Rep., Vol. 33, p. 377 (A), Apr. 15, 1960 PB 144 710

The design and construction of a miniaturized wideband video amplifier utilizing 2N502 transistors is presented. The final design occupies a volume of 0.7 cu in., weighs 5 oz, and operates with 0.2 w input at 12 v. It has a 65 db voltage gain, 60 Mc bandwidth, and one volt output across a 1000-ohm impedance.

8109 THE TRANSISTORIZED TV RECEIVER USING A NEW HORIZONTAL DEFLECTION SYSTEM by T. Miura and K. Mano (Tohoku U.); Rep. Res. Inst. Elect. Commun., Tohoku U., Ser. B, Vol. 12, No. 1, pp. 41-55, 1960

A transistorized circuit for the horizontal deflection system of a TV receiver is described. Experimental results show that the circuit is satisfactory in systems up to 17" - 90° TV receivers. A complete TV receiver, including video detector, video amplifier, sync separator, vertical deflection and horizontal deflection circuits is shown in detail.

8110 THE DISTRIBUTION OF HIGH-DEFINITION TELEVISION SIGNALS BY MEANS OF TRANSISTORIZED EQUIPMENT [in French] by P. Blancheville (Corps Telecommun., Service Etudes RTF); Onde Elect., Vol. 40, pp. 440-449, June 1960

An analysis concerning the possible use of transistors in TV distribution amplifying equipment is presented. The performance required from such equipment in order to maintain the signal quality is examined and the corresponding methods of measurement described. The basic properties of transistors are reviewed and an analysis is given of the principles of an arrangement which meets the previously determined requirements. The possibilities of development in the design of television equipment using semiconductors is dealt with.

TELEPHONY AND TELEMETRY

8111 A TRANSISTOR AMPLIFIER WITH HEAVY FEEDBACK FOR 12-CHANNEL OPEN-WIRE CARRIER SYSTEMS by A. W. Thies (Postmaster Genl. Dept., Melbourne); Proc. IRE, Austl., Vol. 21, pp. 91-98, Feb. 1960

After a brief outline of the laws controlling single-loop feedback amplifier design, the merits of the three fundamental transistor connections in feedback circuits at high frequencies are compared. Cascaded common-emitter stages are recommended for most applications. A three stage amplifier which uses silicon transistors and operates at frequencies from 92 to 143 kc with approximately 40 db of feedback is described. Properties of hybrid coil feedback are discussed.

Speech-Path Switches for All-Electronic Telephone Exchange Systems - See 8092

Lightning Protection for Transistor Repeaters - See 8154

8112 NEW APPLICATIONS OF ELECTRONICS IN POWER INSTALLATIONS [in French] by R. Colin and L. Bousquet (Ctr. Natl. d'Etudes des Telecommun.); Onde Elect., Vol. 40, pp. 733-741, Oct. 1960

The application of semiconductor devices in power supplies employed in the regulation and conversion of current in telecommunication centers is described. A sketch of the general problems encountered in designing such systems is presented. Two replacement systems for rotary machine equipment are discussed in detail. One system comprises a transistorized tone generator, the other a power control device that employs transistors and thyratrons. A large portion of the article is devoted to this latter device which seems likely to have wide application in the electronics field.

8113 MICROMINIATURE MULTICHANNEL PULSE-POSITION-MODULATION SYSTEM INCORPORATING TRANSISTOR-MAGNETIC-CORE CIRCUITRY by H. Kihn, R. J. Klensch, and A. H. Simon (RCA); RCA Rev., Vol. 21, pp. 199-227, June 1960

An experimental five-channel time-division multiplex system incorporating a microminiature transistor-core ring counter for both the transmitter modulator and receiver sampler is described. The pulse-position modulation of the transmitter modulator results from the variable time triggering of a transistor-core pulse generator by the variation of either the transistor input voltage or ferrite-core coercive-force thresholds. The sampling rate used in the system is 15 kc with an upper limit set only by the transistor and core high-frequency cutoff. Channel cross talk as low as -40 db may be obtained by suitable adjustment of operating parameters. Increased isolation can be obtained by reduction of repetition rate and use of a faster transistor such as the 2N139 or equivalent. Power consumption is approximately 200 milliwatts at the 15 kc rate. Linearity is adequate (of the order of several per cent) for voice communication, but could be improved by optimization of drive and by trigger-current shaping to compensate for hysteresis-loop curvature.

RADAR AND MICROWAVES

8114 RADAR DUPLEXING BY FERRITE AND GAS DISCHARGE DEVICES by D. H. Pringle and G. S. Baldcock (Ferranti); Solid State Phys. Electronics and Telecommun., Academic

ADAR AND MICROWAVES (Cont'd)

ress, Inc., 1960, Vol. 3, pp. 384-395

adar duplexing by ferrite and gas discharge devices is discussed. A circulator employing a gyrator, a circulator employing Faraday rotation, and a ferrite pulsed attenuator for use with the circulators, are considered. A ferrite duplexer has virtually infinite life, greater stability during life, no "spike" leakage, much shorter recovery time, and provision for isolation from aerial mismatch without a separate ferrite isolator required. The TR duplexer, on the other hand, has smaller bulk and weight, provides passive protection, provides adequate crystal protection, requires no additional pulse circuitry, can cover a wide frequency band easier than a complete ferrite duplexer, and has no low frequency limitation.

censors as Code Converters - See 8040

Microwave Generator - See 8087

Microwave Power Source - See 8101

Millimeter Wave Generator - See 8088 and 8090

TAPE RECORDERS

1115 POCKET-SIZE DICTATING MACHINE by L. Hannemann (Protona); Electronics, Vol. 33, p. 73, Oct. 28, 1960

A miniature six transistor tape recorder is described. The instrument utilizes a two track tape magazine, transistorized voltage regulators, and a three stage resistance-coupled amplifier. The tape speed permits 30 minutes of recording per track. The battery-operated recorder weighs 2 lbs and measures 3-15/16 x 5-11/16 x 1-9/16.

1116 MAGNETIC RECORDING TAPE by D. K. Hausen (Commonwealth Engrg.); U.S. Pat. 2,923,642, Issued Feb. 2, 1960

Magnetic recording tapes which have large storage capacities because of the use of magnetic layers on both sides of the tape are discussed. Film of aluminum is utilized to provide magnetic shielding between the magnetic layers. In one tape an aluminum film is applied to both sides of a Mylar tape, a magnetic layer about 0.001 mm thick is applied to both aluminum films, and the recording layers are covered by a protective coating of Mylar film. In another tape the central region consists of a strip of aluminum. Successive layers of Mylar, magnetic material, and Mylar are applied on both sides of the aluminum film. Two parallel magnetic tracks may be produced on each side of the tape.

1117 THE MECHANICAL CONSIDERATIONS OF MAGNETIC RECORDING HEADS by M. B. Martin (Data Rec. Instr. Engrg.); Brit. IRE, Vol. 20, pp. 877-883, Nov. 1960

The mechanical limits imposed on magnetic recording heads by the required performance specification are discussed. The performance criteria of a multi-track head are normally: sensitivity and the variation in sensitivity between tracks, the short wavelength response, high-frequency losses, bias sensitivity and cross talk between adjacent tracks. The manufacturing problems associated with multi-track heads are discussed in relation to the effects of mechanical variations on the head performance.

Assessment of Magnetic Tape for Data Storage - See 8131

Magnetic Tape Recording of Digital Data - See 8130 and 8132

Magnetic Readout Head - See 8127

COMPUTERS

8118 TRANSISTOR-RESISTOR LOGICAL CIRCUITS by P. D. T. Hawker (Mullard); Electronic Applic., Vol. 21, No. 1, pp. 32-40, 1960-61

The operation of a basic transistor-resistor logic circuit is described and the design and performance equations are derived. The simplicity of the circuit leads to economy, reliability and ease of design. By way of illustration, circuits using the switching transistors type OC46 and OC47 are designed. Modifications to the basic circuit which give greater gain or faster operation are included.

8119 THE "SYMMAG" A HIGH-SPEED STATIC MAGNETIC SWITCH [in French] by M. Dumaire (Soc. Electronique et Automatisme); Onde Elect., Vol. 40, pp. 561-664, Oct. 1960

The Symmag, which is related in principle to magnetic pulse-amplifiers and is a device developed for the commercial production of binary counter circuits, is described. It is usable up to frequencies of several hundred kilocycles. Its principle and characteristics show possible application in the field of industrial calculation where reliability and convenience are of primary importance.

8120 MULTISTABLE MAGNETIC CORE CIRCUITS by G. A. Hardenbergh; U.S. Pat. 2,958,787, Issued Nov. 1, 1960

Several circuits employing magnetic cores which are capable of more than two states of magnetic retentivity are described. Magnetic cores which exhibit a high ratio of limiting remanent state flux density to saturated flux density have been found to undergo a change in flux density which is proportional to the integral of the applied electrical force. The application of a predetermined number of magnetizing impulses, each with a particular amplitude and duration, will change the magnetic state of the core by predetermined increments between its limiting states. These predetermined intermediate steps may be used to store other than binary information. This principle forms the basis for several multistable devices which are described, including a shift register and a counting circuit.

8121 A MAGNETIC MATRIX SWITCH AND ITS INCORPORATION INTO A COINCIDENT CURRENT MEMORY by K. H. Olsen (MIT); U.S. Gov. Res. Rep., Vol. 33, p. 183 (A), Feb. 12, 1960 PB 144 069

A multi-position switch, capable of handling pulses shorter than one usec, constructed from magnetic cores, is described. Windings on the magnetic cores, when matrix-connected, control selection of the switch output. These windings can be excited with either direct current or pulses. This switch is capable of transmitting power efficiently and the magnetic cores from which it is made are inexpensive, rugged, and promise reliability and long life. Two such switches pulse the 16 coordinate rows and the 16 coordinate columns of a coincident-current magnetic-core memory. The complete cycle-time of the memory, including the switch setup time, reading of information, and rewriting of information, is less than 4 usec.

COMPUTERS (Cont'd)

Design of the magnetic-matrix switch is facilitated by an equivalent-circuit technique.

8122 GATING SYSTEM FOR A DIGITAL COMPUTING DEVICE by E. Goto (Kokusai DDK); U.S. Pat. 2,956,173, Issued Oct. 11, 1960

A gating system for the control of transmission of signals in a digital computing device comprising parametrically excited resonators (parametrons) is described. Exciting currents of frequency $2f$ are applied to induce a beat frequency f in a resonant circuit which employs either ferro-magnetic cores or nonlinear capacitors as parametric elements. Binary digits "0" or "1" are represented by the phase "0" or " π " of the oscillation. Gating is accomplished by the control of the exciting current or by the suppression of oscillation in the paramatron by variations in dc bias or damping resistor. Selection circuits, applicable for memory address selectors, shift registers and channel selectors, and frequency converters employing parametrons are cited.

Ring Counters - See 8138

8123 BISTABLE CIRCUIT by E. D. Ostroff (LFE); U.S. Pat. 2,955,211, Issued Oct. 4, 1960

A bistable circuit for application in multistage counters comprising a magnetic core and a resistivity gated switching transistor is described. The transistor is activated only when the bistable core resides in its first stable state and when so activated restores the core to its second state. Alternate input pulses to the circuit are effective in changing the core from the second state to the first; the remaining pulses thus activate the transistor and return the core to its second state. Input pulses are applied to the series connected core set winding and base resistance and coupled to the transistor through a current limiting impedance of either resistance or capacitive shunted resistance elements.

8124 MAGNETIC COUNTER by I. L. Auerbach; U.S. Pat. 2,960,684, Issued Nov. 15, 1960

A magnetic counting device which may be preset to count to a prescribed limit is described. The device is comprised of two series of magnetic cores, the output coils of each of which are connected to a selective switch. Through employment of the selective switch, the counter can be used as a preset counter or as a variable length delay line. The circuit claims the advantages of stability of operating characteristic, minimum maintenance, and absence of moving parts.

8125 A NEW 600 CARDS PER MINUTE READER by H. H. G. Groom (Intl. Computers Tabulators Ltd.); J. Brit. IRE, Vol. 20, pp. 669-674, Sept. 1960

The requirements for a 600 cards/min reader and their fulfillment are discussed. The card transporting mechanism, including the method of feeding individual cards, and the novel stacking system are discussed. Two systems of card sensing are described, one using phototransistors, the other silicon-voltaic cells. The results of checks on card registration and the resulting card clocking system are given. The need to replace some relay logic with faster elements is discussed and some control functions mentioned.

8126 A HIGH-SPEED TAPE READER by R. D. Lacy (Assoc. Automn. Ltd.); J. Brit. IRE, Vol. 20, pp. 661-668, Sept. 1960

A high-speed tape reader featuring photoelectric sensing of the information and simple, low inertia mechanical control of the tape is described. An electromagnetic brake and clutch are operated from a phototransistor sensing the position of the sprocket hole to locate the tape in the reading positions. The action of the brake is virtually free from inertia and the tape can be stopped from maximum speed on any character. The functional elements, the clutch, brake and photo-sensing head are interchangeable between machines. Production models are fitted with adjustable guide rollers for 5, 6, 7, and 8-hole tape. The optical system permits accurate reading of tape on which the holes are incorrectly positioned relative to the edge. Functional tests show that the accuracy and reliability of the reader in service is very good. Over 10^6 characters have been read from standard pattern loops without detecting an error.

8127 MAGNETIC READ HEAD WITH OUTPUT SIGNAL INDEPENDENT OF TAPE SPEED by D. Kerr and E. J. M. Quirk (Ultra Electronics Ltd.); J. Brit. IRE, Vol. 20, pp. 743-748, Oct. 1960

A variable-reluctance magnetic read head designed for use in digital computer output and editing equipment, which can read digits recorded at normal packing densities over a wide range of tape speeds down to zero, is described. Each head is a "double" head, consisting of a variable reluctance read head and a conventional write head. The centerline separations between the read and write sections is one digit interval; with the 100 digit per inch system used, this separation is 0.01 in. The packing density is a function of the separation between the read and write sections only when the head is used for digit-by-digit checking of a writing operation. Eight such heads are built as one unit having external physical dimensions of 1.5" \times 1.1" \times 0.75" and can be accommodated across standard one-half inch wide magnetic tape. Attention is drawn to the suitability of the reading head for use in off-line editing equipment where the tape speed can be reduced to correspond with the speed of operation of mechanical teleprinters or typewriters, simplifying the tape transport mechanism and circuitry.

Magnetic Recording Heads for Input-Output Units - See 8117

8128 ELECTRIC CHARGE STORAGE APPARATUS by G. D. Bruce; U.S. Pat. 2,925,585, Issued Feb. 16, 1960

A circuit for charging and discharging a capacitor in such a manner that it may be used as a storage element in an electronic memory device is described. The circuit employs a p-n-p junction transistor in both charging and discharging circuits. In the charging circuit, the capacitor is connected in series with a battery that maintains charge on the capacitor. In the discharging circuit, the capacitor is connected across the base and collector electrodes in such a manner that discharge is opposed by the high reverse base-collector impedance.

8129 MAGNETIC INTEGRATOR FOR THE PERCEPTION PROGRAM by J. K. Hawkins (Ford); 1960 IRE Int'l. Conv. Rec., Part 2, pp. 88-95, 1960

A magnetic component possessing storage and signal output properties suitable for circuit realization of the W-type memory element postulated in Perceptron-type systems is described. Stored value or "weight" of the element can be made to increase or decrease in incremental steps by the application of volt-time pulses derived from a logical function of the activity

COMPUTERS (Cont'd)

of associated A-units. Readout is accomplished nondestructively by means of a field applied in a direction orthogonal to normal storage flux. The readout voltage is proportional to the net value of stored flux, both in sign and magnitude. Properties of the integrator of interest in Perceptron system analysis are discussed, and test results presented.

8130 INSTRUMENTATION MAGNETIC RECORDING by P. E. Axon (Ampex Ltd.); J. Brit. IRE, Vol. 20, pp. 723-734, Oct. 1960

A survey of the general field of instrumentation magnetic recording is presented. The individual requirements for analog and digital recorders are examined and the influence of the requirements on mechanical design, electronic equipment, and magnetic tape is illustrated.

8131 ASSESSMENT OF THE RELIABILITY OF MAGNETIC TAPE FOR DATA PROCESSING by R. Noble (MSS Rec. Ltd.); J. Brit. IRE, Vol. 20, pp. 737-742, Oct. 1960

The testing of many specimens of tape for drop-outs, over a wide range of operating conditions, is described. All specimens showed the same characteristic behavior and lead to the conclusion that there is a drop-out distribution which is inherent in the structure of tape and independent of any foreign particles or mechanical damage introduced in the manufacturing process or subsequent handling. The observed distribution permits use of a simple mathematical expression in terms of the two major variables of operation; drop-out discrimination level and pulse packing density. A simple theory of the origin of the observed behavior is given, and a method of tape testing is suggested which appears to be more basic than the present "go-no-go" type of test. The method permits batch testing for most purposes and saves valuable time in the selection of suitable tape even if complete testing is warranted.

Magnetic Recording Tape - See 8116

8132 SOME ENGINEERING ASPECTS OF MAGNETIC TAPE SYSTEM DESIGN by D. W. Willis and P. Skinner (Decca Radar); J. Brit. IRE, Vol. 20, pp. 867-876, Nov. 1960

Attempts to evaluate some of the effects encountered in the design of a digital magnetic tape system are described. Proposals are made for the evaluation of many of these effects in terms of specific measurements on waveforms generated by standard tapes, rather than in terms of dimensional tolerances. Suitable standard tapes are defined in the appendices, together with description of some methods by which they might be prepared; some selected definitions of related terms are also given. By adopting the technique of worst-case design, specifications can be placed on the performance parameters of the system and its components, which are consistent with design for the standard of reliability demanded of modern data processing systems. Such a technique necessarily leads to a modest system specification. Some of the factors described can be removed from the system by proper design, and the method described permits such improvements to be evaluated. In general, the system performance is limited ultimately by noise and by random mechanical effects.

8133 MAGNETIC TAPE DIGITAL RECORDING FOR NUCLEAR RESEARCH by F. H. Wells, I. N. Hooton, and J. G. Page (Atomic Energy Res. Estab.); J. Brit. IRE, Vol. 20, pp. 749-

757, Oct. 1960

Two magnetic tape digital recording techniques developed for nuclear physics research are described. Both 1-in 16-track and 1/4-in 4-track systems are used with maximum bit packing densities of 200 and 400/in., respectively. The tape writing and reading technique uses a return to zero method chosen to facilitate "drop out" detection; a "0" is written by a short duration current pulse of one polarity and a "1" by a similar pulse of reverse polarity. The absence of a pulse on any track during reading indicates a "drop out" and the particular event is then rejected. This error check permits the use of tape systems with overall drop out performance as bad as 1 in 160 bits.

8134 A METHOD OF STORING BINARY INFORMATION IN FERRITE MEMORY CORES WITH NON-DESTRUCTIVE READ-OUT by J. K. A. Olsson (Tel. Ericsson); Solid State Phys. Electronics and Telecommun., Academic Press, Inc., 1960, Vol. 3, pp. 404-410

The 0-flux nondestructive ferrite core readout method in which the binary digits "1" and "0" are represented by the demagnetized state and a remanent state, respectively, of the core is described. The technique is useful in matrix systems which utilize direct word selection. Methods for writing the two digits are discussed and some measurements made on two different cores are presented. The low pulse currents required in the readout permit the use of transistor drive circuits. A small memory built as a programming unit is briefly described and it is pointed out that the 0-flux method makes possible a trinary memory element if both remanent states and the demagnetized state are used.

Coincident Current Core Memory - See 8121

8135 DATA STORAGE DEVICES by R. J. Froggatt and N. D. Robinson; U.S. Pat. 2,958,855, Issued Nov. 1, 1960

A buffer data storage device for use with information handling apparatus is described. The circuit comprises a storage matrix of magnetic cores and transistor shifting registers used to step information from the storage matrix to the output device. Diodes are employed to prevent backward propagation, and an indicator and detector circuit are provided to signal an empty or full condition of the storage matrix.

Parametric Memory Address Selectors - See 8122

8136 ELECTRICAL CONTROL CIRCUITS by R. W. Larisch (Bell Labs.); U.S. Pat. 2,957,088, Issued Oct. 18, 1960

A control circuit which automatically resets sequential stepping devices upon interruptions in power is described. A relay circuit alternately couples a capacitor to the base of a gating transistor; upon the failure of an output pulse the capacitor attains full charge and activates the transistor which then applies a resetting potential to the sequential circuit. The connection and disconnection of the capacitor at frequencies lower than output frequency ensures proper resetting since more than one application of potential may be necessary to reset the device.

8137 MAGNETIC CONTROL CIRCUITS by P. Mallory (Bell Labs.); U.S. Pat. 2,955,212, Issued Oct. 4, 1960

A magnetic control circuit employing a double helix configuration as a three-dimensional, flux-limited magnetic structure is described. Plurality of flux-limited legs enables the structure to selectively steer flux from input signals to accomplish logic

COMPUTERS (Cont'd)

operations. In particular, the circuit described is employed to perform a parity check for a four-bit binary code. Combinations of inputs representing an odd number of "1" bits energize a "check" winding; even number combinations energize a "fail" winding. The circuit is then restored to repeat the operation.

8138 MAGNETIC SYSTEMS by V. L. Newhouse (RCA); U.S. Pat. 2,957,165, Issued Oct. 18, 1960

A magnetic system that may be employed as a stepping register or ring counter and in which noise signals are substantially suppressed is described. The output winding of one magnetic core is coupled through a unilateral impedance to the input winding of a succeeding core. Bias voltage, developed across the advance winding during the application of advance pulses, is applied to predetermined unilateral impedances to control information flow. Noise is suppressed during operation by a biased charge diode that acts to block transmission of noise pulses from one core to another. Three shift-registers employing the above circuit techniques are cited.

8139 DIODELESS MAGNETIC SHIFTING REGISTER by H. M. Robbins and H. R. Kaiser; U.S. Pat. 2,958,852, Issued Nov. 1, 1960

A magnetic core shift register employing no diodes or other unilateral current elements is described. The circuit employs pairs of capacitor coupled saturable magnetic cores arranged in cascade. Application of a shift pulse to the first of the cores results in the transference of the binary digit from the first to the second core. Successive shift pulses move the digit sequentially through the matrix. The register may be operated in either direction and requires three magnetic binary elements per binary bit stored.

Shift Registers in Storage Units - See 8135

Magnetic Shift Registers - See 8120

Parametric Shift Registers - See 8122

Magnetic Tape Recording of Analog Data - See 8130

8140 CIRCUITS FOR CALCULATING THE FUNCTIONS $U_1^{\frac{m}{\sqrt{U_2}}}$ AND $U_1/\sqrt[m]{U_2}$ (FOR $2 \leq m \leq 3$) USING THE ELECTROSTATIC CAPACITANCE OF A P-N JUNCTION by L. S. Berman; *Radio Engrg.*, Vol. 15, No. 10, pp. 102-105, 1960

Simple circuits for approximating functions of the $U_1^{\frac{m}{\sqrt{U_2}}}$ and $U_1/\sqrt[m]{U_2}$ types, where $2 \leq m \leq 3$, are described. The circuits utilize the dependence of p-n junction capacitance on the applied voltage.

8141 ELECTRICAL CIRCUIT by C. F. Winder and E. M. Jones (Baldwin Piano); U.S. Pat. 2,956,171, Issued Oct. 11, 1960

A photocell assembly, featuring a static arrester, which is employed in analog to digital optical encoders, is described. Breakdown and destruction of the photoconductive mass is curtailed by utilizing either a pair of spaced electrodes (of the type used in static discharging of antennas) or a Zener diode. Predetermined voltage breakdown occurs in the arrester before the photocell can be damaged.

8142 A SIMPLE ANALOGUE TO DIGITAL CONVERTER WITH NONLINEARITY COMPENSATION by W. N. Jenkins (Brit.

Iron Steel Res. Assoc.); *J. Brit. IRE*, Vol. 20, pp. 518-522, July 1960

An analog to digital converter which combines a high-speed electromechanical switch with a transistor switching amplifier is described. The electromechanical switch is a motor driven uniselector; a chain of high stability resistances is connected around the two levels of the switch to form a potential divider. A signal from this potential divider is subtracted from the unknown input voltage in the range 0-10 volts and the difference appears across the input of the switching amplifier. When balance is reached the amplifier signal reverses in sign and the switching amplifier energizes a high-speed relay to stop the motor uniselector. Balance is achieved in 1/2 second and the accuracy of digitizing is 1 part in 100. The converter is extremely flexible in output coding and gives complete nonlinearity compensation for any function with suitable connections on the spare levels of the motor uniselector. It is very simple and cheap to construct and can be used to digitize from most types of potentiometric recorder.

POWER

Power Supplies for Telecommunication Systems - See 8112

8143 AN ANALYSIS OF A MAGNETORESISTIVE VOLTAGE REGULATOR by H. Berger and R. K. Crooks (Battelle Mem. Inst.); *Proc. IRE*, Vol. 48, p. 2041(L), Dec. 1960

An experimental and analytical investigation of the feasibility of using magnetoresistive effects in InSb for voltage regulation is discussed. An equation which describes the control action of a magnetoresistive regulator is presented. The calculated and experimental performances of a magnetoresistive regulator are compared for the case in which the load resistance equals the resistance changes of the magnetoresistance element. Good agreement between the two is found. Voltage regulation of 1 per cent for 20 per cent variations in loop and input voltage are feasible without additional amplification in the feedback circuit. Single InSb magnetoresistive elements can be used for regulation at low voltages (< 10v) and medium currents (< 10a) and multiple elements for regulation at higher ratings.

8144 NEW HIGH POWER D-C CONVERTER CIRCUITS by J. R. Howiski (Mullard); *Mullard Tech. Commun.*, Vol. 5, pp. 104-114, Apr. 1960

A two transistor dc converter which provides 100 w output from 28 v supply with less than 3 per cent change in output for maximum spreads in transistor characteristics is described. Operating range is -10° to $+80^{\circ}\text{C}$. With matched transistors and a resistive load, 130 w at 90 per cent efficiency is obtainable. A saturating drive transformer controls transistor switching and a linear output transformer steps up the output. The transistors are initially biased into conduction for reliable starting. The output transformer does not saturate and magnetizing current is small compared to load current. Transformer design equations are developed. A voltage doubler circuit, three timing circuits, and a bridge converter which provides 200 w from a 56 v supply with an efficiency of 80 per cent are also presented.

INSTRUMENTATION

145 DIRECT-READING NOISE FIGURE MEASURING DEVICE
by G. Bruck (Avco); Proc. IRE, Vol. 48, p. 1342(L), July 1960

A noise figure meter which measures power, rather than voltages, is described. A multivibrator gates a noise source on during a period t_1 and off during a period t_2 . Simultaneously the output of the instrument under test is gated during t_1 into thermistor T_1 and during t_2 into thermistor T_2 of a thermistor bridge. When the product of t_1 and the power into T_1 is equal to the product of t_2 and the power into T_2 , the bridge is balanced. Under balanced conditions, the noise figure can be determined from $F = RF_0/1 - 2R$, where F_0 is the ratio of the power of the noise source to thermal power, and R is the ratio E/E_0 , where E_0 is the output of a voltage reference and E is the reading of an indicator to which the reference voltage is applied. The performance of the system can be checked easily by reversing the two thermistors.

146 A MULTI-RANGE ELECTROMETER AMPLIFIER USING VARIABLE FEEDBACK by J. H. Leck and W. E. Austin (U. Liverpool); Electronic Engrg., Vol. 32, pp. 106-107, Feb. 1960

A simple electrometer amplifier which has been found both accurate and reliable over a period of twelve months for the measurement of positive ion currents down to 10^{-15} a is described. By using a miniature electrometer tube in conjunction with a high gain transistor dc amplifier having a large overall negative feedback, the advantage of simplicity is combined with that of high accuracy and adequate sensitivity. The temperature instability of the transistor dc amplifier has been overcome by using a silicon transistor in the first stage and operating with an input from a constant current source.

Hysteresis Loop Tracer for Thin Magnetic Films - See 7953

Low Frequency Magnetic Field Measurements with Hall Generators - See 8034

147 PHOTOELECTRIC COMPARATOR FOR RAYLEIGH FRINGE ELECTROPHORESIS PATTERNS by C. C. Curtain (Baker Med. Res. Inst., Melbourne); J. Sci. Instr., Vol. 37, pp. 190-193, June 1960

A photoelectric fringe comparator for scanning electrophoresis plates, based on a microdensitometer, a Schmitt-trigger operated counter and a recording milliammeter is described. The basis of the microdensitometer is a standard Zeiss binocular microscope with a mechanical stage driven by a reduction gear-box. A considerable simplification in the electronic circuit of the densitometer is achieved by using highly sensitive type DRP 90 cadmium sulphide photoconductive cells.

148 ELECTRICAL INSTRUMENT WITH THERMISTOR SENSING ELEMENT by M. Rogoff (McDermott Controls); U.S. Pat. 3,026,299, Issued Feb. 23, 1960

The use of a thermistor to indicate a change of state of a medium in which it is immersed or to indicate a change from a stationary to a moving medium, or vice versa, is discussed. A heating coil is wound around the thermistor. A change in the state or of the motion of a medium can be detected by the resulting change in the heat-dissipating characteristics of the medium. The heat generated by the heating coil is dissipated more rapidly by a high thermal conductivity liquid or a liquid in motion than by a gaseous or stationary medium. In the former case, the temperature of the thermistor is not raised; in the latter it is raised. The speed of response of the device in detecting a change of state from liquid to gas is increased by utilizing a draining tube to remove the last few drops of liquid.

Acoustical Firing Indicator - See 8105

8149 TRANSISTOR CUP ANEMOMETER by R. R. McGregor (CSIRO); J. Sci. Instr., Vol. 37, pp. 189-190, June 1960

A remote indicating cup anemometer in which transistors are used to obtain a compact instrument is described. The device is capable of registering wind speeds down to 0.2 m/s and operates off small dry batteries.

8150 DETERMINING CLOSURE TIME IN MISSILE CONTROL VALVES by R. L. Kissner (Con. Avionics); Electronics, Vol. 33, pp. 88-89, Oct. 14, 1960

A circuit which determines the exact time of closure of a solenoid-actuated pilot valve following the application of a current to the solenoid is described. The two transistor circuit differentiates the solenoid current twice. The trailing edge of the output pulse occurs at the exact time of valve closure. Similar circuits can determine the time interval between de-energizing a valve and its arrival at a discrete position. A valve operation analyzer utilizing the circuit is described. The analyzer was designed primarily for missile applications.

Ammonia Beam Maser in Portable Frequency Standard - See 8097

8151 A TUNNEL DIODE CRYSTAL CALIBRATOR by L. G. Cox (Natl. Res. Coun., Ottawa); J. Brit. IRE, Vol. 20, pp. 621-624, Aug. 1960

A series tunnel diode circuit with five possible modes of operation is described and a diagram showing the ratios of circuit constants is given. A tunnel diode crystal calibrator with a relatively flat output in the HF band is discussed, and circuit details of a 100 kc or 1000 kc calibrator are cited.

8152 INEXPENSIVE GRAPH PLOTTER USED FOR FIVE-TRACK PAPER TAPE by L. Molyneux and E. E. Schneider (U. Durham); J. Sci. Instr., Vol. 37, pp. 425-431, Nov. 1960

A device to produce a graph from data in the form of five-track paper tape is described. The rate of plotting is 20 points per minute at an accuracy of up to one part in 1000. Apart from a standard ten-millivolt potentiometric recorder and tape reader, the device requires 21 transistors, 2 tubes and 22 relays.

8153 ELECTRONICS IN THE POSTAL FIELD [in French] by P. Chouquet (Ctr. Natl. d'Etudes des Telecommun.); Onde Elect., Vol. 40, pp. 742-746, Oct. 1960

Devices used for the control of machines employed in the sorting of letters and parcels and also in selective conveyors are described. These devices, which at first used electromechanical relays, now use transistor circuits. Two examples are briefly described, one being applicable to a semi-automatic machine, the other to a fully-automatic machine. Finally, the problems of future applications are considered.

8154 LIGHTNING PROTECTION FOR TRANSISTOR REPEATERS by R. W. Blackmore and B. A. Pickering (Brit. Telecomm. Res. Ltd.); ATE J., Vol. 16, pp. 153-168, Oct. 1960

The introduction of plastic-sheathed small diameter coaxial cable used in conjunction with transistor carrier telephony repeaters means that a new standard of lightning protection must be provided to prevent damage to repeater equipment. The nature of a lightning discharge is briefly considered and an explanation of the resulting voltage surges likely to appear in buried and aerial coaxial cables is given. Protection methods are then discussed and a scheme developed for use with transistor repeaters is described.

SUBJECT INDEX

A

- Absorption,
 Impurity Induced Infrared 7918
- Absorption:
 Lines of Cr³⁺ in Ruby 7979
 in Mn-ZnF₂ Crystals 7980
- Spectrum of:
 Electron in One-Dimensional Deep Trap 7930
 YGG 7978
- Acceptor Occupation Statistics, Dislocation 7914
- Acoustical Firing Indicator 8105
- Activation Energies in Semiconducting Compounds 7907
- Activators, Atomic Wave Functions of 7925
- Adiabatic Temperature Changes in Magnetic Cycles of Ferrimagnets 7952
- Alkali Alloy Systems, Nuclear Magnetic Resonance in 7972
- Alkali Halide Phosphors,
 Crystal Structure and Spectra of 7989
 Luminescence in 7989
- Alkali Halides,
 Effect of Pressure on:
 Color Centers in Ag Doped 7854
 the M Center in 7915
 Luminescence of 7983
 Spin-Lattice Relaxation in 7967
- Alkalis, Wave Representation Energy Band Calculation for 7906
- Alloying Processes of Si 7846
- Alloys,
 Antiferromagnetism in Dilute 7961
 Measurement of the Thermal Conductivity of 8000
 Specific Heat of Dilute 7998
- Alumina-Chromic Oxide Systems, Lattice Spacings and Distortion in 7850
- Aluminum Antimonide Junctions, Dendritic Inclusions in 8016
- Aluminum Antimonide-Indium Antimonide System, Conductivity and Other Properties of 7938
- Aluminum Tantalide Inclusions in AlSb Junctions 8016
- Aluminum-Zinc Alloys During Tension, Diffusion of Zn in 7859
- Amplifiers,
 Diode:
 Loaded Helix 8061
 Stabilization of the Gain of 8070
 Increasing the Input Impedance of 8078
- Ion Current Measuring 8146
- Narrow-Band 8057
- Negative Conductance: Low Noise Coupling of 8076
- Parametric: 8007, 8060, 8071
 Bandwidth of 8102
 Ferroelectric 8074, 8075
 Ferromagnetic Longitudinal Pumping 8072
 Low Noise Coupling of 8076
 Measurement of Noise Figure of 8067
 Operation and Applications of 8046
 Optimum Noise Performance of 8068
 Reduction of Pump Power in Ferromagnetic 8073
 Theory of 8065
 Wide Band Travelling Wave 8066
 X-Band Super-Regenerative 8069
- Tecnetron 8031
- Transistor:
 Balanced Chopper 8059
 Carrier System 8111
 Class B 8080
 High Frequency 8058
 IF 8062
 Measurement of Current Gain in 8021
 Push-Pull 8064
- Tunnel Diode: 8009, 8010, 8054
 Coupling Elements in IF 8063
 Hybrid Coupled 8077

- Large Bandwidth 8079
Super-Regenerative 8096
- Varactor: Gain Stabilization of 8070
Video 8106, 8107, 8108
- Analog:
 Calculation of Mathematical Functions 8140
 to Digital:
 Converter 8142
 Encoders 8141
- Anemometer, Transistorized 8149
- Anisotropy of:
 CdS Elastic Constants 8004
 Photoconductivity in Pyrographite 7996
- Annealing of Thin Solid Films, X-Ray Reflection Studies of 7871
- Anthracene,
 Effect of Disorder on Lifetime of Positrons in 7928
 Free Carrier Generation in Photoconducting 7927
- Antiferromagnetic:
 Interaction Shift in Mn-ZnF₂ Crystals 7980
 Ordering in Stacking Fault 7963
 Susceptibility at Moderate Magnetic Fields 7962
- Antiferromagnetism, Theory of 7998
- Antiferromagnetism in Dilute Alloys 7961
- Atomic:
 Radii in Semiconducting Compounds 7907
 Structure Distortion in Alumina-Chromic Oxide System 7850
 Wave Functions of Activators 7925
- Automatic Sorter 8153
- Avalanche Breakdown, Theory of 8025
- B
- Band:
 Calculation for Alkalies, Wave Representation Energy 7906
 Structure of:
 Alkali Halide Phosphors 7989
 Ge in External Magnetic Field 7909
 Luminescent ZnS-In 7991
- Barium Titanate,
 Growth of 7920
 Motion of Domains in 7958
 Permittivity of 7920
 Spiral Growth Layers on Crystals of 7876
- Bilateral Switches 8092
- Binary:
 Compounds, Energy Gaps of 7907
 Counter, Magnetic Switch for 8119
- Bismuth, Hole Component of the Fermi Surface in 7910
- Bismuth Telluride,
 Anisotropic Diffusion of Cu into 7863
 Thermal Conductivity of 8001
- Bismuth Telluride-Selenide, Influence of Oxygen Content on Electrical and Thermoelectric Properties of 7919
- Bistable Counting Circuit, Magnetic Core 8123
- Bloch Wall Energy Density of Magnetoplumbite 7957
- Boron-Li Ions in Si, Relaxation Process for Recombination of 7867
- Brass, Radiation Enhanced Diffusion in 7861
- Breakdown Characteristics of Si p-Sp-n Rectifiers 8015
- Bridgman Method of Single Crystal Growth, Horizontal Modification of 7878
- Broadband Nonreciprocal Transmitters 8041
- C
- Cadmium Doping in InAs 7878
- Cadmium Sulfide,
 Elastic Constants of Hexagonal 8004
 Growth of 7880
 Production of Dislocation Etch Pits on 7855
 Surface Noise in 7951

- Calcium Chloride Impurity in KCl Crystals, Vacancy Association with 7868
- Calcium Fluoride, Paramagnetic and Optical Spec of Yb³⁺ in 7976
- Capacitor Storage Element 8128
- Carbonyl Iron Powder, Magnetization Curve in 7955
- Card Reader Using Photoelectric Sensing Devices 8125
- Carrier:
 Concentration of Vitreous Materials 7949
 Density of:
 AlSb-InSb 7938
 GaAs-Ga₂Se₃ 7942
 Generation in Photoconducting Anthracene, Free 7927
 Lifetime in Transistor Bases 8024
 Systems, Feedback Amplifiers for 8111
- Cellulose, Temperature Dependence of Conductivity of 7936
- Center Law of Lattice Vibration Spectra 7917
- Ceramic Rutile, Stability and Aging of 7901
- Characteristic Frequency and Center Frequency, Equivalence of 7917
- Charge:
 Control Parameters in Transistor Switching Circuit Design 8091
 Densities, Effect of Crystalline Fields on 7926
 Screening, Classification of Solids by Free Electron 7903
- Chopper for DC Amplifier, Balanced Transistor 8055
- Chromic Oxide-Alumina Systems, Lattice Spacing and Distortion in 7850
- Chromium in Ruby, Absorption Lines of 7979
- Circuit Analysis, Use of Multiterminal Networks in 8052
- Circulators,
 Ferrite 8114
 Large Bandwidth Tunnel Diode Amplifiers Using 8079
- Cleavage Faces of LiF Single Crystals, X-Ray Observation of 7872
- Cohesive Properties of Solids, Free Electron Bond Effect on 7903
- Collector Avalanche Breakdown, Theory of 8025
- Color Centers in Ag Doped Alkali Halides, Effect of Pressure on 7854
- Composition Limits of Stability of PbTe 7849
- Compressibility of F and M Centers in Alkali Halide Crystals 7915
- Computer:
 Capacitor Storage Element 8128
 Card Readout Device 8125
 Control Circuit 8136, 8137
 Counters - See Counters
 Ferrite Core Storage 8134, 8135
 Logic Circuits - See Logic Circuits
- Magnetic:
 Storage Element 8129
 Tape Storage 8130, 8131, 8132, 8133
 Memory Units - See Memory
- Punched Tape Readout Device 8126
- Readout, Magnetic Head for 8127
- Shift Registers - See Shift Registers
- Switching Circuits - See Switching Circuits
- Conduction:
 Band Occupancy Function After Collision 7908
 in Si, Low Temperature Impurity 7943
- Conductivity:
 of Cellulose, Temperature Dependence of 7936
 in Doped Quenched KCl Crystals, Decay of 7868
 of GaAs-Ga₂Se₃ 7942
 in Ge, Fluctuations of 7940, 7941
 of High Vanadium Phosphate Glass 7944
 of InSb 7937
 in PbTe, Type Dependence on Composition of 7849
 in Semiconductors, Thermally Stimulated 7935
 of Sodium Aluminosilicate Glass 7939
- Control Circuit, Computer 8136, 8137

SUBJECT INDEX (Continued)

- Converters,
Analog-Digital 8142
High Power DC Transistor 8144
Power 8112
Conveyor, Selective 8153
Copper:
Diffusion into Bi_2Te_3 7863
in Mg-Cr Ferrites, Addition of 7896
Copper Chloride, Antiferromagnetic Susceptibility of 7962
Costa-Ribeiro Effect, Anisotropy in Single Crystal Naphthalene of the 7897
Counters, Magnetic Core 8120, 8123, 8124
Critical Field for Superconductivity in Nb_3Sn 7946
Cross Relaxation:
by a Four Spin Flip Mechanism 7965
in Spin Systems 7950
Cyclotron Gating Circuits 8094
Crystal:
Calibrator Employing Tunnel Diodes 8151
Growth - See Growth of
Structure and Spectra of Alkali Halide Phosphors 7989
Crystalline Field Effects on Charge Densities and Magnetic Form Factors 7926
Crystals,
Cleavage Faces of LiF 7872
Preparation of VHF Quartz 8048
Current Drift Calculation in Junction Transistors 8055
Cutoff:
Characteristics of Si p-Sp-n Rectifiers at Breakdown 8015
Frequency in Junction Transistors 8024
Czochralski Method in PbTe Crystal Growth 7877
- D
- Data Storage on Magnetic Tape 8130, 8131, 8132
Defects, Structure of 7852
Defects in:
Ge, Neutron Irradiation 7929
LiF Crystals 7856
Quartz 7853
Deflection Systems, Television Receiver Transistorized 8109
De Haas-van Alphen Effect in Graphite, Field Dependence of 7931
Delay Line, Variable Length Magnetic 8124
Demagnetization in Ferrimagnets, Adiabatic 7952
Dendritic:
Growth:
of Ge 7888, 7890, 7892
of Ge, Dislocations in 7893
on Ge Dendrite Surfaces 7891
Theory 7889
Inclusions in AlSb Junctions 8016
Density Meters, Thermistor 8148
Deposition of Thin Films of Germanium 7885, 7887
Detector, Tunnel Diode Super-Regenerative 8096
Deuteron Energy on Irradiation Damage in W, Effect of 7902
Diamond,
Decay of Persistent Polarization in 7995
Electron Diffraction and Secondary Electron Emission Studies of a (100) Semiconducting Surface of 7870
Four Spin Flip Mechanism in 7965
Luminescence in Semiconducting 7987
Diamonds, Synthesis of 7898, 7899
Dicing, Semiconductor 7900
Dictating Machine, Transistor 8115
Dielectric Resonator for Inductive Capacity Measurement 7921
Dielectrics, Thermal Conductivity Tensor of 7999
Diffraction Studies of Pyrographite, X-Ray 7851
Diffusion,
Effect of Pressure on 7860
Radiation Enhanced 7861
Diffusion:
into Au-Ni System, Isothermal 7864
Coefficients, Effects of Strain Upon 7859
of Cu into Bi_2Te_3 , Anisotropic 7863
Doping of Si 7858
Lengths, Measurement of p-n Junction Minority Carrier 8008
Model 7852
of P into Si, Effect of Oxide Layers on 7862
Process for Ge n-p-n Transistors 8028
of S and Se into GaAs 7865
Digital:
Computer Magnetic Readout Head 8127
Storage:
System, Design of 8132
Unit for Nuclear Research 8133
Diode:
Loaded Helix Microwave Amplifier 8061
Phase Shifters, Variable Capacitance 8051
UHF Harmonic Generators 8099
Diodes,
Junction:
Dendritic Inclusions in AlSb 8016
Double Diffusion Oxide Masking in Diffused 8017
Protective Resin Surface Treatment for Ge and Si 8019
Silver Bonded:
Capacitance and Cutoff Frequency of 8007
Fabrication of 8007
Tunnel:
Design and Application of 8010
Design, Fabrication, and Operation of 8009
Microwave Frequency Characteristics of 8012
Operating Mode Biasing of 8054
Directivity of Crystal Properties, Theory of 7905
Dislocation:
Acceptor Occupation Statistics 7914
Cross-Glide in LiF Crystals 7856
Multiplication in LiF Crystals 7856
Dislocations in:
CdS, Decoration of 7855
Ge Dendrites 7893
Solids, Theory of 7903
Distortion in Alumina-Chromic Oxide Systems 7850
Distribution:
Coefficient of Te in Melt Grown InSb Crystals 7847
of Impurities During Zone Equalization 7866
Domain:
Growth, Kinematic Theory of Ferroelectric 7923
Nucleation Centers in BaTiO_3 , Motion of 7958
Structure, Effects of Heat Treatment on Magnetic 7873
Width of Magnetoplumbite, Thickness Dependence of 7957
Doping:
of InAs with Cd 7878
Si by Diffusion 7858
Double Tetrode Transistor 8023
Drift Transistors, TV Signal Amplifiers Using 8106
Duplexer, Ferrite 8114
- E
- Elastic Constants of Hexagonal CdS 8004
Electric:
Field Effect on Electron Mobility in InSb 7933
Fields, Properties of InSb in Pulsed High 7934
Electrical Properties of $\text{Bi}_{2-x}\text{Te}_3\text{x}$, Influence of Oxygen Content on 7919
Electroluminescence,
Temperature Dependence of 7985
Very Low Frequency Excitation of 7985
Electroluminescence:
in Diamond 7987
in GaP 7990
of Insulated Particles, Model for 7984
in (Zn, Hg)S and (Zn, Cd, Hg)S Phosphors 7988
Electromagnetic Wave Polarization by Gyromagnetic Rods 8042
Electrometers, Transistor Amplifier for 8146
Electron:
Bound States, Calculation of Wave Functions and Energies of 7930
- Diffraction of a (100) Semiconducting Diamond Surface 7870
Emission of a (100) Semiconducting Diamond Surface 7870
Impact Ionization, Occupancy State Probability Function in 7908
Mobility in InSb 7933
in One-Dimensional Deep Trap, Absorption and Emission Spectra of 7930
Electronegativities in Semiconducting Compounds 7907
Emission:
Bands:
in Sn, Pb, and Sb Activated Phosphors 7925
of Zn-Hg Phosphors 7988
Spectrum of:
Electron in One-Dimensional Deep Trap 7930
Luminescent ZnS-In 7991
Emitter Junction, Characteristics of Imperfect 8026
Encoders,
Analog to Digital 8141
Optical 8141
Energy, Calculation of Lattice Free 7916
Energy:
Band Calculation in Solids, Technique for Electronic 7906
Gap:
of GaAs-Ga₂Se₃ 7942
in Ge, Pressure Dependence of 7913
Gaps of Semiconducting Compounds 7907
Levels:
of Holes 7911
in Paramagnetic Crystals 7977
Spectrum of Ge and Si, Effect of Deformation on Hole 7912
Entropy in Spin Systems 7950
Epitaxial Growth of Ge from GeI₂ 7885
Equivalent:
Circuit for:
Gyrators 8056
Tecnetrons 8032
Tunnel Diodes, Low and Microwave Frequency 8012
Hybrid-π Circuit for Junction Transistors 8027
Esaki Diode - See Tunnel Diode
Etch Pits in CdS 7855
Exchange:
Constant of Magnetoplumbite 7957
Interaction of Fe³⁺ and Mn²⁺ in Spinel Structures 7966
Excited Levels of Activator Ions in Alkali Halides 7983
- F
- Feedback Amplifiers for Carrier Systems 8111
Fermi Surface in Bi, Hole Component of the 7910
Ferrimagnetic Compounds Containing Fluorine, Properties of 7904
Ferrimagnets, Adiabatic Demagnetization and Specific Heat in 7952
Ferrite:
Devices, Radar Duplexing with 8114
Hall Generators 8033
Loaded Waveguide Transmitters, Broadband Nonreciprocal 8041
Microwave Frequency Doublers 8100
Resonators, Oscillations of 8037
Scanners, Properties and Applications of 8040
Sphere, Susceptibility of 7954
Ferrites,
Compositions and Properties of 7896
Ferromagnetic Resonance in 7959
Relaxation Processes in 7964
Resonance Absorption Linewidths in Mg-Mn 7960
Ferroelectric:
Domain Growth, Kinematic Theory of 7923
Parametric Amplifiers 8074, 8075
Properties of Thin Films of Pb(Ti-Zr-Sn)O₃ 7922
Ferromagnetic, Magnetization of a Dilute Suspension of a Multidomain 7955

SUBJECT INDEX (Continued)

Ferromagnetic:
 Materials, Longitudinal Oscillations in 8005
 Parametric:
 Amplifier, Reduction of Pump Power in 8073
 Amplifier Utilizing Longitudinal Pumping 8072
 Resonance, Effect of Circularly Polarized Radiation on 7959
 Field:
 Amplification in Zn-CdS-Mn Phosphors 7982
 Dependence of:
 De Haas-van Alphen Effect in Graphite 7931
 Domain Motion in BaTiO₃ 7958
 Exciton Creation in InSb 7934
 Spin-Lattice Relaxation in Neodymium Ethyl-Sulfate 7968
 Effect Transistors, Fabrication of 8029
 Filamentary Crystals, Growth of 7895
 Films,
 Deposition of 7886
 Disproportionation of GeI₂ in the Growth of Ge 7885
 Flux Measurements of Thin Magnetic 7953
 Formation of:
 Ge Single Crystal 7887
 Phosphor 7894
 Magnetic Anisotropy Constant of 7956
 Photoconductivity of Metal-Free Phthalocyanine 7992
 X-Ray Reflection Studies of Thin Solid 7871
 Filter Structures for Parametric Amplifiers 8066
 Filters, Thermistors in Low Frequency 8036
 Flow Meters, Thermistor 8148
 Fluoride Crystals, Optical Absorption in 7980
 Fluorine in Hexagonal Ferrimagnetic Compounds 7904
 Flux Measurement of Thin Magnetic Films 7953
 Forward Characteristics of Junctions, Two-Carrier Theory of 8014
 Free Carrier Generation in Photoconducting Anthracene, Extrinsic Model of 7927
 Frequency:
 Characteristics of Tunnel Diodes 8012
 Converters, Parametric 8065, 8122
 Dividers, Transistorized 8097
 Dividers Utilizing Hall Generators 8098
 Doublers,
 Diode UHF 8099
 Ferrite Microwave 8100
 Mixers, Ferrite Microwave 8100
 Multiplier,
 Parametric 8097
 Transistor and Diode VHF to X-Band 8101
 Fringe Comparator Employing Photodevices 8147

G

Gain:
 in Double Tetrode Transistor 8023
 Stabilization of Varactor Amplifiers 8070
 Gallium Arsenide,
 Diffusion of S and Se in 7865
 Growth of 7882
 Gallium Arsenoselenides, Conductivity and Other Properties of 7942
 Gallium Phosphide,
 Growth of 7882
 Luminescence and Photovoltaic Effects in 7990
 Galvanomagnetic:
 Effect in Crystals, Theory of 7905
 Properties of Pyrographite 7948
 Gating Systems,
 Parametric 8122
 Superconductive 8094
 Generator,
 Harmonic: VHF to X-Band 8101
 Parametric:
 Microwave 8087
 Millimeter Wave 8088
 Tone 8112

Germanium,
 Conductivity Fluctuations in 7940, 7941
 Effect of Deformation on Hole Energy Spectrum of 7912
 Formation of Single Crystal Films of 7887
 Magneto-Optic Effect in 7909
 Microwave Hall Mobility in 7932
 Neutron Irradiation Defects in 7929
 Peltier Effect in 8003
 Pressure Dependence of Energy Gap in 7913
 Resistivity Gradient Dependence of Volume Peltier Effect in 8003
 Solubility of Interstitial Impurities in 7869
 Surface Transverse Magnetoresistance Effects on 7947
 Temperature Dependence of Refractive Index of 7994
 Germanium:
 Dendrites, Growth of 7888, 7889, 7890, 7891, 7892, 7893
 Films, Disproportionation of GeI₂ in the Growth of 7885
 Transistors,
 Double Diffusion Process for 8028
 Fabrication of 8029
 Valence Band Structure in External Magnetic Field 7909
 Gold Activated Zn-CdS-Mn Phosphors 7982
 Gold-Ni System, Kirkendall Effect in the 7864
 Graph Plotter, Transistorized 8152
 Graphite, Field Dependence of De Haas-van Alphen Effect in 7931
 Growth of:
 BaTiO₃ 7920
 CdS Crystals 7880
 Crystals, Theory of 7875
 Cu₂O Single Crystals 7883
 Dendrites, Theory of 7889
 Diamonds (Synthesis of) 7898, 7899
 Films 7886
 Ge:
 Dendrites 7888, 7890, 7891, 7892, 7893
 Films 7885, 7887
 Group III-V Compounds 7882
 Hexagonal HgS Crystals 7881
 InAs Crystals 7878, 7882
 InP 7882
 MnBi Films, Effect of Heat Treatment on 7873
 p-Type GaP Phosphors 7990
 PbTe Crystals by Czochralski Method 7877
 Phosphor Films 7894
 Phosphors 7988, 7991
 Quartz 7884
 Si Films from Silanes 7879
 Whiskers from Solid Metal 7895
 (Zn,Hg)S Phosphors 7988
 ZnS-In Phosphors 7991
 ZnS Single Crystals 7874
 Gyrorators, Equivalent Circuit of 8056
 Gyromagnetic Rods, Polarization of Electromagnetic Waves by 8042

H

Hall:
 Coefficient of:
 InSb 7937
 Si, Low Temperature Measurement of 7943
 Effect in:
 AlSb-InSb 7938
 Pyrographite 7948
 Vitreous Materials 7949
 Generators,
 Characteristics of 8034
 Frequency Dividers Utilizing 8098
 Magnetic Field Measurements with 8034
 Output Multiplication in 8033
 Mobility in Ge, Microwave 7932
 Harmonic:
 Approximation Calculation of Lattice Specific Heat and Free Energy 7916

Coupling in Ruby 7970
 Generators,
 Ferrite Microwave 8100
 UHF 8099
 VHF to X-Band 8101
 High Frequency Amplifiers, Design of 8058
 Hole:
 Component of the Fermi Surface in Bi 7910
 Energy Spectrum of Ge and Si, Effect of Deformation on 7912
 Holes, Energy Levels of 7911
 Hot Electrons in Nonpolar Crystals, Variational Treatment of 7924
 Hybrid-π Circuit for Junction Transistors 8027
 Hysteresis Loop Tracer for Thin Magnetic Films 7953

I

IF Amplifiers,
 Transistorized 8062
 Tunnel Diodes as Coupling Elements in 8063
 Impurities,
 Growth of Synthetic Quartz Affected by 7884
 Interstitial Solubility in Ge and Si 7869
 Zone Equalization and Distribution of 7866
 Impurity:
 Concentration Dependence of Refractive Index of Ge 7994
 Conduction in Si, Low Temperature 7943
 Induced Infrared Lattice Vibration Absorption at Isolated Frequencies 7918
 Inclusions in AlSb Junctions 8016
 Indium Antimonide,
 Conductivity and Other Properties of 7937
 Electron Mobility in 7933
 Magnetoresistive Voltage Regulator Employing 8143
 Orientation of Te Distribution Coefficient in 7847
 Thermal Conductivity of 8001
 Indium Antimonide in Pulsed High Electric Fields Properties of p-Type 7934
 Indium Arsenide,
 Growth of 7882
 Preparation and Properties of 7878
 Indium-Ge Junctions, Properties of 8013
 Indium Phosphide, Growth of 7882
 Inductive Capacities in Millimeter Range, Measurement of 7921
 Insulated Particles, Model for Electroluminescence of 7984
 Interface Motion, Theory of 7875
 Ion Current Measurement, Amplifier for 8146
 Ionization,
 Classification of Solids by Ease of 7903
 Occupancy State Probability Function in Electrons Impact 7908
 Iron,
 Phase Transformation by Differential Thermal Analysis of α-γ 7848
 Self Diffusion Coefficient During Compression of 7859

Iron:
 Powder, Magnetization Curve in Carbonyl 7955
 in Spinel Structure, Exchange Interaction of 7966
 Irradiation:
 Defects in Ge, Neutron 7929
 Effects on Resistivity of W, Deuteron 7902
 Islands in Semiconductor Slices, Production of 7900

J

Junctions,
 Formation of Diffused 7858, 8017
 Measurement of Minority Carrier Diffusion Lengths in 8008
 Properties of In-Ge 8013
 Two-Carrier Theory for Forward Current in 8014

SUBJECT INDEX (Continued)

- unctions in:
 Si, Formation of Diffused 7858
 SiC, Formation of 8018, 8030
- K**
- Inematic Theory of Ferroelectric Domain Growth 7923
- inetics of:
 Luminescence of Alkali Halides 7983
 Phthalocyanine Photoconductivity 7992
 Kirkendall Effect in the Au-Ni System 7864
 night Shift in Ta Metal 7973
- L**
- Band Tunable Lasers 8044
- attice:
 Constant of Conduction of Cellulose 7936
 Free Energy, Calculation of 7916
 Phase Transition on F and M Centers in Alkali Halide Crystals, Effect of 7915
- Spacings in Alumina-Chromic Oxide Systems 7850
- Specific Heat, Calculation of 7916
- Vibration:
 Absorption, Impurity Induced Infrared 7918
 Spectra, Center Law of 7917
- ayer Geometry in Pyrographite 7851
- ead Telluride,
 Composition Limits of Stability of 7849
 Growth of 7877
 Thermal Conductivity of 8001
- ife Expectancy of Transistors 8020
- ifetime of Positrons in Anthracene, Effect of Disorder on 7928
- ight Stimulation in Luminescence Kinetics 7986
- ightning Protection for Transistor Repeaters 8154
- inear Sweep Circuit, Transistorized 8085
- iquid-Solid Interface Studies of Ge Dendrites 7892
- ithium-Boron Ions in Si, Relaxation Process for Recombination of 7867
- ithium Fluoride,
 Cleavage Faces of Single Crystals of 7872
 Dislocation Multiplication in Crystals of 7856
- ogic Circuits,
 Design and Performance of Transistor-Resistor 8118
- Magnetic: 8119
 Core 8120
- ow Frequency Wave Filters, Thermistors in 8036
- uminescence, Very Low Frequency Excitation of 7985
- uminescence:
 of Alkali Halide Phosphors 7989
 of Alkali Halides 7983
 Decay in AgCl 7981
 of GaP 7990
 Kinetics, Light Stimulation in 7986
 in Semiconducting Diamond 7987
- uminous:
 Films, Formation by Evaporation of 7894
 ZnS-In, Optical Properties of 7991
- M**
- Magnesium-Manganese Ferrites, Resonance Absorption Linewidths in 7960
- Magnetic:
 Anisotropy Constant in Single Crystal Films 7956
 Control Circuit 8137
 Core:
 Counters 8120, 8124
 Logic Circuits 8120
 Matrix Switch, Design of Core for 8121
 Multiplexer 8113
 Multistage Bistable Counting Circuit 8123
 Shift Registers 8120, 8139
 Storage Units 8134, 8135
 Delay Line 8124
 Field Measurements, Hall Generators for 8034
- Fields, Antiferromagnetic Susceptibility at Moderate 7962
- Films,
 Effects of Heat Treatment on Growth and Domain Structure of MnBi 7873
 Flux Measurement of Thin 7953
- Form Factors, Effect of Crystalline Field on 7926
- Materials, Elastic Switching Properties of Toroidal Square Loop 8039
- Memory for Perceptron System 8129
- Readout Head for Digital Computer 8127
- Recording Heads, Mechanical Limitations of 8117
- Resonance, Thermodynamics of 7950
- Shift Register and Ring Counter 8138
- Switch, High Speed 8119
- Tape,
 Assessment of Data Storage on 8131
 High Storage Capacity of 8116
 Storage of Analog and Digital Data on 8130
- Tape:
 Storage Unit, Application in Nuclear Research of 8133
 System for Digital Data, Design of 8132
 Transfer Circuits 8093
- Magnetization:
 vs Applied Magnetic Field in Nb₃Sn 7946
 of a Dilute Suspension of a Multidomain Ferromagnetic 7955
- Magneto-Optic Effect in Ge 7909
- Magnetoplumbite, Thickness Dependence of Domain Structure of 7957
- Magnetoresistance:
 Effects on Ge, Surface Transverse 7947
 of InSb 7937
 Voltage Regulators, Analysis of 8143
- Manganese in Spinel Structure, Exchange Interaction of 7966
- Manganese Bismuthide Films, Effects of Heat Treatment on Growth and Domain Structure of 7873
- Manganese Chloride, Antiferromagnetic Susceptibility of 7962
- Manganese-Magnesium Ferrites, Relaxation Processes in 7964
- Manganese Zinc Fluoride Crystals, Optical Absorption in 7980
- Manganous Sulfide, Specific Heats of Polymorphic Forms of 7963
- Masers,
 Operation and Applications of 8046
 Pumping by a Four Spin Flip Mechanism in 7965
 Theory of 8043
 Tunable:
 L-Band 8044
 X-Band 8045
- Mathematical Functions, Analog Calculation of 8140
- Matrix Switch for Coincident Current Memory 8121
- Measurement of:
 Current Gain in Transistors 8021
 Inductive Capacities in Millimeter Range 7921
 Magnetic Anisotropy Constants of Single-Crystal Films 7956
 Surface Magnetoresistance in Ge 7947
 Surface Noise in CdS 7951
- Medical Measurements, Transistor Application in 8104
- Memory:
 Address Selector, Parametric 8122
 for the Perceptron System 8129
 Unit, Magnetic Core Matrix Switch for 8121
- Mercury Sulfide Crystals, Growth of Hexagonal 7881
- Metallic Bonds, Classification of Solids by 7903
- Metals, Measurement of the Thermal Conductivity of 8000
- Meteorological Meters, Anemometer 8149
- Microphones, Piezoelectric 8105
- Microwave:
 Amplifier, Diode Loaded Helix 8061
 Frequencies, Fabrication of Semiconductor Devices for 8017
 Hall Mobility in Ge 7932
 Parametric Amplifiers 8060
 Power Absorption in Yttrium Garnets 8038
- Military Electronics, Piezoelectric Firing Indicator for 8105
- Millimeter Wave:
 Generation, Parametric 8088
 Modulator, Fabrication and Performance of a Ge p-i-n 8006
 Oscillators 8090
- Minority Carrier Diffusion Lengths in p-n Junctions, Measurement of 8008
- Missile Control Valves, Circuit for Determining Closure Time in 8150
- Mixers, Measurement of Noise Figure of 8067
- Mobility:
 of AlSb-InSb 7938
 of GaAs-Ga₂Se₃ 7942
 in InSb, Electron 7933
 of Vitreous Materials 7949
- Modulator, Ge p-i-n Millimeter 8006
- Molybdenum, Thermal Conductivity of 8000
- Multiplexer, Five Channel Magnetic Core-Transistor 8113
- Multipliers, Hall Effect 8033
- Multiterminal Network Elements, Analysis of Circuits by 8052
- Multi-Track Recording Heads, Mechanical Limitations of 8117
- Multivibrator,
 Free-Running Complementary 8083
 Temperature Stability of 8084
- Muscle Potential, Detection Circuit for 8104
- N**
- Naphthalene, Anisotropy of the Costa-Ribeiro Effect in 7897
- Negative:
 Conductance Amplifiers using Tunnel Diodes 8079
- Resistance:
 in Network Synthesis 8050, 8053
 Oscillator 8086
- Neodymium Ethyl-Sulfate, Spin-Lattice Relaxation in 7968
- Network Synthesis with Negative Resistance Concept 8050, 8053
- Neutron Irradiation Defects in Ge 7929
- Nickel:
 During Tension, Diffusion of H Through 7859
 Thin Films, Deposition of 7886
- Nickel-Au System, Kirkendall Effect in the 7864
- Nickel-Zn Ferrites, Deposition of Thin Films of 7886
- Niobium Stannide, Critical Field for Superconductivity in 7946
- Noise:
 in CdS, Surface 7951
- Figure:
 Meter, Thermistor 8145
 in Parametric Amplifiers: 8068
 and Converters 8065
 and Mixers 8067
- Nonpolar Crystals, Variational Treatment of Warm Electrons in 7924
- Nonunilateral Electron Devices in Narrow-Band Amplifiers, Analysis of 8057
- Nuclear:
 Magnetic Resonance:
 in Alkali Alloy Systems 7972
 of Ta¹⁸¹ in Ta 7973
 Paramagnetic Resonance of Na²³ and Cl³⁵ 7974
 Quadrupole Interactions in Crystals, Volume Dependence of 7974
- Nucleation Mechanisms of Interface Motion 7875

SUBJECT INDEX (Continued)

O

Occupancy State Probability Function in Electron Impact Ionization 7908
 Occupation Statistics, Dislocation Acceptor 7914
 Optical:
 Absorption in Mn-ZnF₂ Crystals 7980
 Constants of Hexagonal Se Single Crystals 7997
 Encoders, Analog to Digital 8141
 Properties of:
 Luminescent ZnS-In 7991
 Pyrographite 7996
 Spectra in Paramagnetic Crystals 7977
 Spectrum of Yb³⁺ in CaF₂ 7976

Oscillation Conditions 8081
 Oscillations in Ferromagnetic Materials, Internal Friction of Longitudinal 8005
 Oscillators,
 Microwave Parametric 8087
 Negative Resistance 8086
 Transistor:
 Polyphase High Frequency 8081
 Sinusoidal 8082
 Tunnel Diode: 8009, 8010, 8054
 Millimeter Wave 8090
 Voltage Tuning in 8089

Oxidation of Thin Solid Films, X-Ray Reflection Studies of 7871
 Oxide Layers, Effect on Diffusion of P in Si 7862
 Oxygen Content on Electrical and Thermoelectric Properties of Bi_xTe_{3-x}Se_x, Influence of 7919

P

Paramagnetic:
 Crystals,
 Energy Levels in 7977
 Optical Spectra in 7977
 Resonance:
 Absorption of Fe³⁺ and Mn²⁺ in Spinel Structures 7966
 of V⁴⁺ in TiO₂ 7975
 of Yb³⁺ in CaF₂ 7976
 Solute in Metals, Antiferromagnetic Ordering of 7961

Parametric:
 Amplifiers,
 Ferroelectric 8074, 8075
 Ferromagnetic 8072
 Filter Structures for 8066
 Noise in 8066
 Optimum Noise Performance of 8068
 Reduction of Pump Power in Ferromagnetic 8073
 Wide Band Travelling Wave 8066
 X- and S-Band 8060
 X-Band Super-Regenerative 8069
 Amplifiers: 8007, 8071
 and Converters 8065
 and Converters, Bandwidth of Lower Sideband of 8102
 and Mixers, Measurement of Noise Figure of 8067

Frequency Multiplier 8097
 Generator,
 Microwave 8087
 Millimeter Wave 8088
 Phase Shifters 8051

Parametron Application in Computer Circuitry 8122

Pb(Ti-Zr-Sn)O₃, Ferroelectric Properties of Thin Films of 7922

Peltier Effect in Ge, Resistivity Gradient Dependence of Volume 8003

Perceptron System, Magnetic Memory for 8129
 Periods of De Haas-van Alphen Effect in Graphite 7931

Permittivity:
 of BaTiO₃, Effect of Si Ion Replacement on 7920
 in Millimeter Range, Measurement of 7921

Phase:

Diagram Determination in Alkali Alloy Systems 7972
 Diagrams of Si 7846
 Shifters, Variable Capacitance Diode 8051
 Transformation, Effect of High Pressures on α-γ Iron 7848
 Phonon Scattering in Nonpolar Crystals 7924
 Phosphate Glass, Conductivity of High Vanadium 7944
 Phosphor Films Formation by Evaporation 7894
 Phosphors,
 Crystal Structure and Spectra of Alkali Halide 7989
 Emission Bands in Sn, Pb, and Sb Activated 7925
 Field Amplification of Zn-CdS-Mn 7982
 Growth of 7988, 7991
 Light Stimulation of ZnS-Cu 7986
 Photo- and Electroluminescence in (Zn, Hg)S and (Zn, Cd, Hg)S 7988
 Phosphorus Diffusion in Si Through Oxide Layers 7862

Photocells,
 Card Reader Using 8125
 Fabrication and Performance of Position Sensitive 8035
 Photocconductivity of:
 Additively Colored KBr, Pulse 7993
 CdS 7951
 Metal-Free Phthalocyanine Films 7992
 Photodevice Application in Fringe Comparator 8147

Photoelectric:
 Card Reader 8125
 Punched Tape Reader 8126
 Photoluminescence in (Zn, Hg)S and (Zn, Cd, Hg)S Phosphors 7988
 Photoresponse of p-n Junctions 8008
 Phototransistor:
 Card Reader 8125
 Modification, Photocell Obtained from 8035
 Punched Tape Reader 8126
 Photovoltaic Effects in GaP 7990
 Phthalocyanine Films, Photoconductivity of Metal-Free 7992

Piezoelectric:
 Crystals, Reduction of Temperature Frequency Shift by Stressing 8047
 Microphones 8105
 Polarization in Diamond, Decay of 7995
 Polarized Light Determination of Optical Constants of Se Crystals 7997
 Polishing of Quartz Crystal Surfaces 8048, 8049
 Polymorphism in Alkali Halide Phosphors 7989
 Positrons in Anthracene, Effect of Disorder on Lifetime of 7928
 Postal Sorter 8153
 Potassium Bromide, Pulse Photoconductivity of Additively Colored KBr 7993

Potassium Chloride, Vacancy Association with CaCl₂ Impurity in 7868
 Power:
 Converters 8112, 8144

Gain of Narrow-Band Amplifiers Employing Nonunilateral Electron Devices 8057
 Regulators 8112
 Preset Counter 8124

Pressure Effect on:
 Color Centers in Ag Doped Alkali Halides 7854
 Diffusion 7860

 the M Center in Alkali Halide Crystals 7915
 Protection of Repeating Equipment from Lightning 8154

Pulse:
 Generator, Transistor 8103
 Photoconductivity of Additively Colored KBr 7993
 Width Modulator 8095

Pyrographite,

 Galvanomagnetic Properties of 7948
 Optical Properties of 7996
 X-Ray Diffraction Studies of 7851

Q

Q Factor Increase in Quartz Crystals 8049
 Quantum Effects on Valence Band Structure in Ge 7909

Quartz,
 Defects in Natural and Synthetic 7853
 Effect of Impurities on Growth of Synthetic 788-
 Quartz Crystals,
 Increase in Q of 8049
 Preparation of VHF 8048

R

Radar Duplexing with Ferrite Devices 8114

Radiation:
 Enhanced Diffusion 7861
 Induced Complex Decay of Positrons in Anthracene 7928

Reader for:
 Cards, Photoelectric 8125
 Punched Tape, Photoelectric 8126
 Readout, Nondestructive Memory 8134
 Readout Head for Digital Computer 8127
 Recombination of Li-B Ions in Si, Relaxation Process for 7867

Rectification of Ratios of Fused Junctions in SiC 8030

Rectifiers, Breakdown Characteristics of Si 8015
 Refining, Continuous Zone 7857

Reflection Curves of Annealed or Oxidized Metal Films 7871

Refractive Index of Ge, Temperature Dependence of 7994

Registers, Magnetic Shift 8138

Regulators, Power 8112

Relaxation in:
 Alkali Halides 7967
 MgMn Ferrites 7964
 Neodymium Ethyl Sulfate 7968
 Ruby 7969, 7970
 Ruby, Concentration and Temperature Dependence of 7971

Reliability of Transistors 8020

Repeaters, Lightning Protection for 8154

Reset Circuit for Sequential Stepping Devices 8136

Resistivity Gradient Dependence of Volume Peltier Effect in Ge 8003

Resonance:
 Absorption Linewidths in Mg-Mn Ferrites 7960
 in Alkali Alloy Systems 7972
 of Ta¹⁸¹ in Ta, Nuclear Magnetic 7973
 Tuning of Spherical Resonators 8037
 of V⁴⁺ in TiO₂ 7975

Resonator for Inductive Capacity Measurement, Dielectric 7921

Resonators, Oscillations of 8037

Reverse Characteristic of Ge Tunnel Diode, Pressure Dependence of 8011

Ring Counters, Magnetic 8138

Ruby,
 Absorption Lines of Cr³⁺ in 7979
 Concentration Dependence of the Relaxation Time in 7971

Spin-Lattice:
 Relaxation in 7969
 Relaxation and Harmonic Coupling in 7970
 Temperature Dependence of the Relaxation Time in 7971

Ruby Lasers,
 Tunable:
 L-Band 8044
 X-Band 8045

Rutile, Stability and Aging of Ceramic 7901

SUBJECT INDEX (Continued)

S

- Scanners, Properties and Applications of 8040
- Shear Dislocation Mechanism of Interface Motion 7875
- Selenium:
 - Diffusion in GaAs 7865
 - Single Crystals, Optical Constant of Hexagonal 7997
- Semiconductors,
 - Thermally Stimulated Conductivity in 7935
 - Thermoelectric Efficiency of 8002
- Shift:
 - Reduction in Piezoelectric Crystals, Stress Technique Temperature Frequency 8047
- Registers 8135
- Registers,
 - Magnetic: 8138
 - Core 8120, 8139
 - Parametric 8122
- Shockley Equation, Imperfect Emitter Junction Characteristics Applied to 8026
- Signal Transfer Circuits 8093
- Silanes, Production of Si by Decomposition of 7879
- Silica on Mo, Deposition of Thin Films of 7886
- Silicon,
 - Alloying Processes of 7846
 - Decomposition of Silanes in the Production of 7879
 - Diffusion:
 - Doping of 7858
 - Through Oxide of P in 7862
 - Effect of Deformation on Hole Energy Spectrum of 7912
 - Low Temperature Impurity Conduction in n-Type 7943
 - Phase Diagrams of 7846
 - Replacement Ion Effect on the Permittivity of BaTiO₃ 7920
 - Solubility of Interstitial Impurities in 7869
 - Silicon Carbide,
 - Deposition of Thin Films of β - 7886
 - Formation of Junctions in 8018, 8030
 - Silicon p-Sp-n Rectifiers, Breakdown Characteristics of 8015
 - Silicon Tetrachloride, Growth of Si by Decomposition of 7879
 - Silver, Self Diffusion Coefficient During Compression and Torsion of 7859
 - Silver Chloride, Luminescence Decay in 7981
 - Silver Doped Alkali Halides, Effect of Pressure on Color Centers in 7854
 - Sinusoidal Oscillator, Transistor 8082
 - Sodium Aluminosilicate Glass, Conductivity of 7939
 - Solubility of Interstitial Impurities in Ge and Si 7869
 - Sorter, Automatic Postal 8153
 - specific:
 - Heat, Calculation of Lattice 7916
 - Heat of:
 - Dilute Alloys 7998
 - Ferrimagnets 7952
 - Polymorphic Forms of Manganese Sulfide 7963
 - Speech-Path Switches for Direct Coupled Connections, Semiconductor 8092
 - spin:
 - Degeneracy Dependent Statistics, Acceptor State 7914
 - Flip Mechanism,
 - Cross Relaxation by 7965
 - Diamond 7965
 - Maser Pumping by 7965
 - Lattice Relaxation in:
 - Alkali Halides 7967
 - Neodymium Ethyl Sulfate 7968
 - Ruby 7969, 7970
 - Systems, Theory of Entropy and Cross-Relaxation in 7950
 - Wave Theory of Ferromagnetism 7952

- Spinel Structure, Exchange Interaction of Fe³⁺ and Mn²⁺ in 7966
- Spiral Growth Layers on BaTiO₃ Crystals 7876
- Stacking Fault, Antiferromagnetic Ordering in 7963
- Steering Circuits, Magnetic 8137
- Storage:
 - of Data on Magnetic Tape 8130, 8131, 8132
 - on High Capacity Magnetic Tape 8116
 - System, Magnetic Core Matrix Switch for 8121
 - Unit,
 - Capacitor 8128
 - Magnetic:
 - Core 8134, 8135
 - Tape 8133
 - Strain Enhanced Diffusion 7859
 - Structure of Magnetic Films, Effects of Heat Treatment on 7873
 - Sulfur Diffusion in GaAs 7865
 - Superconductive:
 - Gating Circuits 8094
 - Transition, Thermal and Electrodynamic Properties of 7945
 - Transition in Thin Wires and Films 7945
 - Superconductivity in Nb₃Sn, Critical Field for 7946
 - Surface Transverse Magnetoresistance Effect on Ge 7947
 - Surfaces,
 - Protective Treatment for Device 8019
 - Quartz: Polishing of 8048, 8049
 - Susceptibility:
 - at Moderate Magnetic Fields 7962
 - of Small Ferrite Spheres 7954
 - Sweep Circuit, Transistorized Linear 8085
 - Switches for Direct Coupled Connections, Semiconductor Speech-Path 8092
 - Switching:
 - Circuits,
 - Charge Control Parameters of 8091
 - High Speed Magnetic 8119
 - Tunnel Diodes in 8009, 8010, 8054
 - Properties of Toroidal Square Loop Magnetic Materials 8039
 - SYMMAG High Speed Magnetic Switch 8119
 - Synthesis of Diamonds 7898, 7899
 - Synthetic Quartz, Effect of Impurities on Growth of 7884

T

- Tantalum Metal, Knight Shift in 7973
- Tape:
 - Reader, Photoelectric 8126
 - Recorder, Transistor 8115
 - Recording Heads 8117
 - Storage:
 - Capacity and Properties, Magnetic 8116, 8130, 8131
 - Units, Magnetic 8132, 8133
 - Target Miss Indicator 8105
- Tecneutrons,
 - Equivalent Circuits and Characteristics of 8032
 - Theory and Design of 8031
- Television:
 - Receiver Deflection Systems, Transistorized 8109
 - Signal Amplifiers Using Drift Transistors 8106
 - Transmitters, Transistorized 8110
 - Video Amplifier, Transistorized 8106, 8107, 8108
- Tellurium in InSb, Distribution Coefficient of 7847
- Thermal:
 - Conductivity, Detection of α - γ Iron Phase Transformation by 7848
 - Conductivity:
 - of Bi₂Te₃, PbTe and InSb 8001
 - of Metals and Alloys, Measurement of the 8000
 - of Mo 8000
 - Tensor of Dielectrics 7999
 - Drift in Junction Transistors 8055
 - Excitation Induced Polarization Decay in Diamond 7995
- Thermally Stimulated Conductivity in Semiconductors 7935

- Thermistor Noise Figure Meter 8145
- Thermistors,
 - Measurement of Change of State and Motion of a Medium by 8148
 - Properties of 8036
- Thermoelectric:
 - Efficiency of Semiconductors 8002
 - Properties of Bi₂Te_{3-x}Se_x, Influence of Oxygen Content on 7919
- Thermoluminescence, Defect Measurements in Quartz by 7853
- Thermomagnetic Effect in Crystals, Theory of 7905
- Thin Films of Pb (Ti·Zr·Sn)O₃, Ferroelectric Properties of 7922
- Timing Meter for Missile Control Values 8150
- Tin Whiskers, Tensile Strength of 7895
- Titania, Paramagnetic Resonance of V⁴⁺ in 7975
- Titanium Dioxide, Stability and Aging of 7901
- Tone Generators 8112
- Transfer Circuits, Magnetic 8093
- Transistor:
 - Amplifiers - See Amplifiers
 - Converters, High Power DC 8144
 - Frequency Divider 8097
 - Graph Plotter 8152
 - Linear Sweep Circuit 8085
 - Multiplexer 8113
 - Multivibrator, Free-Running Complementary 8083
 - Polyphase Oscillators, Oscillation Conditions for 8081
 - Pulse Generator 8103
 - Ratings and Reliability 8020
 - Repeaters, Lightning Protection for 8154
 - Resistor Logic Circuits, Design and Performance of 8118
 - Sinusoidal Oscillator 8082
 - Switching Circuit Design, Charge Control Parameters in 8091
 - Tape Recorder 8115
- Transistors,
 - Double:
 - Diffusion Process for Ge n-p-n 8028
 - Tetrode 8023
 - Field-Effect: Method of Fabricating 8029
 - Germanium: Method of Fabricating 8028, 8029
 - Junction:
 - Characteristics of:
 - Imperfect Emitter 8026
 - p-n-p 8022
 - Collector Avalanche Breakdown in 8025
 - Current Drift Calculation of 8055
 - Double Diffusion Oxide Masking in Fabrication of 8017
 - Equivalent Hybrid- π Circuit for 8027
 - Minority Carrier Injection into Base of 8024
 - Measurement of Current Gain in 8021
 - Photo-: Application in Punched Tape Reader of 8126
 - Protective Resin Surface Treatment for Ge and Si 8019
- Transmitters,
 - Broadband Nonreciprocal 8041
 - Transistorized TV 8110
- Trapping Kinetics of Additively Colored KBr, Analysis of 7993
- Traps,
 - Absorption and Emission Spectra of Electron in One-Dimensional Deep 7930
- Traps in CdS 7951
- Travelling Wave:
 - Masers, Theory of 8043
 - Parametric Amplifiers, Wide Band 8066
- Triboluminescence in Diamond 7987
- Tungsten, Effect of Deuteron Energy on Irradiation Damage in 7902
- Tunnel Diode:
 - Amplifiers - See Amplifiers
 - Circuits 8151
 - Crystal Calibrator 8151
 - Oscillators,

SUBJECT INDEX (Continued)

- Millimeter Wave 8090
 Voltage Tuning in 8089
 Super-Regenerative Detector and Amplifier 8096
 Tunnel Diodes,
 Equivalent Circuit and Frequency Characteristics of 8012
 Pressure Dependence of Reverse Characteristic of Ge 8011
 Tunnel Diodes as Coupling Elements in IF Amplifiers 8063

U

- Ultra High Frequency Harmonic Generators 8099
 Ultrasonic Drilling of Semiconductor Slices 7900

V

- Vacancy Association with CaCl_2 Impurity in KCl Crystals 7868
 Valence Band Structure of Ge in External Magnetic Field 7909
 Vanadium in TiO_2 , Paramagnetic Resonance of 7975
 Vanadium $^{4+}$ Concentration on Conductivity of High V Phosphate Glass, Effect of 7944
 Vanadium Phosphate Glass, Conductivity of High 7944
 Vapor:
 Decomposition, Formation of Ge Single Crystal Films by 7887
 Phase Diffusion of P in Si, Effect of Oxide Layers on 7862

Varactor Diode:

- Parametric Amplifier 8069
 Phase Shifters 8051
 Vibration Spectra, Center Law of Lattice 7917
 Video Amplifier, Transistorized 8107, 8108
 Vitreous Materials, Hall Effect in and Other Properties of 7949
 Voltage Regulators, Analysis of Magnetoresistive 8143

W

- W-Type Memory Element 8129
 Wall Orientation in Ferroelectric Domain Growth of BaTiO_3 7923
 Warm Electrons in Nonpolar Crystals, Variational Treatment of 7924
 Wattmeter, Thermistor 8145
 Wave:
 Functions of Activators, Atomic 7925
 Representation Energy Band Calculation for Alkalies 7906
 Whiskers, Growth of 7895
 Wurtzite Structure, Synthesis of ZnS with 7874

X

- X-Band Masers, Tunable 8045
 X-Ray:
 Diffraction Studies of Pyrographite 7851
 Reflection Studies of Annealing and Oxidation in Thin Solid Films 7871

Y

- Ytterbium in CaF_2 , Paramagnetic and Optical Spectra of 7976
 Yttrium Gallium Garnet, Absorption Spectrum of 7978
 Yttrium Iron Garnet,
 Adiabatic Demagnetization and Specific Heat in 7952
 Microwave Power Absorption in 8038

Z

- Zinc-CdS-Mn Phosphors, Field Amplification of 7982
 Zinc-Mercury Phosphors, Photo- and Electroluminescence in 7988
 Zinc-Ni Ferrites, Deposition of Thin Films of 7886
 Zinc Sulfide,
 Formation by Evaporation of Thin Luminescent Films of 7894
 Synthesis of Single Crystals of 7874
 Zinc Sulfide-Cu Phosphors, Light Stimulation of 7986
 Zinc Sulfide-In Phosphors, Optical Properties of Luminescent 7991
 Zincblende, Synthesis of ZnS with 7874
 Zone:
 Equalization, Concentration Distribution in a Billet During 7866
 Rifining, Continuous 7857

AUTHOR INDEX

- | | | | | | |
|---------------------------|-----------------------|-------------------------|--------------------------|-------------------------|-------------------------|
| Adawi, I. 7924 | Blaise, J. 8105 | Cherry, W. H. 7945 | Endo, I. 8092 | Good, Jr., R. H. 7932 | Hudson, D. E. 7995 |
| Agaev, Ya. 7938 | Blancheville, P. 8110 | Chih-ch'ao, L. 7937 | Eppler, R. A. 7854 | Gorter, C. J. 7962 | Hughes, R. 8061 |
| Albers, Jr., W. A. 7947 | Bloembergen, N. 7972 | Cheung, P. 8153 | Fabri, G. 7928 | Gorton, H. C. 8016 | Hulme, K. F. 7847 |
| Albin, J. 8093 | Blumberg, W. E. 7967 | Claussen, W. F. 7948 | Farnsworth, H. E. 7870 | Gourary, B. S. 7930 | Ian'-Shen, S. 8037 |
| Allen, R. B. 7862 | Boesch, F. T. 8053 | Coleman, P. D. 7921 | Faust, Jr., J. W. 7888, | Graham, J. 7850 | Ida, I. 8048 |
| Allgaier, R. S. 7849 | Boiko, I. I. 7935 | Colin, R. 8112 | 7889, 7890, 7893 | Grannemann, W. W. | Iofe, V. A. 7939 |
| Andreyev, V. S. 8098 | Bolef, D. I. 8004 | Conrad, G. 8061 | Feltin'sh, I. A. 7942 | Grimmeiss, H. G. 7990 | Jackson, R. B. 8082 |
| Antell, G. R. 7882 | Bossard, B. B. 8069 | Cosenza, F. 8104 | Finegold, L. 8011 | Groom, H. H. G. 8125 | Jacobs, I. S. 7955 |
| Aoki, Y. 8074 | Bousquet, L. 8112 | Cottini, C. 7928 | Finlayson, D. M. 7980 | Gruenberg, H. 8073 | Jaentsch, O. 8015 |
| Arai, Y. 8048 | Bowlden, H. J. 7909 | Cottrell, A. H. 7903 | Fishbein, W. 8069 | Guentert, O. J. 7851 | Jenkins, W. N. 8142 |
| Arams, F. R. 8044 | Boyd, E. L. 7956 | Cox, L. G. 8151 | Fisher, S. T. 8102 | Gutowsky, H. S. 7974 | John, H. F. 7888, 7889, |
| Armstrong, R. A. 7970 | Boyett, H. 8041 | Crooks, R. K. 8143 | Fock, M. V. 7986 | 7890, 7893, 8019 | |
| Arnold, Jr., G. W. 7853 | Bozorth, R. M. 7946 | Curtain, C. C. 8147 | Fox, A. G. 8042 | Johnston, W. G. 7856 | |
| Atkins, K. R. 7943 | Brandt, N. B. 7910 | Curtis, Jr., O. L. 7929 | Fredericks, W. J. 7985 | Jones, E. M. 8141 | |
| Auerbach, I. L. 8124 | Brebrick, R. F. 7849 | Czyzak, S. J. 7880 | Freeman, A. J. 7926 | Jordan, A. G. 8096 | |
| Austin, W. E. 8146 | Brini, D. 8022 | Daniels, J. J. 7968 | Frei, E. H. 7904 | | |
| Axon, P. E. 8130 | Brisott, J. J. 7846 | Danielson, G. C. 7932 | Freitas, L. G. 7897 | Kaczér, J. 7957 | |
| Ayres, W. P. 8100 | Brophy, J. J. 7951 | Davis, D. D. 7946 | Froggett, R. J. 8135 | Kaiser, H. R. 8139 | |
| Bagno, S. 8104 | Brophy, V. A. 7874 | de Jager, J. T. 8070 | Frost, E. 8069 | Kambouris, G. N. 8021 | |
| Baker, L. R. 8035 | Bross, H. 7905 | DeLoach, B. C. 8071 | Fukui, H. 8012 | Kamysheva, L. N. 7920 | |
| Baldcock, G. S. 8114 | Broudy, R. M. 7914 | Denton, R. T. 8072 | Gaertner, W. W. 8009 | Kanai, Y. 7933 | |
| Baranskii, P. I. 8003 | Brown, C. S. 7884 | de Ronde, F. C. 8006 | Galt, J. K. 7952 | Kearns, D. R. 7992 | |
| Barrack, C. M. 8033 | Brown, E. 7852 | Deschamps, R. 8028 | Gatti, E. 7928 | Kembadjian, H. 8059 | |
| Barsukov, Yu. K. 8013 | Brown, L. 7954 | Dienes, G. J. 7861 | Gelles, I. L. 7965 | Kerr, D. 8127 | |
| Beale, J. R. A. 8029 | Bruce, G. D. 8128 | Dominick, F. J. 8045 | Gemperle, R. 7957 | Khlystov, A. S. 7896 | |
| Bean, C. P. 7955 | Bruck, G. 8145 | Donovan, R. 7943 | Gennon, S. 8059 | Khovostenko, G. I. 7935 | |
| Beaufoy, R. 8091 | Budnick, J. I. 7973 | Doronkin, E. F. 8084 | Gerber, E. A. 8047 | Kilkson, R. 7883 | |
| Beauzee, C. 7858 | Burrus, C. A. 8090 | Downey, E. J. 8051 | Germann, E. 7928 | Kihn, H. 8113 | |
| Belov, K. P. 7960 | Butcher, P. N. 8043 | Drickamer, H. G. 7854, | Gerritsen, H. J. 7975 | Kilkson, R. 7883 | |
| Belov, V. F. 7960 | Butler, K. H. 7925 | 7915 | Gianino, P. D. 8045 | Kingston, D. L. 7881 | |
| Bennett, A. I. 7891, 7892 | Cahn, J. W. 7875 | Drial, A. 8022 | Gill, J. C. 7971 | Kiss, M. J. 8101 | |
| Bennett, L. H. 7973 | Calvin, M. 7992 | Cardona, M. 7913 | Gilman, J. J. 7856 | Kissner, R. L. 8150 | |
| Berger, H. 8143 | Carlin, H. J. 8050 | Duinker, S. 8040 | Girifalco, L. A. 7859 | Kita, S. 8007 | |
| Berman, L. S. 8140 | Carlson, R. O. 7863 | Dumaire, M. 8119 | Gittleman, J. I. 7945 | Klein, C. A. 7948 | |
| Bernheim, R. A. 7974 | Carter, W. S. 7963 | Dunlap, Jr., W. C. 7887 | Glicksman, M. 7934 | Klement, F. D. 7989 | |
| Bernstein, H. 7862 | Catalano, S. B. 7885 | Effer, D. 7882 | Glikin, N. V. 7876 | Klensch, R. J. 8113 | |
| Bir, G. L. 7912 | Chang, K. K. N. 8061 | Elco, R. 8096 | Goldstein, B. 7865 | Knight, R. D. 7900 | |
| Birkhol, U. 8002 | Chang, Y. F. 8014 | Elmgren, J. A. 7995 | Goldstein, I. 8060, 8075 | Koelmans, H. 7990, 7991 | |

AUTHOR INDEX (Continued)

- Kohra, K. 7872
 Koller, L.R. 7894
 Kolomiets, B.T. 7949
 Kornfeld, M.I. 7941
 Kotzebue, K.L. 8068
 Krumme, J.B. 7987
 Krupicka, S. 7964
 Kunin, V.I. 7901
 Kunzler, J.E. 7952
 Kurilo, P.M. 8003
 Kurtz, A.D. 7862
 Lacy, R.D. 8126
 Lade, R.W. 8086
 Lainé, D.C. 8046
 Larisch, R.W. 8136
 Lasher, G.J. 7965
 Lebedev, V.I. 8078
 Lebedev, V.V. 8000
 Leck, J.H. 8146
 Leonov, D. 8099
 Leivo, W.J. 7987
 Lentz, J.J. 8094
 Lewis, H.R. 7975
 Liebman, F. 8104
 Lim, M. 8057
 Lindsay, J.E. 8080
 Link, G.L. 7958
 Liu, S.H. 7932
 Loferski, J.J. 8008
 Lomasson, T.E. 8103
 Longini, R.L. 7891
 LoSasso, L.A. 8063
 Low, W. 7976, 7977, 7979
 Lowell, R. 8101
 Lukes, F. 7994
 Lur'e, M.S. 7922
 Maeda, K. 7984
 Mallery, P. 8137
 Manganne, R. 8105
 Mano, K. 8081, 8109
 Maradudin, A.A. 7918,
 7930
 Marcel, P. 7879
 Marcus, P.M. 7906
 Marinace, J.C. 7887
 Marsh, J. 7870
 Marshall, W. 7998
 Martin, A.V.J. 8031,
 8032
 Martin, M.B. 8117
 Mascarenhas, S. 7897
 Mattei, J.I. 8105
 Mayer, L. 7873
 Mazurov, M.E. 8098
 McClure, J.W. 7914
 McGregor, R.R. 8149
 McInnes, I.G. 8106
 Meechan, C.J. 7864
 Melamed, N.T. 8004
 Melcher, J.L. 8100
 Memelink, O.W. 8006
 Menes, M. 8004
 Messenger, G.C. 8010
 Meyer, H.J.G. 8006
 Miasek, M. 7908
 Miller, S.L. 8011
 Minomura, S. 7915
 Mirlin, D.N. 7940,
 7941
 Miura, T. 8109
 Molyneux, L. 8152
 Moore, W. 7927
 Movshovich, M.E. 8062
 Mullin, J.B. 7847
 Munakata, M. 7944
 Munushian, J. 8051
 Murphy, E.J. 7936
 Murray, R.P. 8054
 Muss, D.R. 7902
 Nachtrieb, N. 7860
 Naess, E. 8108
 Nakamura, T. 7923
 Nasledov, D.N. 7937,
 7938, 7942
 Nathan, M.I. 8011
 Nazarova, T.F. 7949
 Newhouse, V.L. 8138
 Nii, R. 8001
 Ninomiya, T. 7868
 Nishina, Y. 7932
 Noble, R. 8131
 Oguey, H.J. 7953
 O'Hara, S. 7892
 Ohkura, H. 7993
 Okwit, S. 8044
 Olsen, K.H. 8121
 Olsson, J.K.A. 8134
 Onuki, M. 7993
 Ostroff, E.D. 8123
 Overhauser, A.W. 7961
 Pace, J.H. 7969
 Page, J.G. 8133
 Pappalardo, R. 7978
 Parratt, L.G. 7871
 Paul, W. 7913
 Pell, E.M. 7867
 Pfann, W.G. 7857
 Pickering, B.A. 8154
 Pikus, G.E. 7912
 Pistol'kovs, A.A. 8037
 Plendl, J.N. 7917
 Plyavin, I.K. 7983
 Polonskii, Ju.A. 7901
 Popova, A.A. 7960
 Potter, F.J. 8058
 Prewitt, C.T. 7851
 Pringle, D.H. 8114
 Prosser, V. 7997
 Prudnikov, I.N. 8098
 Pulfer, J.K. 8089
 Pustynskii, I.N. 8107
 Quirk, E.J.M. 8127
 Rashba, É.I. 7935
 Nathan, M.I. 8011
 Reynolds, D.C. 7880,
 7881
 Rieckhoff, K.E. 7968
 Rimai, L. 7972
 Robbins, H.M. 8139
 Robertson, I.S. 7980
 Robinson, B.J. 8070
 Robinson, N.D. 8135
 Robinson, N.O. 8097
 Rogoff, M. 8148
 Romanenko, V.N. 7866
 Rood, J.W. 8099
 Rupprecht, G. 7996
 Ruth, R.P. 7885, 7887
 Sager, G. 8058
 Samelson, H. 7874
 Sampson, D.F. 7969
 Sard, E.W. 8079
 Scherer, P.M. 7931
 Schieber, M. 7904
 Schlax, T.R. 8086
 Schloemann, E. 7959
 Schlosser, H. 7906
 Schneider, E.E. 8152
 Schossberger, F.V. 7886
 Seeger, C.L. 8070
 Seelbach, W.C. 8039
 Seidensticker, R.G.
 7888, 7890
 Shapiro, D.N. 8062
 Shockley, W. 8017
 Shtivel'man, K.Ya. 7911
 Shtrikman, S.S. 7904
 Shveikin, V.I. 8024
 Sie, J.J. 8077
 Siegmund, A.E. 7950
 Sigorskii, V.P. 8052
 Silver, M. 7927
 Simon, A.H. 8113
 Simons, S. 7999
 Sines, G. 7895
 Skinner, P. 8132
 Smagin, A.G. 8049
 Smirous, K. 7919
 Smith, T. 7980
 Smith, W.J. 7891
 Smokotin, E.M. 7896
 Solomon, A.H. 8087
 Sorokin, P. 7965
 Spacek, L. 8005
 Spriggs, S. 7886
 Spry, W.J. 7931
 Steele, M.C. 7934
 Steiger, W. 8010
 Sterzer, F. 8087
 Stevenson, A.F. 7916
 Stevenson, I.R. 8020
 Stevenson, R.W.H.
 7980
 Stitch, M.L. 8097
 Stourac, L. 7919
 Strauss, A.J. 7878
 Strong, H.M. 7899
 Suchet, J.P. 7907
 Sugiura, Y. 7966
 Sugiyama, K. 8007
 Szabo, A. 7970
 Tagoshima, I. 8095
 Takagi, T. 8081
 Tamiya, J. 8076
 Thies, A.W. 8111
 Thomas, Jr., J.E. 7947
 Thomas, L.A. 7884
 Thomson, A.F.H. 8038
 Thorp, J.S. 7969
 Timofeeva, V.A. 7876
 Todd, C.E. 8010
 Tollin, G. 7992
 Tomono, M. 8026
 Toth, R.S. 7883
 Townsend, J.R. 7902
 Trivich, D. 7883
 Trofimenko, A.P. 7935
 Trokhimenko, Ia.K.
 8056
 Tsikin, A.N. 7901
 Vacek, K. 7981
 van Biljon, L. 8025
 van Damme, K.J. 8070
 van den Broek, J. 7962
 van der Ziel, A. 8076
 Van Ommen, B. 8040
 Vartanian, Jr., P.H.
 8100
 Vinukurov, L.A. 7986
 Vital, I.K. 7983
 Wachtel, A. 7988
 Wade, G. 8065
 Wainfan, N. 7871
 Walker, L.R. 7952
 Wallis, R.F. 7909, 7918
 Walmsley, R.H. 7943
 Ward, J.J. 8055
 Watson, R.E. 7926
 Weisbaum, S. 8041
 Weiser, K. 7869
 Weiss, H. 8034
 Wells, F.H. 8133
 Wendel, G. 7982
 Wheatley, C.J. 8064
 Wilkner, E.G. 7967
 Willett, R.M. 8085
 Williams, A.J. 7946
 Willis, D.W. 8132
 Winder, C.F. 8141
 Wöhlers, M.R. 8053
 Wood, D.L. 7978
 Woods, J. 7855
 Wysocki, J.J. 8008
 Yoshida, S. 8092
 Yoshimatsu, M. 7872
 Youla, D.C. 8050
 Zarkhi, L.D. 8027
 Zeender, R.J. 7959
 Zelinka, R.J. 8023
 Zorzy, J. 8060

“Every 24 hours enough technical papers are turned out around the globe to fill seven sets of the twenty-four volume *Encyclopaedia Britannica*. And the output is rising every year. This year's crop: some 60 million papers . . . the laboratory scientist, busy with work of his own, no longer can find enough hours in the day to keep up with all that is published in his field. Even staying on top of the indexes and abstracts of these papers has become an insurmountable task for the lab men. One result is that company after company has found itself duplicating research work that others have done and fully chronicled.”

From the *Wall Street Journal*
Tuesday, December 20, 1960

COMPUTER ABSTRACTS ON CARDS

A quick cumulative reference to the
Technical Literature on Electronic Computers

C 2.25/1.249

1539 COMPUTER DESIGN OF MULTIPLE-OUTPUT LOGICAL NETWORKS by T. C. Bartee (Lincoln Lab., M.I.T.); IRE Trans. on Electronic Computers, Vol. EC-10, pp. 21-30, March 1961

An important step in the design of digital machines lies in the derivation of the Boolean expressions which describe the combinational logical networks in the system. Emphasis is generally placed upon deriving expressions which are minimal according to some criteria. A computer program which automatically derives a set of minimal Boolean expressions describing a given logical network with multiple-output lines is discussed. The program accepts punched cards listing the in-out relations for the network, and then prints a list of expressions which are minimal according to a selected one of three criteria. The basic design procedure and the criteria for minimality are described.

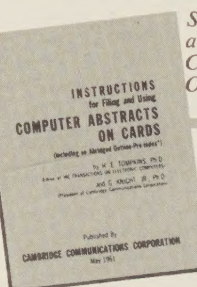
non-cumulative version of the abstracts make it easy to locate information by:

Logical Sequence
Alphabetically by Subject
Alphabetically by Author

COMPUTER ABSTRACTS ON CARDS covers the following topics in the field of electronic computers:

- Logic and Switching Theory (Boolean Functions, Switching Networks, Automata)
- Digital Computers and Systems (Design, Arithmetic Methods, Equipment, Error Detection)
- Devices (Electromechanical, Electron Tube, Semiconductor, Magnetic, Cryogenic, etc.)
- Logic and Waveforming Circuits
- Storage and Input-Output
- Programming and Coding (Programming Languages, Automatic Programming, Algorithms)
- Languages (Natural and Formal Languages, Mechanical Translation)
- Information Retrieval
- Pattern Recognition and Artificial Intelligence
- Mathematics (Number Theory, Numerical Analysis, Probability and Statistics)
- Operations Research and Game Theory
- Information Theory and Noise; Communications Systems
- Analog and Hybrid Computers
- Real-Time Systems and Automatic Control
- Applications of Computers in Science, Engineering, Industry, Government, Business, etc.

Send for free booklet — “Instructions for Filing and Using COMPUTER ABSTRACTS ON CARDS” — including Abridged Classification Outline and Pre-Index.



**CAMBRIDGE
COMMUNICATIONS
CORPORATION**
238 Main St., Cambridge 42, Mass.

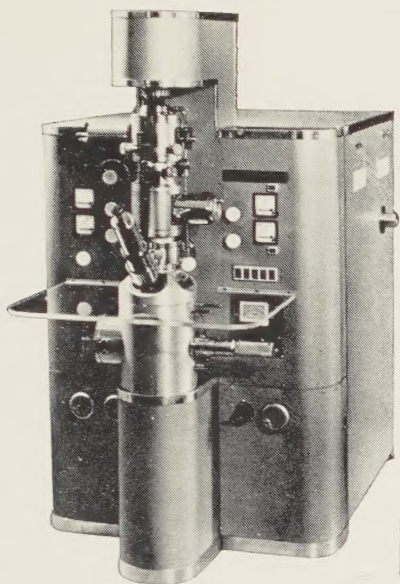
Please send me a copy of “Instructions for Filing and Using COMPUTER ABSTRACTS ON CARDS”.

NAME _____
TITLE _____
COMPANY _____
ADDRESS _____
CITY _____ ZONE _____
STATE _____

COMPUTER ABSTRACTS ON CARDS is designed to provide the engineer or scientist with a cumulative reference file to the technical literature on electronic computers, organized by subject matter. As a subscriber you would receive, every other month, several hundred 3" x 5" cards containing abstracts of recently published papers in the computer field. These abstracts summarize the contents of the papers, enabling you to determine what work has been reported on a given subject and showing you where you can find more detailed information on that subject. In addition to the abstract and the journal reference, each card has a classification number which makes it easy for you to file the card in a logical sequence with all previously issued cards. In this way you can continuously group together abstracts of related references, just as the Dewey Decimal System enables a librarian to group together books on related subjects.

This abstract card file corresponds in some ways to the card file which enables the librarian to locate any book or periodical in the library. However, it has additional advantages which result from the information provided by the abstracts themselves and from the logical (as opposed to alphabetical) organization which permits one to browse through references on related topics as one might browse through the books on a library shelf. An alphabetical Pre-Index is provided with this service to direct the user to the part of the file which is devoted to a given topic. In addition, the same abstracts are supplied in a non-cumulative form with subject and author indexes. Taken together the card file, the Pre-Index, and

FOR SURFACE STUDIES



KE1

Trüb, Täuber Secondary Electron Emission Microscope

for direct viewing of metallic and semiconducting specimens by means of secondary electrons released from ion bombardment of the surface — featuring . . .

- Images free of distortion and deformation
- Enlargement up to 1500 X electronoptically
- Resolution 500–600 Å
- Object temperature 150°–800° C
- Observable surface of the object 25 mm square
- Differentiation of the material

The Instrument Includes . . .

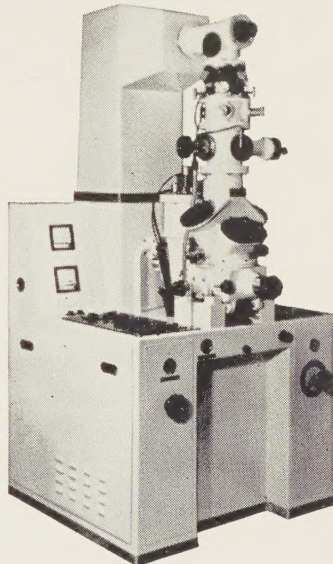
Electrostatic immersion objective
Ion beam system
Revolving contrast diaphragms
2 electromagnetic projectors
Observation chamber with fluorescent image screen
Recording chamber with plate cassette
High-intensity optical microscope
All-metal housing with vacuum equipment including diffusion pump
High-voltage equipment for 45 kV
Measuring instruments and control equipment

Distributed by:

NEW ENGLAND SCIENTIFIC INSTRUMENTS CO.

238 MAIN STREET • CAMBRIDGE 42, MASSACHUSETTS • Kirkland 7-2932

Electron Microscopes • Nuclear Induction Spectrographs • High Voltage Oscilloscopes • Precision Laboratory Instruments • Nuclear Track Microscopes



KD3

Trüb, Täuber Electron Diffractograph

for determining the crystalline structure of surfaces, thin layers, and extremely small quantities of material, including dynamic processes — featuring . . .

- Cold-cathode electron gun with practically unlimited life
- Simple design — dependable operation, extreme flexibility
- Balanced optical system
- High resolving power
- Large variety of specimen holders for various methods of investigation
- Devices for heating and cooling the test specimens (from liquid nitrogen to 1000°C)
- Devices for discharging, etching, surface evaporating
- Various cameras for photographic recording on plates and films
- Unique kinematic recorder

Specifications

Acceleration Voltage —	10 to 50 kV
continuously adjustable:	approx. 2 x 10 ⁻⁵ mm Hg
ripple (fractional):	≈ 10–4
stability:	± 0.1%
Final vacuum:	approx. 2 x 10 ⁻⁵ mm Hg
Magnification with electronic lens:	75X
Minimum line width:	0.001 mm
Minimum diameter of beam for focussing on specimen, without additional diaphragms:	4μ

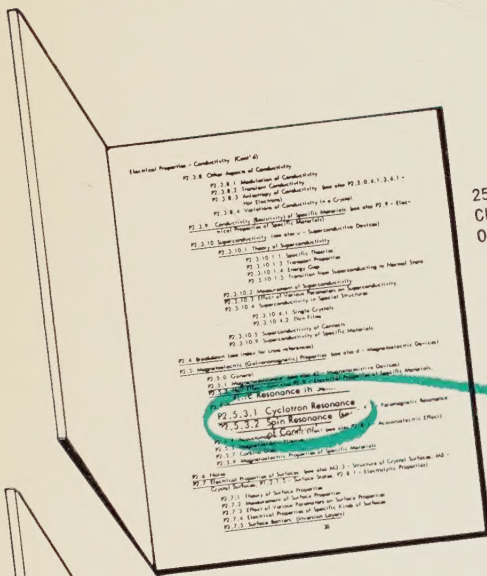
in'for·ma·tion re·triev'al, n. 1. rapid location of technical information on specific topics.

information retrieval system

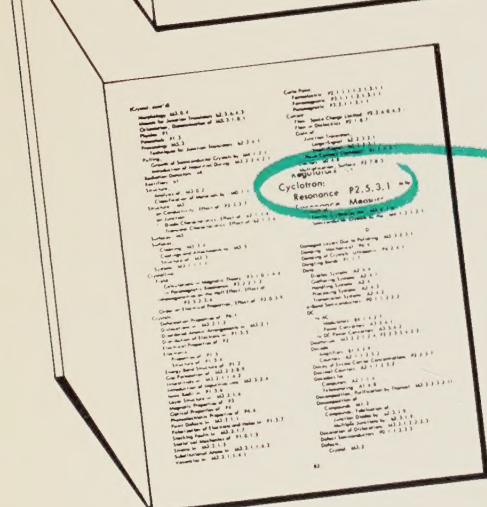
for the

solid state:

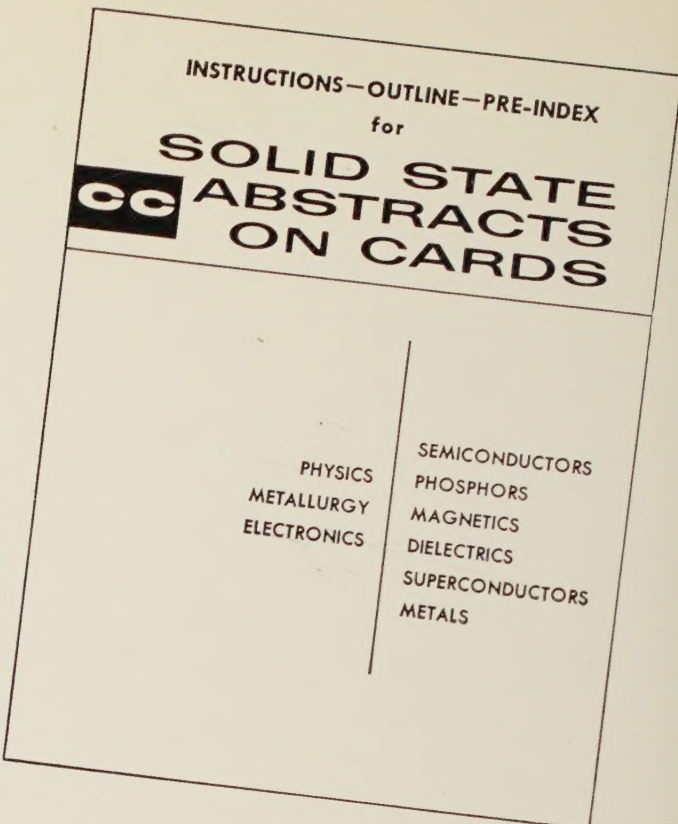
SOLID STATE ABSTRACTS ON CARDS



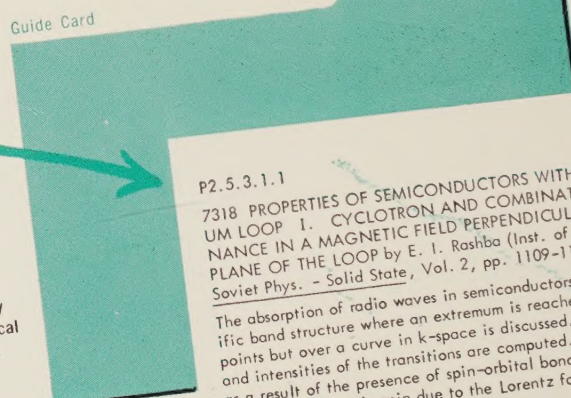
2500-Topic
Classification
Outline



4000-Entry
Alphabetical
Pre-Index



Send for your free copy of our new 120 page book describing this unique system which is now being used in more than 300 solid state laboratories throughout the world.



6000 Abstract
Cards (soon
to be 20,000)

P2.5.3.1.1
7318 PROPERTIES OF SEMICONDUCTORS WITH AN EXTREMUM LOOP 1. CYCLOTRON AND COMBINATIONAL RESONANCE IN A MAGNETIC FIELD PERPENDICULAR TO THE PLANE OF THE LOOP by E. I. Rashba (Inst. of Physics, Kiev); Soviet Phys. - Solid State, Vol. 2, pp. 1109-1122, Dec. 1960

The absorption of radio waves in semiconductors having a specific band structure where an extremum is reached not at isolated points but over curve in k-space is discussed. The frequencies and intensities of the transitions are computed. It is shown that as a result of the presence of spin-orbital bonds, transitions involving a change in spin due to the Lorentz force possess significant power.



CAMBRIDGE COMMUNICATIONS CORPORATION

236 MAIN STREET • CAMBRIDGE 42, MASSACHUSETTS • Tel. 491-0710